An Introduction to Transition Metal Chemistry

A transition metal is an element that has a partly *d* or *f* subshell in any of its common oxidation states. The transition elements are taken to be those of Groups 3-12, plus the lanthanides and actinides.

## Properties Common to the Transition Elements

1. The free elements conform to the metallic bonding model. Thus, their lattices are typically either close-packed or body centered cubic. They generally have high thermal and electrical conductivities, and they are malleable and ductile.

2. Nearly all have more that one positive oxidation state.

3. Nearly all have one or more unpaired electrons in their atomic ground states, and form paramagnetic compounds and ions. Because of this, studies of magnetic properties using experimental tools such as NMR, ESR, and magnetic susceptibility are often employed in this are of chemistry.

4. Low-energy electron transitions are observed for the free elements and their compounds and complexes. The transitions may fall into the infrared, visible, or ultraviolet region; for the visible cases, of course, colored species are the results.

5. The cations of these elements (and often the neutral atoms as well) behave as Lewis acids, and there is a strong tendency to form complexes. Complexes having 2-6 bases (ligands) are common, and species with as many as 14 ligands about a single metal are known.

Oxidation State Tendencies and Their Causes

A key to understanding the chemistry of the transition elements is knowledge of their oxidation state preferences. These preferences can be rationalized through analysis of such factors as **ionization energy (IE)** and **bond energy**.

It is useful to view oxidation states from two perspectives: One is the maximum (the most oxidized) state, and the second is the preferred (most stable) state.

For the first half of the 3d series (Sc-Mn), the maximum state corresponds to the "loss" (or more accurately, the participation in chemical bonding) of all valence electrons.

$$Sc_2O_3,\ TiO_2,\ VO_2{}^+,\ CrO_3,\ MnO_4{}^-$$
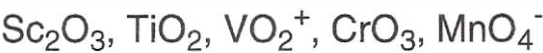
Beyond manganese there is a general decrease in the highest state observed, as demonstrated by the following:

$$FeO_4{}^{2-},\ Co_2O_3 \cdot nH_2O,\ NiO_2,\ CuO^+,\ ZnO$$

The decrease from Fe(VI) to Zn(II) correlates better with the number of vacancies than with the number of occupancies in the valence orbitals of these elements.

Maximum oxidation states also can be examined through binary oxides and fluorides.

Table 15.1 The common binary fluorides and oxides of the elements of the first transition series

					Fluorides					
M^{II}			VF_2	CrF_2	MnF_2	FeF_2	CoF_2	NiF_2	CuF_2	ZnF_2
M^{III}	ScF_3	TiF_3	VF_3	CrF_3	MnF_3	FeF_3	CoF_3			
M^{IV}		TiF_4	VF_4	CrF_4	MnF_4					
M^{V}			VF_5	CrF_5						

					Oxides					
M^I									Cu_2O	
M^{II}		TiO	VO	CrO	MnO	FeO	CoO	NiO	CuO	ZnO
M^{III}	Sc_2O_3	Ti_2O_3	V_2O_3	Cr_2O_3	Mn_2O_3	Fe_2O_3	Co_2O_3			
M^{IV}		TiO_2	VO_2	CrO_2	MnO_2			NiO_2		
M^{V}			V_2O_5							
M^{VI}				CrO_3						
M^{VII}					Mn_2O_7					

Note: The most thermodynamically stable states are shown in boldface type. The most stable oxide of iron is the mixed oxide Fe_3O_4.

For Cr and Mn, a higher state is achieved with oxide than with fluoride. Why?

The preferred state is the one that is the most stable (toward disproportionation or thermal dissociation) and/or the least reactive. Such states are highly dependent on the types of ligands present. Metals in high oxidation states are relatively hard, and so are stabilized by hard bases (e.g. F and O donors). Lower oxidation states are stabilized by softer bases such as S^{2-} and I^-.

Table 15.1 shows that, when bonded only to oxygen or fluorine, higher states (M(III) and/or M(IV)) are preferred by the early elements; M(II) is favored later in the series. This correlates with **IE's**. The energy requirements for the removal of two and three electrons from the 3d elements are plotted below.
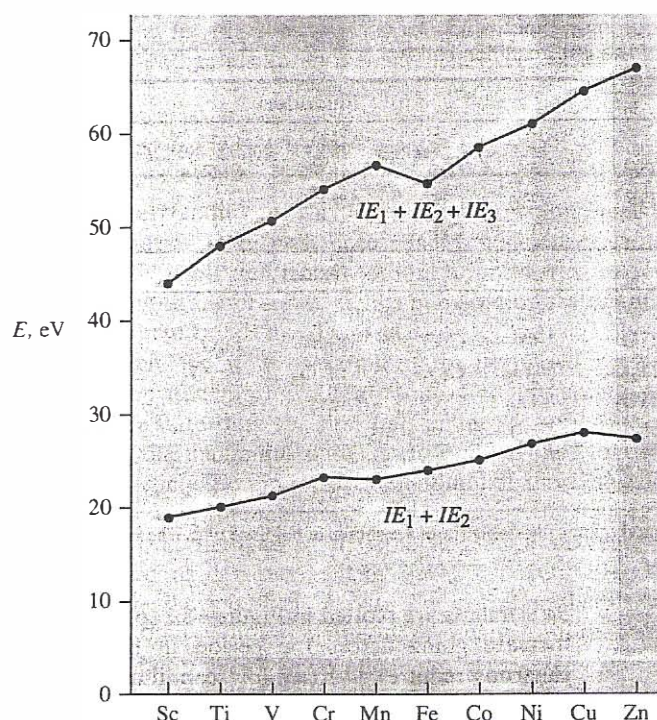
The removal of three e^-'s requires 44.1 eV for Sc and 56.75 eV for Mn, the first element for which the M(II) state is preferred. Hence, Mn^{3+} is destabilized relative to its neutral atom by 12.65 eV (about 1220 kJ/mol) more than is Sc^{3+} versus Sc. The relative destabilization is even greater for Co, Ni, Cu, and Zn. What about Fe?

Comparisons of the 3d, 4d, and 5d Elements

IE's tend to be slightly lower for the 4d elements than for their 3d congeners. For example, the sum of the first three energies of Tc is 52.08 eV, about 8% less than for Mn. These lower IE's and reduced steric interactions (Why?) both favor high oxidation states. Thus, the most stable fluorides of Nb, Mo, Tc and Ru are NbF_5, MoF_6, TcF_6, and RuF_5, respectively. (Compare these to the corresponding 3d elements in the Table 15.1.)

The 5d elements are similar to their 4d congeners (TaF_5, WF_6, etc.), and in some cases still higher oxidation states are stabilized (ReF_7, OsF_6, IrF_4, and PtF_4).

Some Metal Potentials

	M(I)	M(II)	M(III)	M(IV)	M(V)	M(VI)	M(VII)
Sc			-6.09				
Ti		-3.26	-3.62	-3.53			
V		-2.37	-2.63	-2.27	-1.27		
Cr		-1.82	-2.23			1.76	
Mn		-2.36	-0.85	0.10		4.62	5.19
Fe		-0.88	-0.11			6.49	
Co		-0.55	1.25				
Ni		-0.5		2.86			
Cu	0.52	0.67					
Zn		1.52					

- good and stable

+ bad and unstable

Coordination Compounds and Complex Ions

The chemistry of the transition elements is dominated by species in which the metal simultaneously engages in Lewis acid-base interactions (What are these?) with two or more donor ligands. These have long been called *coordination compounds* or *complexes*.

$$M^{m+} + nL^{x-} \longrightarrow [ML_n]^{m-nx}$$

The variable metal oxidation states, great variety of ligands available, and different possible coordination numbers combine to create an enormous number of possibilities for study. However, among the known, stable complexes the number of ligands and the geometric structure about a given metal are far from random.

Low-Coordinate Geometries

Two ligands might be arranged about a central metal in either a linear or an angular manner; linear is more common. Point groups?

Keep in mind that stoichiometry is not predictive of coordination, especially in the solid state. For example, you might assume the coordination number of FeF_2 is two, but in both crystalline FeF_2 and FeF_3, the metals occupy six-coordinate, octahedral interstices of fluoride ion sublattices.

Complexes in which the metal has a coordination number of 3 are relatively uncommon.

(a)

(b)
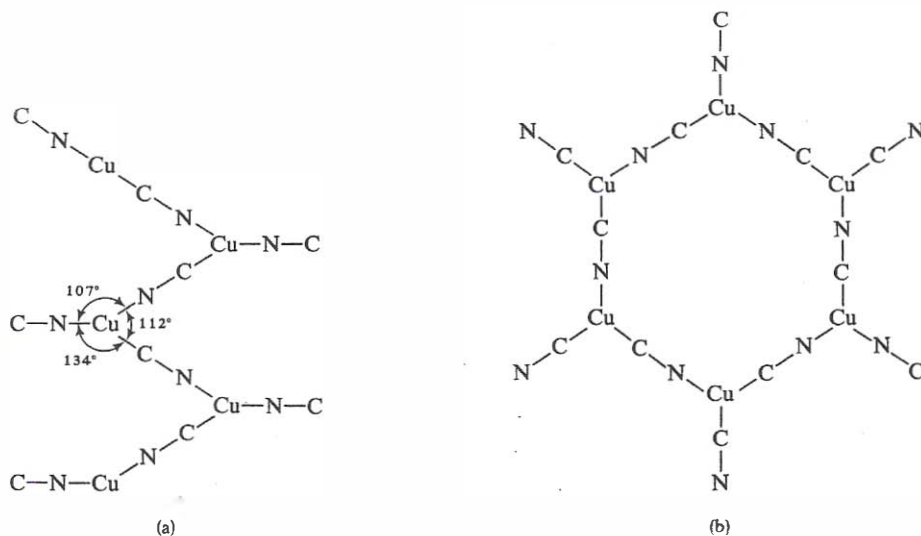
Figure 15.3 The structures of two 3-coordinate Cu^I complexes: (a) the $[Cu(CN)_2]^-$ anion of $K[Cu(CN)_2]$; (b) the $[Cu(CN)_3]^{2-}$ anion of $K_2[Cu(CN)_3] \cdot H_2O$.
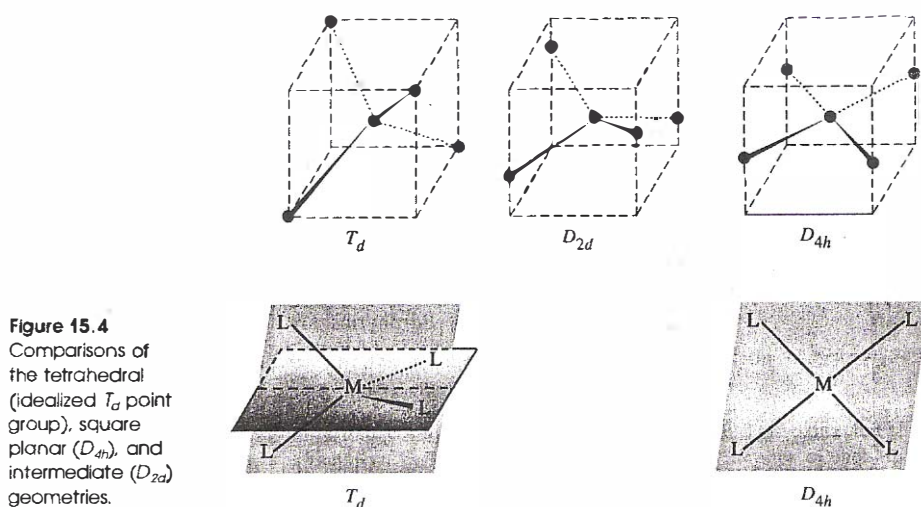
Sterically large ligands often promote trigonal coordination. Two well-known examples are $(Me_3Si)_2N^-$ and $(Me_3Si)_3C^-$, which form trigonal complexes witha majority of the 3d elements. In most such complexes the metal lies in the plane of the three donor atoms, but in $Sc[N(SiMe_3)_2]_3$ the Sc is above the plane (Point group, anyone?).

It is possible (but not common) for three ligands to form an approximately T-shaped geometry about the metal; e.g. $[Rh(P(C_6H_5)_3)_3]^+$, which has a nearly linear P-Rh-P linkage.

Tetrahedral, Square Planar, and Intermediate Geometries

Four-coordinate complexes are usually either tetrahedral or square planar. I assume you all remember their respective bond angles, correct?

There are an infinite number of possible gemoetries between these limiting cases. The situation can be visualized as follows:

Figure 15.4
Comparisons of the tetrahedral (idealized T_d point group), square planar (D_{4h}), and intermediate (D_{2d}) geometries.

The intermediate geometries (variously referred to as flattened, squashed, or distorted tetrahedra) are less common than either the tetrahedral or square planar structures.; e.g. $Cs_2[CuX_4]$ (X = Cl and Br), 100-103°.

The geometry of a given tetracoordinate complex depends on both steric and electronic factors. The tetrahedron is superior from a steric standpoint, because it maximizes the distance between ligands. As we will show later, the number of d electrons determines which possibility is favored electronically.

Some Metal Applications

Sc	High-intensity lights; Al-Sc alloys in aircraft
Ti	Paint base (TiO_2); alloy with Al for aircraft
Zr	Photoflash bulbs, gem stones
V	Steel additive (springs, etc.)
Cr	Stainless steels
W	Filaments in electric lights
Mn	Steel manufacture and additives
Fe	Steels
Co	Pigments (glass, paints and inks)
Ni	Ferrous and nonferrous alloys (nichrome)
Pd	White gold (Au/Pd); resistance in wires, catalysis
Pt	Catalysts
Cu	Electrical conduction purposes; coinage
Ag	Photographic chemicals and jewelry
Au	Jewelry; electrical components
Zn	Autocorrosion coatings; roofings
Cd	Batteries (Ni/Cd); ceramic glazes
Hg	Liquid electrical conductor; fungicide; germicide

Square planar geometry is favored by metal ions having eight d electrons, especially Pd(II), Pt(II), and Au(III). Both geometries are common for Ni(II). The steric effect is more important for nickel than for its $4d$ and $5d$ congeners because of its smaller size. As a result, it is possible to prepare nickel complexes for which the difference in stability between the tetrahedral and square planar geometries is very small.

Table 15.4 The preferred structures of some tetracoordinate Ni^{II} complexes

Complex	Geometry	Complex	Geometry
$NiBr_4^{2-}$	T-4	$NiBr_2(P\phi_3)_2$	T-4
NiI_4^{2-}	T-4	$NiCl_2(P\phi_2Me)_2$	SP
$[Ni(CN)_4]^{2-}$	SP	$NiBr_2(P\phi_2Me)_2$	T-4
$[Ni(NCO)_4]^{2-}$	T-4	$NiI_2(P\phi_2Me)_2$	T-4
$[Ni(P\phi_3)_4]^{2+}$	SP	$NiBr_2(P\phi_2Et)_2$	Either
$[Ni(py)_4]^{2+}$	SP		

Note: T-4 = tetrahedral; SP = square planar.

Certain ligands dictate (or at least strongly favor) square planar geometry.

(a) Terpyridine   (b) Porphyrin framework
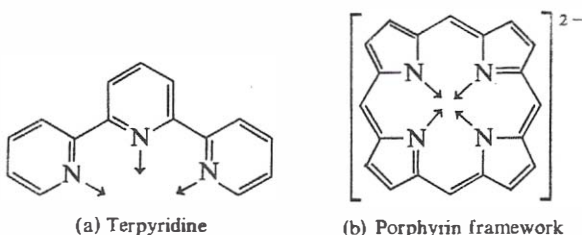
Why and how does the porphyrin remain planar?

Geometric and Optical Isomerism

Stereoisomers differ in their spatial arrangement of atoms. The two broad types of stereoisomerism are *geometric* and *optical* isomerism. Stereoisomerism is possible for certain 4-coordinate complexes having more than one kind of ligand.

For example, geometric (cis-trans) isomers exist for square planar complexes of the type Ma_2b_2, where a and b are nonequivalent donors. No isomerism is possible for tetrahedral Ma_2b_2 compounds. (Note historical significance.)

Although the tetrahedral geometry does not give rise to geometric isomers, the presence of four different ligands creates an asymmetric metal, thereby leading to optical isomerism. Compared to carbon chemistry there are few tetracoordinate metal complexes for which optically pure enantiomers have been isolated; racemization is rapid or below r.t.

Trigonal Bipyramidal, Square Pyramidal, and Intermediate Geometries

Five-coordinate complexes were once rather rare. Some of the earlier complexes that were thought to be 5-coord. actually had coordination numbers (CN) of 4, 6 or other.

The rarity of 5-coord. spawned directed efforts toward their synthesis, and in recent years a large number of such species have been reported.

The CN appears to produce less stable complexes than similar systems having 4 or 6 ligands. As a result, either of two types of decomposition may be observed.

1. $$ML_5 \longrightarrow ML_4 + L$$
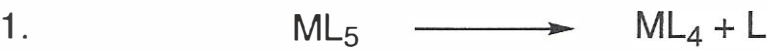
Common in solution chemistry.

2. $$M \longleftarrow L \longrightarrow M$$

Common for complexes containing halide ligands, which can bridge two metal centers.

● = Metal
○ = Halide

(a) $M \bullet_2 Cl_{10}$ (b) Nb_4F_{20}
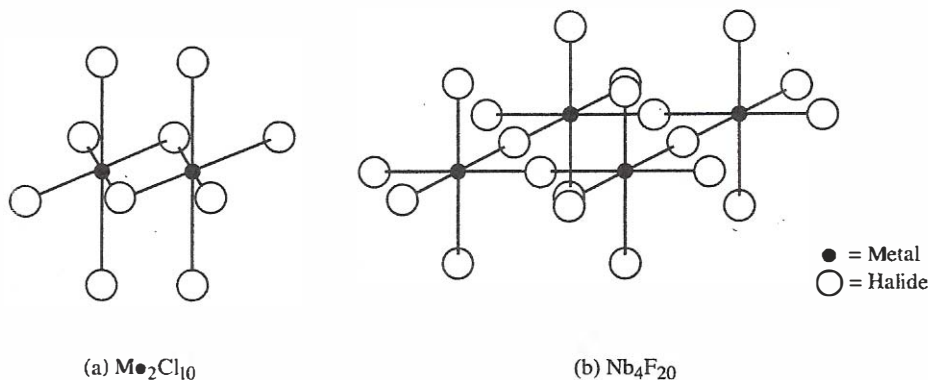
Figure 15.6 The structures of two halide-bridged oligomers.
[Reproduced with permission from Wells, A. F. *Structural Inorganic Chemistry*, 5th ed.; Clarendon: Oxford, 1984; p. 427.]

For complexes that are truly 5-coord., there are two limiting structures and an infinite number of intermediate cases. The limiting geometries are the trigonal bipyramid (TBP) and squre pyramid (SPY), with maximum local symmetries of _____ and _____, respectively.

Does anyone recall which symmetry main group atoms prefer?

The energy difference between the TBP and SPY structures for metal complexes is often small.

The ideal SPY geometry is essentially never encountered. In square pyramidal complexes, the metal ion is normally raised out of the basal plane (30-50 pm) toward the axial group.

This changes the SPY bond angles to (calculated) optimum values of about $104°$ (axial-basal) and $87°$ (basal-basal) from the $90°$ ideal.
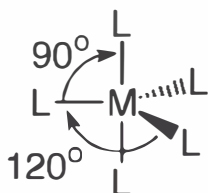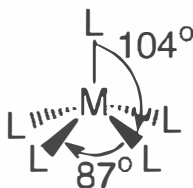
Idealized TBP   Optimized SPY   Idealized SPY
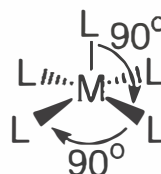
Another way the TBP and SPY geometries become indistinct is through their interconversion: Berry pseudorotation or a similar process. Such interconversion is sometimes facile, resulting in fluxional behavior in solution.
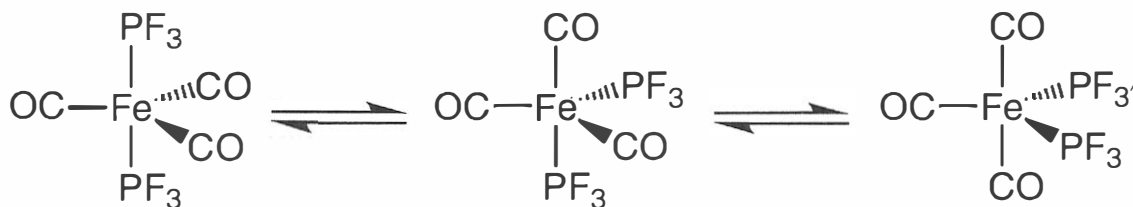
All members of the series $Fe(CO)_x(PF_3)_{5-x}$ have been prepared and exhibit a TBP geometry. In solution it is possible to detect all geometric isomers of $Fe(CO)_3(PF_3)_2$ by IR. However, no individual isomer can be separated from the others because of their rapid interconversion.

The axial and equatorial bond distances in TBP complexes are of interest. For most cases studied to date, the equatorial bonds are longer than the axial linkages. (Review main-group compounds having a 5-coordinate central atom.

Table 15.5 Experimental distances for the axial and equatorial bonds in some trigonal bipyramidal complexes

Complex	Number of d Electrons	d(M–L), ax	d(M–L), eq
$[Fe(N_3)_5]^{2-}$	5	204	200
$[Co(C_6H_7NO)_5]^{2+}$	7	210	198
$[Mn(CO)_5]^-$	8	182	180
$Fe(CO)_5$	8	181	183
$[Co(NCCH_3)_5]^+$	8	184	188
$[Ni(CN)_5]^{3-}$	8	184 (av)	193 (av)
$[Pt(GeCl_3)_5]^{3-}$	8	240	243
$[Pt(SnCl_3)_5]^{3-}$	8	254	254
$[CuCl_5]^{3-}$	9	230	239
$[CuBr_5]^{3-}$	9	245	252
$[CdCl_5]^{3-}$	10	253	256

Note: Bond distances in picometers; av = average values (distorted geometry).

Polydentate ligands can dictate whether a pentacoordinate complex has a TBP, a SPY, or an intermediate geometry.

(a)   (b)
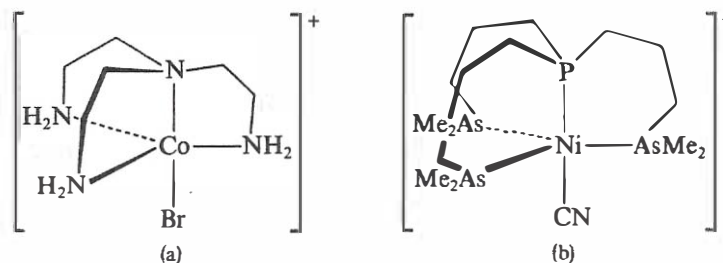
Octahedral and Distored Octahedral Complexes

Among the metal complexes reported to date, the largest percentage contain 6-coordinate metal atoms or ions. All are either octahedral or distorted in some manner from that geometry.

Geometric isomerism is possible for species conforming to the formulas Ma_4b_2 and Ma_3b_3. The Ma_3b_3 isomers are named *fac* (*facial*) and *mer* (*meridional*). In the facial isomer, each set of three common ligands forms a triangular face of the octahedron.


cis   trans   fac   mer
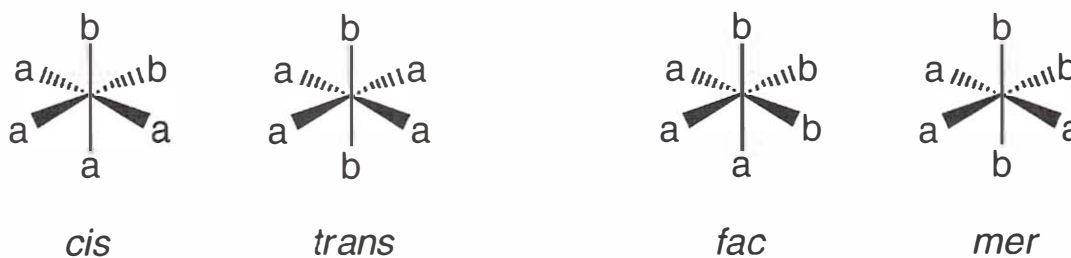
How many geometric isomers for $Ma_2b_2c_2$ and $Mabcdef$ complexes?

Optical isomerism is especially common for octahedral complexes having chelating ligands; eg. EDTA and tris(ethylenediamine). Thus, $[Co(en)_3]^{3+}$ belongs to the D_3 point group; it has neither a mirror plane nor an inversion center, and so is optically active.

Δ Λ
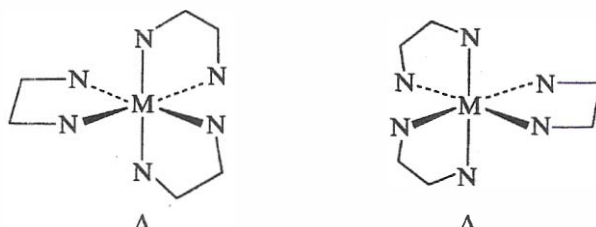
There are three common types of distortion from octahedral geometry. One results from metal-ligand bond shortening or lengthening to two opposite ligands, tetragonal (Jahn-Teller) distortion and destroys the threefold axes of the original octahedron.

Tetragonal (Jahn-Teller) distortion

Trigonal distortion

Twist distortion
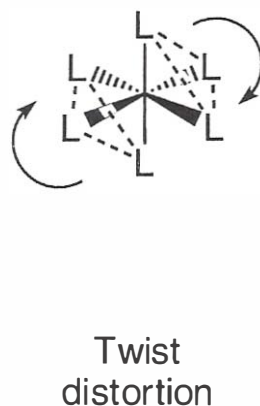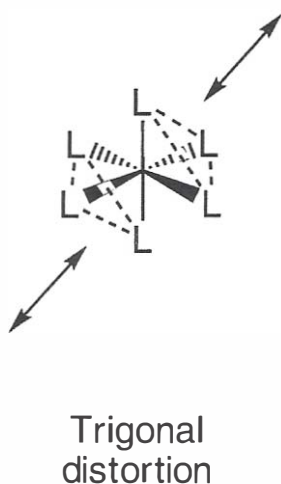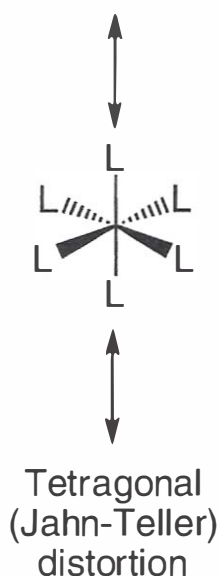
Point group?

A second type of distortion involves bond lengthening or shortening to three facial ligands. This trigonal distortion destroys the C_4 axes of the octahedron, reducing the idealized symmetry to D_{3d}. The result is a trigonal antiprism; very rare for metal complexes but are found in certain ionic lattices (CdBrI).

A third mode of distortion involves the twisting of a triangle of three ligands (ie, one face of the octahedron). In a regular octahedron these triangles are skewed by $60°$ with respect to one another. This geometry is more common in extended lattices (MoS_2) than in discrete complexes ($V(S_2C_2(C_6H_5)_2)_3$ and $Mo(S_2C_2(CN)_2)_3$).
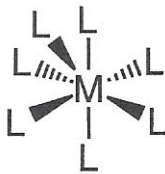
High-Coordinate Geometries

Complexes in which a metal coordinates to 7, 8 or more ligands can no longer be considered rare.
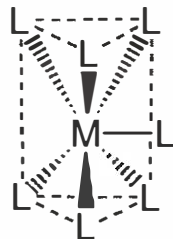
There are three well-established geometries for 7-coordinate complexes: the pentagonal bipyramid, capped octahedron and capped trigonal prism.
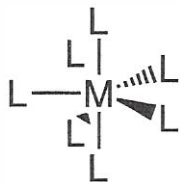
| Pentagonal bipyramid | Capped octahedron | Capped trigonal prism |

At least two of these geometries are likely to lie close to one another in energy for any given complex, and theory suggests (and experiments verify) that they are readily interconvertible; $W(PMe_3)F_6$ at -85°C.

The isolation of 7-coordinate complexes is sometimes facilitated by the incorporation of polydentate ligands:

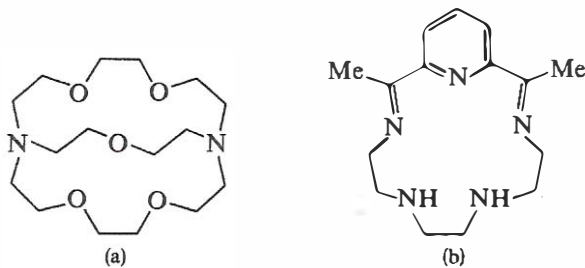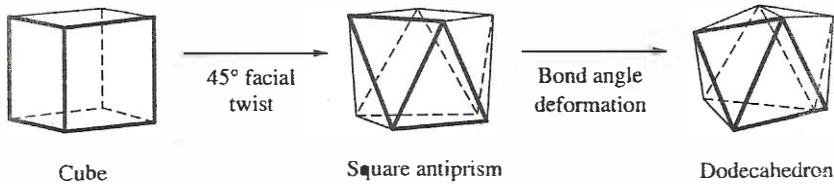**Figure 15.14** Two polydentate ligands that stabilize high-coordinate species: (a) the cryptand ligand of the complex salt $[Co(crypt)]^{2+}[Co(SCN)_4]^{2-}$; (b) the pentadentate ligand pal_{222}.

The best-known 8-coordinate geometries are the cube, the square antiprism, and the dodecahedron.

| Cube | 45° facial twist → | Square antiprism | Bond angle deformation → | Dodecahedron |

13

The relationship between the square antiprism and the cube is the same as between the octahedron and the trigonal prism - twisting one face generates the alternative structure. The energy differences among these geometries are small, interconversions are usually facile, fluxionality is common, and the separation of isomers is often impossible. Most of the known 8-coordinate complexes have large metal ions (4d, 5d, lanthanide, or actinide elements) and/or either small or macrocyclic ligands.

Species having more than eight ligands surrounding a metal are rare. The best-known geometries are the tricapped trigonal prism (9-coordinate), bicapped square antiprism (10), and icosahedron (12).

Structural Isomerism

1. Coordination isomerism. A common type arises when a complex cation and complex anion form a salt. Thus, $[Co(NH_3)_6]^{3+}[Cr(CN)_6]^{3-}$ and $[Cr(NH_3)_6]^{3+}[Co(CN)_6]^{3-}$ both have the molecular formula $CoCrC_6H_{18}N_{12}$.

2. Ionization and hydrate isomerism. Occurs for certain salts containing complex cations. For example, $[(H_3N)_3PtBr]^+NO_2^-$ and $[(H_3N)_3PtNO_2]^{+}Br^-$ are ionization isomers.

3. Linkage isomerism. The potential for isomerism exists in any complex containing ambidentate ligands, and many examples of *linkage isomerism* are known. The earliest and perhaps most thoroughly studied examples contain the NO_2^- ion, as in the pair $[(H_3N)_5CoNO_2]^{2+}$ and $[(H_3N)_5CoONO]^{2+}$.

Also,

Valence Bond Models

Effective Atomic Number (EAN)

The EAN of a metal ion is calculated by adding the electrons of the metal ion to those shared with it through coordination. Just as the octet is useful in formulating the bonding in compounds of the light elements, the notion of an EAN provides a rough guide for bonding in coordination compounds. Quite a few, but not all, metals achieve the EAN of a noble gas through coordination.

Table 9.4 Valence electron count for metals

Complex	Number of electrons on M^{n+}	Number of electrons from ligands	EAN
$Pt(NH_3)_6^{4+}$	$78 - 4 = 74$	$6 \times 2 = 12$	86 (Rn)
$Co(NH_3)_6^{3+}$	$27 - 3 = 24$	$6 \times 2 = 12$	36 (Kr)
$Fe(CN)_6^{4-}$	$26 - 2 = 24$	$6 \times 2 = 12$	36
$Fe(CO)_5$	$26 - 0 = 26$	$5 \times 2 = 10$	36
$Cr(CO)_6$	$24 - 0 = 24$	$6 \times 2 = 12$	36
$Ni(CO)_4$	$28 - 0 = 28$	$4 \times 2 = 8$	36
$Ni(NH_3)_6^{2+}$	$28 - 2 = 26$	$6 \times 2 = 12$	38
$Ni(CN)_4^{2-}$	$28 - 2 = 26$	$4 \times 2 = 8$	34
$Cr(NH_3)_6^{3+}$	$24 - 3 = 21$	$6 \times 2 = 12$	33

The EAN concept has been particularly successful for complexes of low-valent metals (oxid. # $\leq$ II); for complexes having high oxidation numbers (oxid. # $\geq$ II), EAN can be taken only as a rough guide.

This electron-counting scheme is also called the **eighteen-electron rule**, in contrast to the usual octet rule for "simple" compounds. The octet rule applies to main-group elements for which s and p are the only low-energy orbitals to be filled. For transition metals (TM's) the five d orbitals are also included in the valence shell, since they are comparable in energy to the filled s and p orbitals of the same quantum number.

What do NI(II) complexes obey?

Hybridization and Orbital Occupancy

Coordination compounds result from the use of available empty bonding orbitals on the metal for the formation of coordinate covalent bonds. The coordination number and geometry are determined in part by size and charge effects, but also to a great extent by the orbitals available for bonding.

Coord. number	Hybridized orbitals (σ)	Configuration	Strong π orbitals	Examples
2	sp	Linear	p^2, d^2	$Ag(NH_3)_2^+$
3	sp^2	Trigonal planar	p, d^2	BF_3, NO_3^-, $Ag(PR_3)_3^+$
4	sp^3	Tetrahedral		$Ni(CO)_4$, MnO_4^-, $Zn(NH_3)_4^{2+}$
4	dsp^2	Planar	d^3, p	$Ni(CN)_4^{2-}$, $Pt(NH_3)_4^{2+}$
5	$d_z sp^3$ or $d^3 sp$	Trigonal bipyramidal	d^2	TaF_5, $CuCl_5^{3-}$, $[Ni(PEt_3)_2Br_3]$
5	$d_{x^2-y^2}sp^2$, d^2sp^2, d^4s, or d^4p	Tetragonal pyramidal	d	IF_5, $[VO(acac)_2]$
6	d^2sp^3	Octahedral	d^3	$Co(NH_3)_6^{3+}$, $PtCl_6^{2-}$
7	d^5sp or d^3sp^3	Pentagonal bipyramidal	—	ZrF_7^{3-}
7	d^4sp^2 or d^5p^2	Trigonal prism with an extra atom in one tetragonal face	—	TaF_7^{2-}, NbF_7^{2-}
8	d^4sp^3	Dodecahedral	d	$Mo(CN)_8^{4-}$, $Zr(C_2O_4)_4^{4-}$
8	d^5p^3	Antiprismatic	—	TaF_8^{3-}, $Zr(acac)_4$
8	d^3fsp^3 or d^3f^4s	Cubic	—	$U(NCS)_8^{4-}$

*G. E. Kimball, *J. Chem. Phys.* 1940, 8, 188.

Magnetic susceptibility measurements have been used widely to determine the number of unpaired electrons in complexes, and from this information the number of d orbitals used for bond formation usually can be inferred for ions containing four to eight d electrons.

Table 9.6 Electron configurations for some metal complexes in valence bond (VB) terms and classified as high or low spin
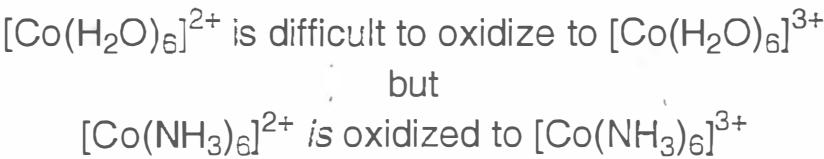
Ion or complex	Configuration											High or low spin
			3d				4s		4p			
Cr^{3+}	1	1	1	—	—	—	—	—	—	—		
$[Cr(NH_3)_6]^{3+}$	1	1	1	1↓	1↓		1↓	1↓	1↓	1↓		*
Co^{3+}, Fe^{2+}	1↓	1	1	1	1		—	—	—	—		
$[Co(NH_3)_6]^{3+}$	1↓	1↓	1↓	1↓	1↓		1↓	1↓	1↓	1↓		Low spin
$Fe(CN)_6^{4-}$												
Co^{2+}	1↓	1↓	1	1	1		—	—	—	—		
$[Co(NH_3)_6]^{2+}$	1↓	1↓	1	1	1		"Ionic" (VB)					High spin
Zn^{2+}	1↓	1↓	1↓	1↓	1↓		—	—	—	—		
$[ZnCl_4]^{2-}$ (tetrahedral)	1↓	1↓	1↓	1↓	1↓		1↓	1↓	1↓	1↓		♭
$[Zn(NH_3)_4]^{2+}$	1↓	1↓	1↓	1↓	1↓		"Ionic" (VB)					♭
Fe^{3+}	1	1	1	1	1		—	—	—	—		
$[Fe(C_2O_4)_3]^{3-}$	1	1	1	1	1	}	"Ionic" (VB)					High spin
$[Ni(NH_3)_6]^{2+}$	1↓	1↓	1↓	1	1							

* All octahedral complexes of Cr^{III} have three unpaired electrons.
♭ All complexes of Zn^{II} are diamagnetic.

The terms **low-spin** (or spin-paired) and **high-spin** (or spin-free) describe the electron population of the d orbitals, as determined from magnetic properties, w/o any assumptions concerning the nature of the bonding.

Stabilization of Oxidation States and Pi Bonding

$$[Co(H_2O)_6]^{2+} \text{ is difficult to oxidize to } [Co(H_2O)_6]^{3+}$$

but

$$[Co(NH_3)_6]^{2+} \text{ is oxidized to } [Co(NH_3)_6]^{3+}$$

The difference in reactivity with ligand type is not so great for other first transition series ions, but in general, coordination with ligand atoms less electronegative than oxygen stabilizes the oxidation state next higher than that of the most stable aqua ion, unless other factors, such as π bonding, are involved.

This is because less electronegative ligand atoms are more effective donors toward the more highly charged ions.

Compounds of the highest oxidation state are strongly oxidizing and are stable only with the most electronegative ligands, F and O, as in fluoride complexes and oxoanions.

$$[FeF_6]^{3-}, \text{ yes, but } [FeI_6]^{3-}, \text{ no}$$

Exceptions: CO, CN⁻, and 1,10-phenanthroline

A ligand atom such as C could give a predominantly covalent coordinate bond with a transition metal atom, leading to the accumulation of negative charge on the metal atom. Let us examine $Ni(CO)_4$.
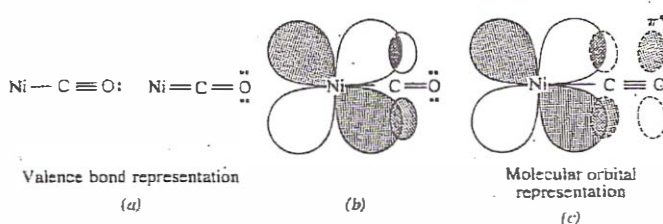

Valence bond representation
(a)   (b)

Molecular orbital representation
(c)

Figure 9.7   Metal–carbon double bonding.

The Ni-C bond distance in $Ni(CO)_4$ is shorter than exptected for a single bond suggesting what?

The VB representation of a contributing structure containing a metal-carbon double bond revelas that particular contributing structure to have a C-O double bond instead of the triple bond in the other main contributing structure.

The sketch of orbitals available for ligand-metal π binding in a molecular orbital (MO) description reveals that if a metal d orbital of appropriate symmetry is filled, electrons can be donated into the CO π^* orbital: a CO double bond.

In either model, the C-O bond is weakened and lengthened while the M-C π-bonding strengthens the M-C bond.

Therefore, CO and CN⁻ stabilize low oxidation numbers where metal electrons are available for M-C π bonding.

The Crystal and Ligand Field Theories

Crystal field theory (CFC) was originally concerned with the electrostatic interactions about a given ion in a solid-state ionic lattice. This model was later applied to coordination compounds and complex ions-for example, for evaluating the repulsions that arise when the electron(s) pairs in a d sub-shell of a metal cation are surrounded by ligand electron pairs in a specific geometric array.
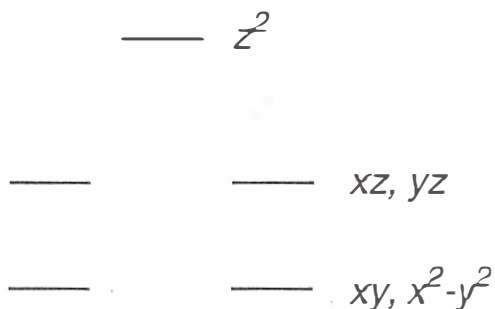
The five d orbitals are degenerate (of equal energy) in gaseous metal ions. The simple electrostatic model (recall Chemical Forces from Chem 318) fails to predict differences of bond energies among complexes of different transition metals

Consider an isolated transition metal ion that has one d electron.

$$\underline{\qquad} \quad \underline{\qquad} \quad \underline{\qquad} \quad \underline{\qquad} \quad \underline{\qquad}$$
$$z^2 \quad\quad xz \quad\quad yz \quad\quad xy \quad\quad x^2\text{-}y^2$$

For a d^1 metal ion in an octahedral field the e^- can go into one of the lower-energy d orbitals, thereby stabilizing the complex. Next, visualize an invasion of this system by two negative charges. The e^- experiences electrostatic repulsion from these charges. If the charge distribution is spherically symmetric, the five d orbitals are destabilized by equal amounts and thus remain degenerate. For any distribution other than spherical, however, the repulsion is different for different orbitals; ie. the d orbital equivalence is destroyed.

For example, two point charges on opposite sides of the metal would occupy positions along the z axis according to group theory convention. We can approach this as a linear ML_2 molecule.

$$\underline{\qquad} \quad z^2$$

$$\underline{\qquad} \qquad\qquad \underline{\qquad} \quad xz,\ yz$$

$$\underline{\qquad} \qquad\qquad \underline{\qquad} \quad xy,\ x^2\text{-}y^2$$

The d^1 system therefore has a doubly degenerate ground state in a linear crystal field (____ point group) with the symmetry label Δ_g assigned to the $d_{xy}/d_{x2\text{-}y2}$ level. The excited states (corr. to occupancy of the Π_g and Σ_g^+ levels, resp.) are accessible through $d \dashrightarrow d\ e^-$ transitions of low energy.

In the pure **crystal-field theory**, we consider that only e⁻'s belonging to the metal occupy the metal's *d* orbitals. The ligand lone pairs are considered to belong entirely to the ligand and to provide an electric field of the symmetry of the ligand arrangement around the metal. The name **ligand-field theory** is used to refer to the approach in present use; it is basically the same as the pure pure crystal field approach, except that covalent interaction is taken into account as necessary.

Octahedral Complexes

The single most common geometry observed for transition metal complexes is octahedral.

Ligand-Field Stabilization Energy

In an octahedral complex oriented as shown below, two of the *d* orbitals, d_{z^2} and $d_{x^2-y^2}$, are directed toward the ligands. The repulsion caused by the e⁻ pairs of the ligands raises the energy of any e⁻'s occupying these orbitals (e_g) more than that of the other three orbitals, d_{xy}, d_{xz}, and d_{yz} (t_{2g}), which are directed at 45° to the axes. The stronger the electric field caused by the ligands, the greater the splitting (energy gap) of the energy levels: $O_h = 10$ Dq or Δ.

d_{xy} d_{xz} d_{yz}

$d_{x^2-y^2}$ d_{z^2} ML_6
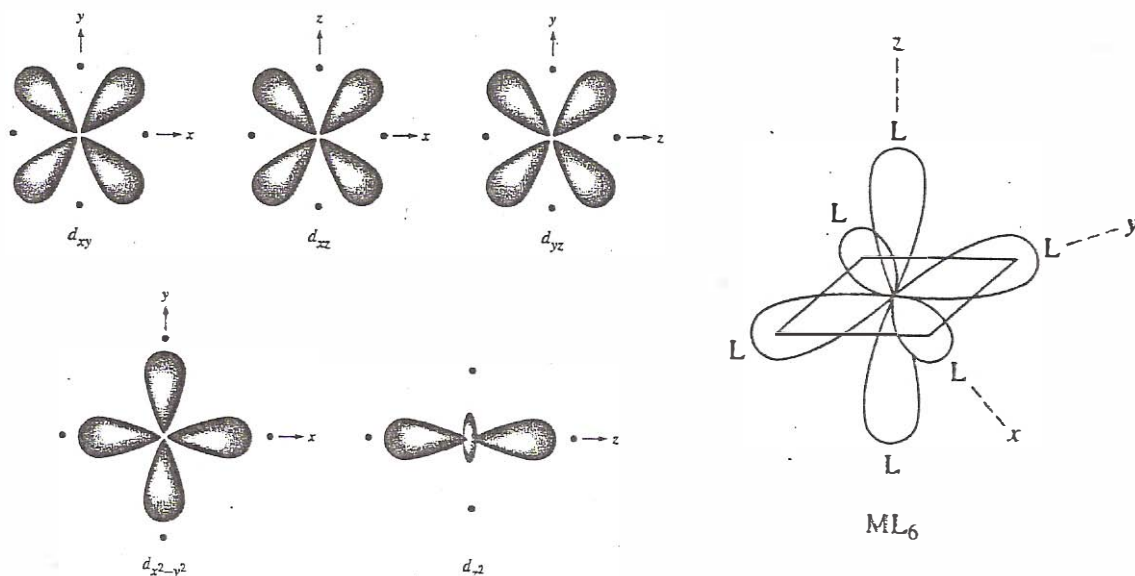
This splitting causes no net change in the energy of the system if all five orbitals are occupied equally because a filled or half-filled orbital set is totally symmetrical. The t_{2g} level is lowered by 4Dq (4/10Δ), and the e_g level is raised by 6Dq (6/10Δ) relative to the average energy of the *d* orbitals.

What is the net change for a d^{10} ion with 6 t_{2g} and 4 e_g e⁻'s?

For all configurations other than d^0, d^5 (high-spin, more on this later), and d^{10}, splitting lowers the total energy of the system as compared to the spherically symmetric case because e⁻'s preferentially occupy the lower-energy orbitals. The decrease in energy caused by the splitting of the energy levels is the **ligand-field stabilization energy** (LFSE).
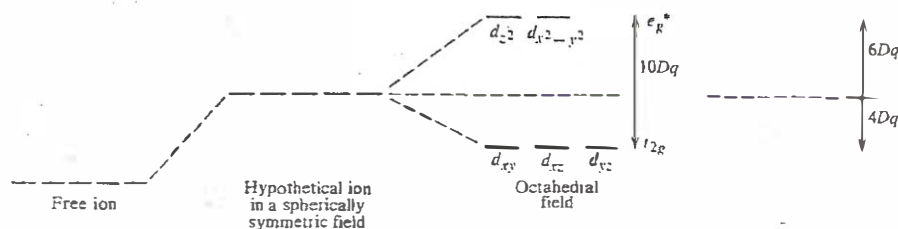

Figure 9.9 Splitting of the d energy levels in an octahedral complex.

Electrons enter the t_{2g} orbitals in accordance with _____'s rule for d^1, d^2, and d^3 configurations.

$[Cr(NH_3)_6]^{3+}$ 3 unpaired e⁻'s = 3(-4Dq) = -12Dq

The LFSE for any octahedral chromium(III) complex is -12Dq, but the value of Dq varies with the ligand.

Two configurations, t^3_{2g}, e^1_g, and t^4_{2g}, are possible for a d^4 ion in the ground state. For $t^3_{2g}e^1_g$, the fourth electron occupies the e_g level, giving four unpaired e⁻'s: LFSE is 3(-4Dq) + 1(6Dq) = -6Dq. For t^4_{2g}, the LFSE is 4(-4Dq) = -16Dq.
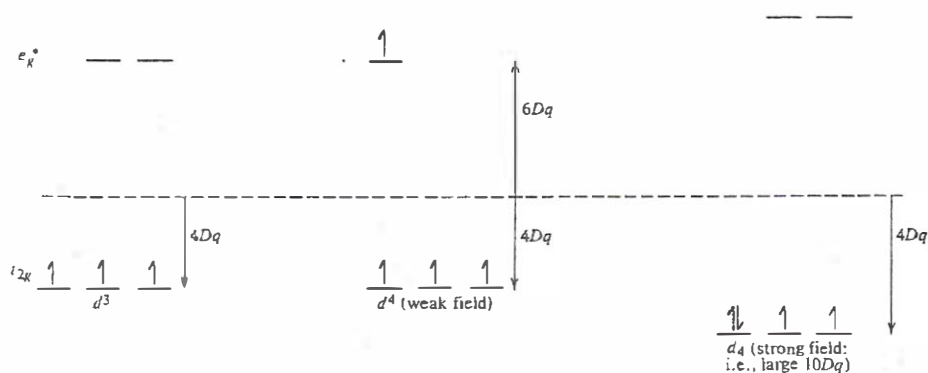
Figure 9.10 Occupation of d orbitals in octahedral complexes for d^3 and d^4 configurations.

Which one of these configurations a given complex adopts depends on the relative magnitudes of the ligand field (Dq) and the unfavorable potential energy of repulsion of two e⁻'s occupying the same orbital with spins paired (the pairing energy, PE). If Dq (and therefore 10Dq) is relatively small compared to the PE, it will be energetically more favorable to expend 10Dq in energy to place the fourth e⁻ in an e_g orbital instead of pairing it with another e⁻ in a t_{2g} orbital: $t^3_{2g}e^1_g$. This is referred to as the **weak-field case**, since the splitting is small with respect to PE, or the **high-spin case**, since there is a maximum number of unpaired spins.

If 10Dq is very large compared to the PE, placing the fourth e⁻ in a t_{2g} orbital produces the t^4_{2g} configuration, the lower energy state. This is referred to as the **strong-field case**, or the **low-spin** (or **spin-paired**) case. The net energy gain in the strong-field case is of smaller magnitude than -16Dq by the amount of energy required for pairing the electron.

Maximum LFSE is obtained for what configuration in what field?

Spectrochemical Series and Factors Affecting Δ

The order of ligand-field strength (decreasing Dq) for common ligands is approximately

$$CN^- > phen \sim NO_2^- > en > NH_3 \sim py > H_2O > C_2O_4^{2-} > OH^- > F^- > S^{2-}$$
$$> Cl^- > Br^- > I^-$$
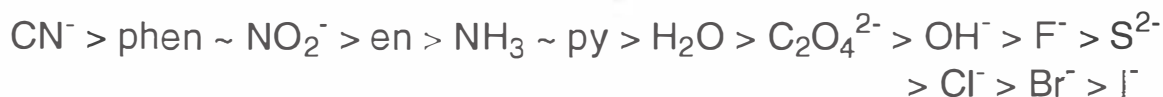
The high ligand-field effect of CN⁻ and 1,10-phenanthroline is attributed to π bonding: therefore, low spin, large Δ, max. occupancy of the t^2_g orbitals.

The splitting (10Dq) increases as the charge on the metal ion increases, because the cation radius decreases with increasing charge and the ligands would be more strongly attracted by the higher charge. The splitting, for the same ligands, increases and the PE decreases for the second and third transition series compared with the first transition series.

Why? 4d and 5d orbitals are larger than 3d orbitals, extend farther from the central atom, and are affected to a greater extent by the ligands.

Because $4d$ and $5d$ orbitals are larger than $3d$ orbitals, it is less energetically unfavorable to pair two e⁻'s in the same orbital; PE's are smaller. PE's for the same number of d e⁻'s also increase with increasing oxidation number, be-cause of increased e⁻ repulsion resulting from the contraction of d orbitals with increasing positive charge.

Δ, kJ/mol	Complex
274	$[Co(NH_3)_6]^{3+}$
408	$[Rh(NH_3)_6]^{3+}$
490	$[Ir(NH_3)_6]^{3+}$

Distorted Octahedral Complexes

Tetragonal distortion from octahedral geometry involves the lengthening or shortening of two trans M-L bonds. The major rotational axis corresponds to the direction of distortion, defined as the z axis. This type of distortion was pre-dicted on theoretical grounds by Jahn and Teller. The **Jahn-Teller Theorem** *predicts that distortion will occur whenever the resulting splitting of energy levels yields additional stabilization.*

If an octahedron is elongated along the z axis by stretching the metal-ligand distances along this axis, the degeneracy of the t_{2g} and e_g orbitals is lowered. Because the ligand field decreases rapidly as the distance is increased, the ligand field is lowered along z and for the e_g orbitals, d_{z^2} is lowered in energy, while the $d_{x^2-y^2}$ orbital is raised in energy. Withdrawing the ligands along the z axis decreases the ligand-ligand repulsion and tends to shorten the metal-ligand distances along the x and y axes, thereby, increasing their interaction with the metal.
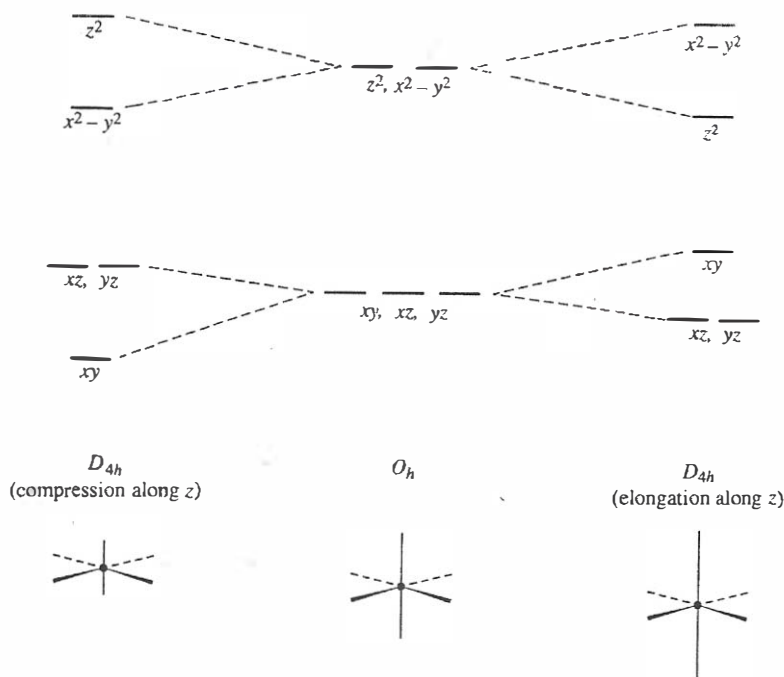
What about the t_{2g} orbitals? Please explain.

The best-known cases of Jahn-Teller distortion involve hexacoordinate d^9 (particularly, Cu^{II}) complexes. They are generally tetragonal (D_{4h} with four short M-X distances in a plan and two long M-X distances perpendicular to the plane) as expected from the Jahn-Teller effect.

If we can remember the definition of the Jahn-Teller Theorem then what does it predict for octahedral d^1, d^2, and d^3 complexes?

Square Planar Geometry

Extreme tetragonal elongation of an octahedron ultimately leads to the complete removal of two opposite ligands, giving a square planar complex. The most favorable electron configuration for planar complexes is d^8-for example, Ni^{2+}, Pt^{2+}, and Au^{3+}-in which splitting can be great enough to bring about pairing of all electrons.

Figure 16.7
Comparison of the relative d orbital energies for octahedral, Jahn-Teller distorted (elongated), and square planar complexes.
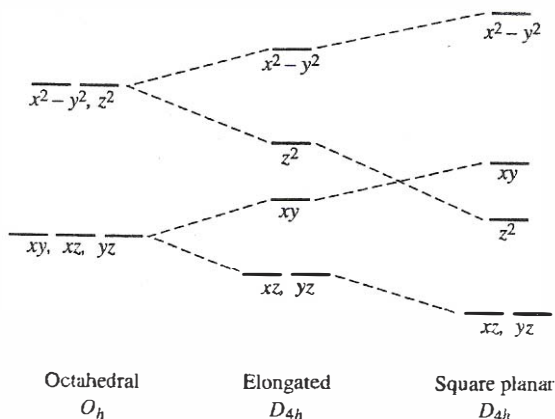
Four of the five orbitals are relatively stable; the fifth (d_{x2-y2}) lies very high in energy (note its torus), and its occupancy is strongly destabilizing. Only those d^8 complexes with sufficient crystal field splitting to be low spin exhibit square planar geometry. For example, CN^- creates a larger Dq unit than does fluoride (2X). Hence, the equilibrium favors the reactants when L = CN, but the product when L = F.

$$NiL_4{}^{2-} + 2L^- \rightleftharpoons NiL_6{}^{4-}$$

Tetrahedral Complexes

A tetrahedral arrangement is the structure of least ligand-ligand repulsion for a four-coordinated metal ion. The ligand field splitting is smaller in tetrahedral complexes because there are only four ligands and they do not approach along the direction of any of the d orbitals. The Δ for T_d geometry is 4/9's that of an O_h geometry. Because of the small splitting, Δ is almost always less than the pairing energy; ie., nearly all T_d complexes are high spin.

Figure 16.8
Comparison of the crystal field theory diagrams for cubic, octahedral, and tetrahedral geometries;
$\Delta_t = \frac{1}{2}\Delta_c = \frac{4}{9}\Delta_o$
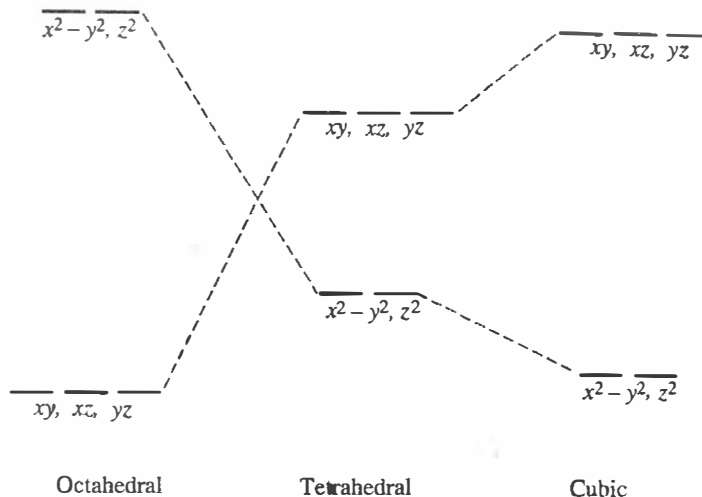
Molecular Orbital Theory

I STRONGLY advise you all to review this either per your Chem 318 notes or by other means.

We follow the same approach for a molecular-orbital (MO) description of a metal complex, ML_n, that we used for other molecules, AX_n. Even though metal complexes are not special cases, they often exhibit features that justify separate discussion. In transition metal complexes, the participation of the $(n-1)d$ orbitals is particularly important.

Consider σ bonding in an octahedral complex, ML_6^{n+}. M is a transition metal ion, such as Cr^{3+}, and L is a Lewis base, such as $:NH_3$. In the complex each $:NH_3$ molecule has a filled orbital directed toward the metal ion.

Shown below is the MO diagram for an octahedral complex.
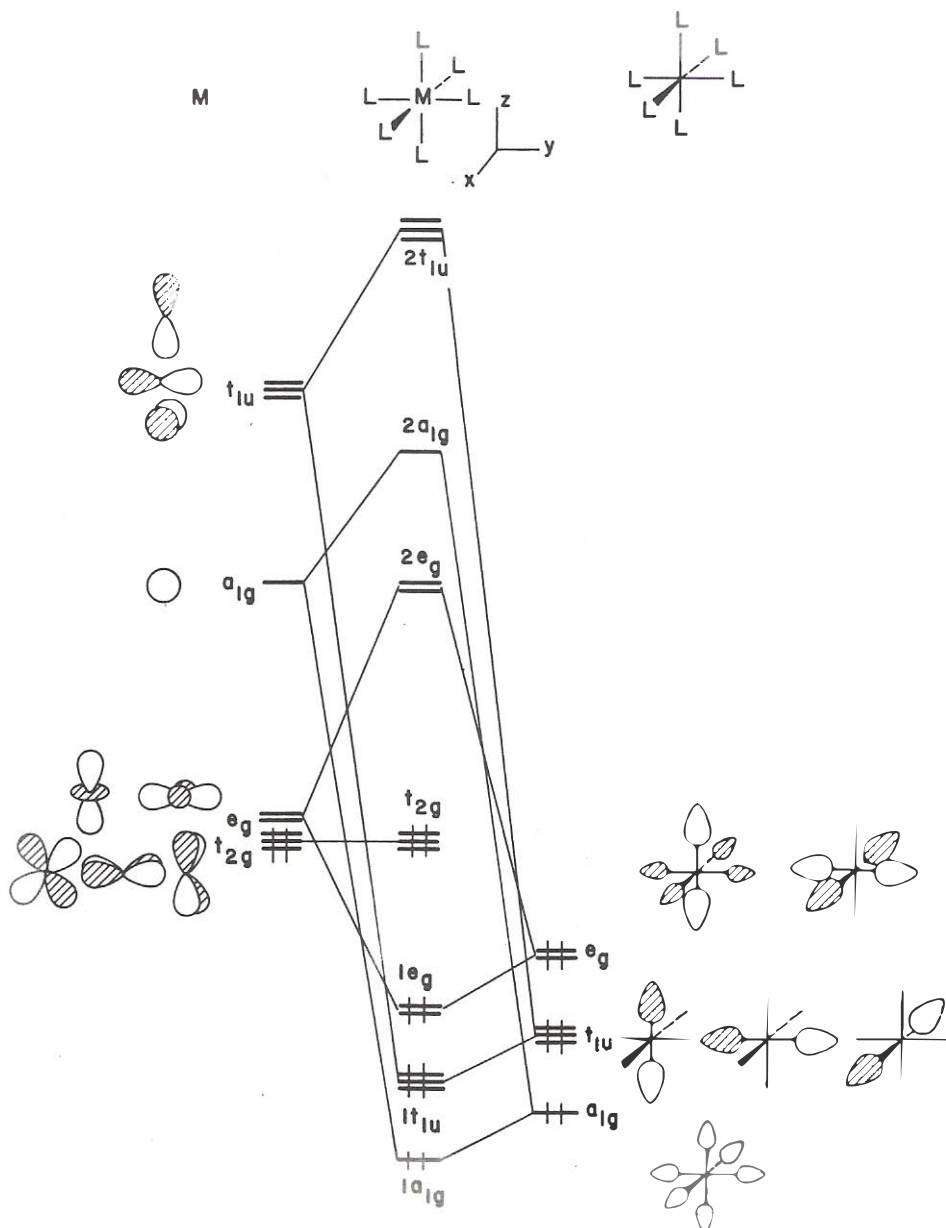
Now, what does this mean? Let us examine further.

There are six lone pairs directed toward the metal in an octahedral arrange-
ment. On the left side of the interaction diagram are the nine atomic orbitals
(AO's) of M. On the right side of the diagram are drawn the ligand group
orbitals (LGO's) of the ligand σ orbitals. With this information, we should be
able to obtain the following representations:

a_{1g}
Metal
s orbital

a_{1g}
LGO

a_{1g}
MO

p_x

p_y
t_{1u} MO's

p_z

d_{z^2}

e_g MO's
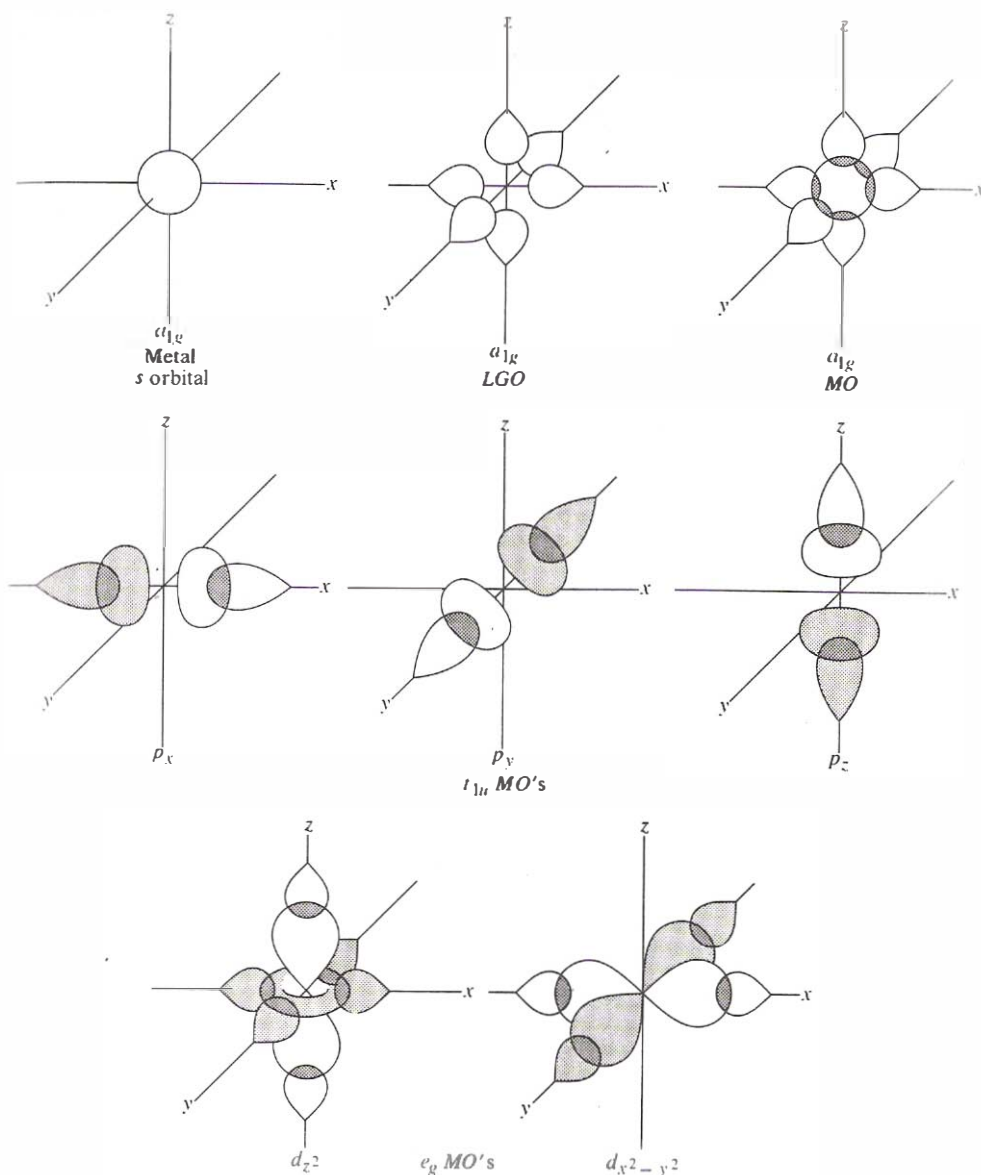
$d_{x^2-y^2}$

Construct the MO diagram for $[Cr(NH_3)_6]^{3+}$.

The major conclusions to be drawn are the following:

1. The σ overlap involves one s-, three p-, and two d-type metal orbitals, and
in that sense is consistent with sp^3d^2 hybridization. The d_{x2-y2} and d_{z2} orbitals
overlap with σ-type MO's of e_g symmetry.

2. There are three unpaired e⁻'s, located in degenerate, nonbonding metal orbitals having t_{2g} symmetry.

3. A total of 18 e⁻'s would be needed to completely fill all the bonding and nonbonding orbitals. However, since the t_{2g} level is nonbonding, the maximum possible number of bonding e⁻'s is 12.

4. The MO diagram shows that an octahedral compound is likely to be stable when t_{2g} is either completely filled or empty.

The former case is more likely for transition metals and one can think of the six e⁻'s in t_{2g} as three sets of lone pairs which are localized on the metal. Together with the 12 e⁻'s from the M-L bonding levels creates a situation where 18 valence e⁻'s are associated with the metal.

Function of the Ligand σ Donor Strength

We are interested in the HOMO, t_{2g}, and the LUMO, $2e_g$. The energy gap between these MO's is a function of the ligand σ donor strength (in the absence of π effects).
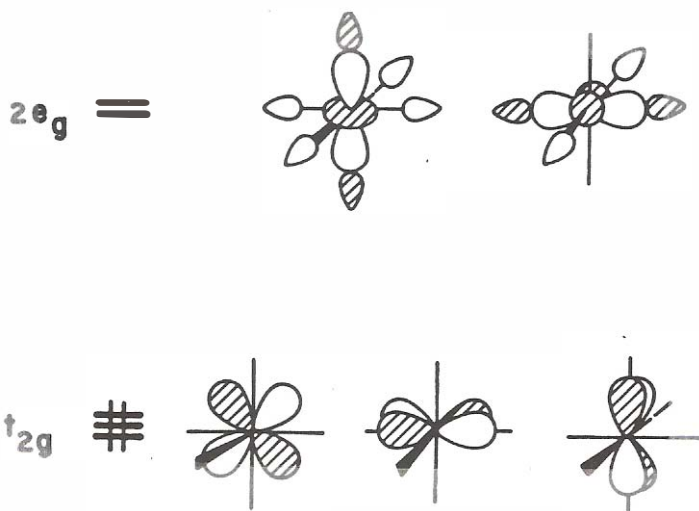
Raising the energy of the ligand lone pairs causes the energy gap between the e_g and the metal d set to diminish. Consequently there is a stronger interaction; the antibonding $2e_g$ set is destabilized sot the t_{2g} - e_g energy gap increases.

Overlap between the ligand lone pairs and metal e_g can also play an obvious role. A strong σ donor set of ligands creates a sizeable energy gap between the molecular t_{2g} and $2e_g$ levels; singlet ground state (all six e⁻'s in the t_{2g} level for an 18-e⁻ complex), low spin complex. Observed for many organometallic compounds.

low spin	intermediate spin	high spin
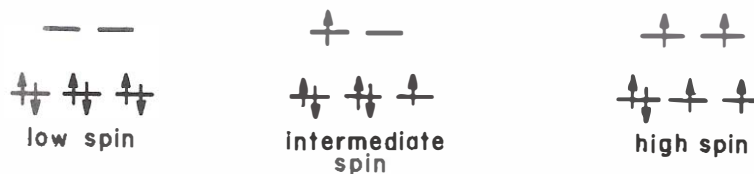
Classical coordination complexes, where L = NH_3, H_2O, halogen, and so on, sometimes behave differently; splitting is not so large because L is highly electronegative. Therefore, the ground state may be one that contains some spins unpaired-an intermediate spin system, or a maximum of unpaired spins-a high spin system. The splitting is in delicate balance with the spin pairing energies, consequently, the high-spin-low-spin energy difference is often very tiny.

What would happen if we would try to add more than 18 e⁻'s into the MO's of an ML_6 complex? Analysis anyone?

Square Planar Complexes

Substitution

In square planar complexes, the four ligands lie in the xy plane, and the metal p_z and d_{z2} orbitals are σ bonding; susceptible to attack by Lewis bases along the z axis.

Let us consider substitution of one ligand for another on *trans*-Pt(t)(L)$_2$X, whereX is the leaving group, T is the ligand *trans* to the leaving group and the L's are ligands *cis* to the leaving group.

$$Pt(T)L_2X + Y \longrightarrow Pt(T)L_2Y + X$$

retention of configuration
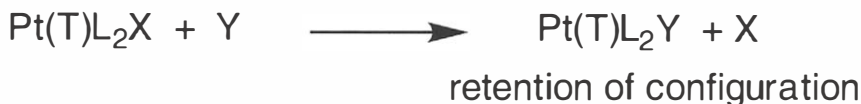
Studies of the kinetics of the rxn show a dependence on the concentration of the entering ligand

$$Pt(NO_2)(Py)_2Cl + Py \longrightarrow Pt(NO_2)(Py)_3 + Cl^-$$

[Py](M)	$k_{obs}(\times 10^3 s^{-1})$
0.02	0.703
0.05	0.832
0.10	1.35
0.20	1.86
0.30	2.20
0.40	2.96
0.50	3.60
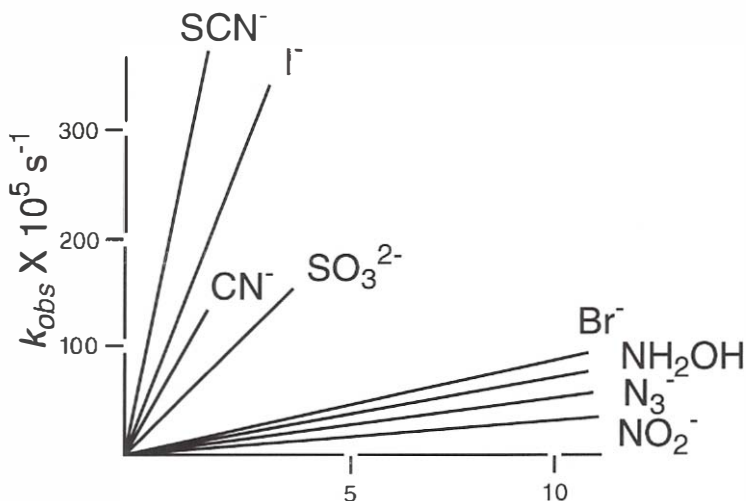
Under pseudo first order conditions, plots of ln [metal complex] vs. time are linear with a slope of k_{obs}. Varying the initial concentration of the ligand gives plots such as that shown above; k_1 is the intercept and k_2 is the slope. Thus the rate law for the rxn

$$trans\text{-}Pt(T)L_2X + Y \longrightarrow trans\text{-}Pt(T)L_2Y + X$$

has a ligand-independent and a ligand-dependent term.

$$\text{Rate} = k_1[trans\text{-}Pt(T)L_2X] + k_2[trans\text{-}Pt(T)L_2X][Y]$$

This tells us that there are two competing processes.

Square Planar Complexes

The ligand-independent pathway could have several possible explanations; the one that is generally accepted involves attack of the solvent on the square planar complex; solvent becomes the entering Nu: in the rate-determining step.

$$Pt(NO_2)(Py)_2Cl \xrightarrow{+S} Pt(NO_2)(Py)_2ClS \xrightarrow{-Cl^-} Pt(NO_2)(Py)_2S$$

$$Pt(NO_2)(Py)_2S \xrightarrow{+Py} Pt(NO_2)(Py)_3S \xrightarrow{-S} Pt(NO_2)(Py)_3$$

and/or

$$Pt(NO_2)(Py)_2Cl \xrightarrow{+Py} Pt(NO_2)(Py)_3Cl \xrightarrow{-Cl^-} Pt(NO_2)(Py)_3$$
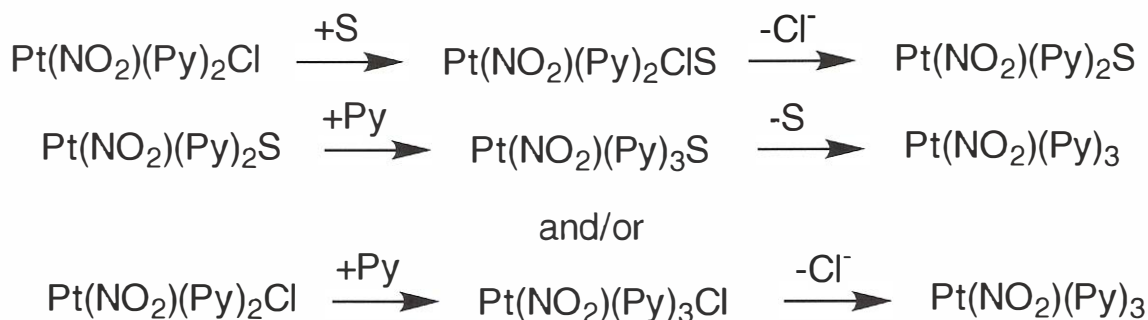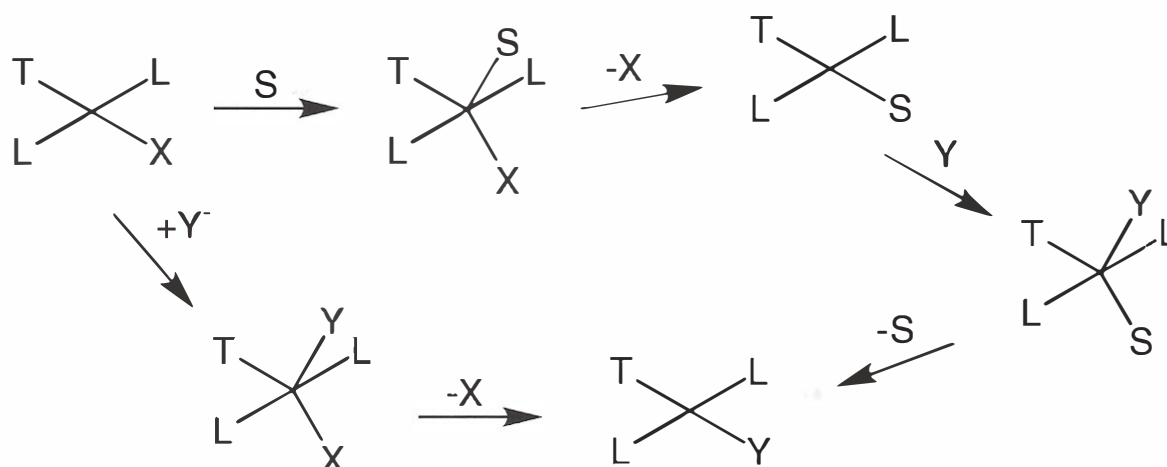
Nonzero values for both k_1 and k_2 indicate the reactions of this type follow two different pathways as shown above (competition).

The similarity of the two pathways is a strong feature in support of this mechanism, especially since the solvents often used, H_2O, CH_3OH, etc., have e$^-$ pairs and can be nucleophiles. The large excess in solvent conc. makes up for the generally lower nucleophilicity of the solvent. That the first order step is not dissociation of a ligand but is dependent on the nature of the solvent is shown by the solvent dependence of k_1 for many rxns. This strong dependence of k_1 on the nature of the solvent is consistent with direct nucleophilic attack by the solvent on the square planar complex.

A good example is the chloride ion exchange of the isotopically labelled complex $trans$-Pt(py)$_2$Cl*$_2$.

solvent	k_1, s^{-1}	k_2, L/mol·s
DMSO	3.8×10^{-4}	
H$_2$O	3.5×10^{-5}	
CH$_3$NO$_2$	3.2×10^{-5}	
EtOH	1.4×10^{-5}	
CCl$_4$		10^4
C$_6$H$_6$		10^2
(CH$_3$)$_2$C=O		10^{-2}

The Trans Effect

Substitutions in square planar complexes are influenced to a remarkable extent by a moiety that might appear to be uninvolved in the process-the ligand trans to the eventual leaving group. The *trans effect* is defined as "the effect of a coordinated group upon the rate of substitution reactions of ligands opposite to it." The experimental evidence for the trans effect is dramatic.

Effect of Solvent on the Rate Constant for the First Order Step

$$trans\text{-Pt(PEt}_3)_2(L)Cl^- + Py \longrightarrow trans\text{-Pt(PEt}_3)_2L(Py) + Cl^-$$

solvent	$k_1 (X10^4 s^{-1})$
dichloromethane	0.06
methanol	0.7
nitromethane	8.0
acetone	3100

Also, consider the following rxn:

$$[Pt(NH_3)Cl_3]^- + NH_3 \longrightarrow Pt(NH_3)_2Cl_2 + Cl^-$$

Two geometric isomers are possible for the product. In the absence of other factors, a statistical distribution of 2/3 *cis* and 1/3 *trans* is expected; however, the product mixture comprises more than 99% of the *cis* isomer.

The following *trans*-effect order has been developed:

CO, CN$^-$, C$_2$H$_4$ > PR$_3$, H$^-$ > CH$_3^-$ > C$_6$H$_5^-$, NO$_2^-$, I$^-$, SCN$^-$ > Br$^-$, Cl$^-$

> Py, NH$_3$, OH$^-$, H$_2$O
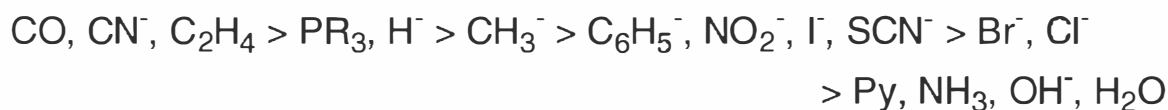
This order spans a factor of 10^6 in rate and holds for all square planar Pt complexes thus far examined.

Before discussing the origin of the *trans* effect, we must distinguish between the *trans* effect and the **trans influence** of a ligand. The *trans* effect concerns the effect of the ligand on the rate of substitution of the ligand that is *trans*. The *trans* influence is the effect of the *trans* ligand on ground state properties such as bond lengths and infrared stretching frequencies.

The difference is similar to the difference between kinetics and thermodynamics; thermodynamics concerns ground state measurements while kinetics concerns the difference in energy between the ground state and the transition state.

Similarly, the *trans* influence provides info. on the ground state influence of a *trans* ligand while the *trans* effect involves the effect of the *trans* ligand on both the ground state and the transition state.

A number of explanations have been offered for the *trans* effect. The best explanation considers both the sigma-donating and pi-acceptance capabilities of the ligand.

Two trans ligands must bond with the same metal *p*-orbital. If one of the bases is a significantly better σ donor than the opposite ligands, then the strength of the interaction of the latter with the metal will be reduced.
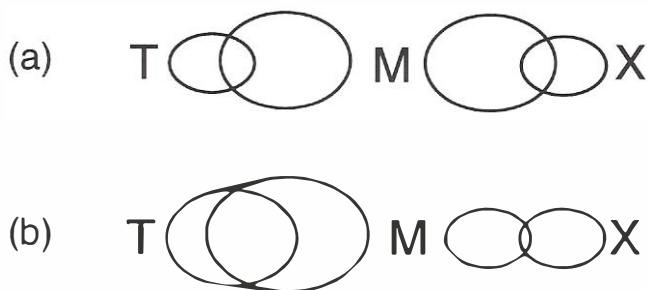
Weak (a) and a strong (b) sigma-donor ligand.

As primarily a ground state effect, the *trans* effect arising from sigma donation should parallel the order of *trans* influence.

$$H^- > PR_3 > SCN^- > I^-, CH_3^-, CO, CN^- > Br^- > Cl^- > NH_3 > OH^-$$

This order is similar to the general order of *trans*-effect ligands with some very notable exceptions (CO and CN⁻ are badly out of order). Discrepancies between the *trans*-effect order and the *trans*-influence order may be attributed to transition state effects.

Ligands that have a substantially larger *trans* effect than would be predicted from their *trans* influence are ligands with pi-bonding capabilities; stabilization of the transition state by pi-accepting ligands. Such ligands remove electron density from the metal and stabilize the transition state; the trans bond is weakened and more easily cleaved.

$$C_2H_4, CO > CN^- > NO_2^- > SCN^- > I^- > Br^- > Cl^- > NH_3 > OH^-$$
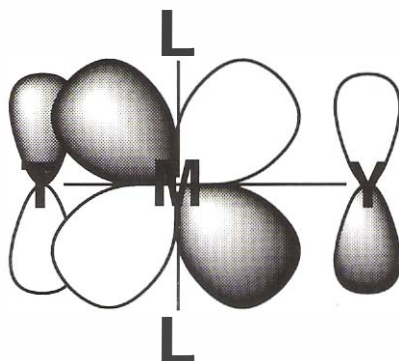
Supporting evidence for this is found in bond distances. Pt-Cl bonds tend to be longer (weaker) when trans to a π acceptor ligand such as PR_3 or C_2H_4.

Complex	Trans Ligand	d(Pt-Cl), pm
$PtCl_4^{2-}$	Cl^-	233
$[Pt(NH_3)Cl_3]^-$	NH_3	232
	Cl^-	235
$[Pt(H)Cl_3]^{2-}$	H^-	232
	Cl^-	230
cis-$Pt(PMe_3)_2Cl_2$	PMe_3	238
$Pt(C_2H_4)Cl_3$	C_2H_4	234
	Cl^-	230

Other Effects on the Rate

cis Effect

The electronic effect of the *cis* ligands is relatively small.

$$cis\text{-}Pt(PEt_3)_2LCl + Py \longrightarrow cis\text{-}Pt(PEt_3)_2LPy + Cl^-$$
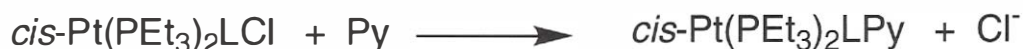
L	$k \times 10^2\ (s^{-1})$
Cl^-	1.7
$C_6H_5^-$	3.8
CH_3^-	6.0

Compare to the effect of the *trans* ligand on rate in substitutions on *trans*-Pt(PEt)$_3$)$_2$L(Cl),

L	k (s^{-1})
PEt$_3$	1.7 X 10^{-2}
CH$_3^-$	1.7 X 10^{-4}
Cl$^-$	1.0 X 10^{-6}

In general the *cis* effect is small and its order is variable unless steric factors are involved. Steric effects provide one of the best means of differentiating a dissociative mechanism from an associative one.

Associative mechanism: the initial step involves the introduction of a new species into the first coordination sphere-the formation of an extra bond to the metal. This is followed by bond rupture and the movement of a (former) ligand away from the metal, returning the first sphere to its original population.

Dissociative mechanism: the initial step is bond cleavage and the creation of a vacancy in the first sphere; a species from the second sphere then fills that vacancy.

For a dissociative rxn there is usually an increase in rxn rate with increasing steric interactions, a steric acceleration. For an associative rxn that involves an increased coordination number, increasing steric size decreases the rate of reaction.

Steric Effects on the Rates of Square Planar Substitutions Rxns (25°C).

Complex	k$_{obs}$ (s^{-1})
cis-Pt(PEt)$_3$)$_2$LCl	
L = phenyl	8.0 X 10^{-2}
L = *o*-tolyl	2.0 X 10^{-4}
L = mesityl	1.0 X 10^{-6}
trans-Pt(PEt)$_3$)$_2$LCl	
L = phenyl	1.2 X 10^{-4}
L = *o*-tolyl	1.7 X 10^{-5}
L = mesityl	3.4 X 10^{-6}

Leaving-Group Effects

To investigate the effect of the leaving group on the rate of substitution one must keep the *cis* and *trans* groups constant.

Pt(dien)X$^+$ complexes

In dissociative reactions a large dependence on the nature of the leaving group can be expected since the bond from the metal to the leaving group is broken in the transition state. For associative rxns the effect of the leaving group depends on the extent of bond breaking in the transition state.

The Effect of the Leaving Group X on Rate of Substitution of Pt(dien)X$^+$ with Py.

$$Pt(dien)X^+ + Py \longrightarrow Pt(dien)Py^{2+} + X^-$$

$\underline{X}$	$\underline{k_{obs}\ (s^{-1})}$
NO_3^-	very fast
H_2O	1900
Cl^-	35
Br^-	23
I^-	10
N_3^-	0.8
SCN^-	0.3
NO_2^-	0.05
CN^-	0.02

The order of leaving-group dependence is almost the inverse of the *trans*-effect order. This reflects the fact that the *trans* effect depends on the strength of bonding and the more strongly bound ligands dissociate more slowly from the five-coordinate intermediate.

Effect of the Entering Nucleophile

There is a dependence on the nucleophilicity of the entering ligand. We can explain this by looking at the polarizability or softness of the ligand; soft nucleophiles prefer soft substrates and hard ligands prefer hard substrates. The observation that larger donors are effective nucleophiles towards Pt(II) indicates that Pt(II) is a soft center.

In describing the nature of a nucleophile one correlates the reactivity with other properties of the ligand; linear free-energy relationship (LFER).

$$trans\text{-}PtL_2Cl_2 + Y \longrightarrow trans\text{-}PtL_2ClY + Cl^-$$

The Effect of the Entering Nucleophile on Reaction at $trans\text{-}PtL_2Cl_2$.

Y	$L = Py$	$L = PEt_3$
Cl^-	0.45	0.029
NH_3	0.47	-
NO_2^-	0.68	0.027
N_3^-	1.55	0.2
Br^-	3.7	0.93
I^-	107	236
SCN^-	180	371
PPh_3	249,000	-

Note the similarity of the order of ligand nucleophilicities to the *trans*-ligand effect. How do we explain this?

Solvent Effects

Solvent effects are important in substitution rxns on square planar complexes. Depending on the relative nucleophilicities of the solvent and of the entering ligand, the observed rate law may be dependent on or independent of the ligand.

$$trans\text{-}Pt(Py)_2Cl_2 + {}^{36}Cl^- \longrightarrow trans\text{-}Pt(Py)_2Cl({}^{36}Cl) + Cl^-$$

Effect of Solvent on the Chloride Exchange Reaction

solvent	$k\,(10^{-5}s^{-1})$
DMSO	380
H_2O	3.5
EtOH	1.4
PrOH	0.4

solvent	$k\,(M^{-1}s^{-1})$
CCl_4	10^4
C_6H_6	10^2
$t\text{-}BuOH$	10^{-1}
$Me_2C(O)$	10^{-2}
DMF	10^{-3}

Activation Parameters

A few examples are shown on the following page. Negative values for both entropy and volume of activation are significant. These values imply an associative mechanism. The first-order path and the second-order path have very similar activation parameters which suggests the mechanistic similarity in both paths.

Dissociative Properties

Dissociative processes are possible for square-planar, 16 e⁻, organometallic complexes. (see IC 1991, 30, 4007).

$$\text{cis-Pt(R)}_2\text{S}_2 + 2\text{S'} \longrightarrow \text{cis-Pt(R)}_2\text{S'}_2 + 2\text{S}$$

Instead of the more typical associative process the primary evidence cited for S dissociation has been:

1. positive values for the volume of activiation;

2. independence of the rate on the nature of the entering group;

3. saturation kinetics;

4. identical rates for substitution and solvent exchange, and;

5. positive values for the entropy of activation.

Dissociative reactions for SP OC may be more important than for SP coordination complexes because a strong donor ligand is important to facilitate dissociation. The characteristics of diss. processes are quite different from ass. rxns.

Lack of dependence on the nature of the incoming ligand is shown in the replacement of DMSO from $\text{cisPt(Ph)}_2\text{(DMSO)}_2$.

$$\text{cis-Pt(DMSO)}_2\text{(Ph)}_2 + \text{L-L} \longrightarrow \text{cis-Pt(L-L)(Ph)}_2 + 2\text{DMSO}$$
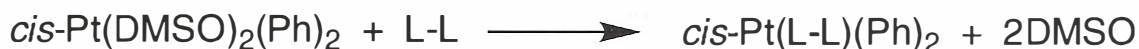
L-L = dppe or o-phen   k = 2.0 s⁻¹ for both dppe and o-phen

ACTIVATION PARAMETERS FOR SQUARE-PLANAR SUBSTITUTION REACTIONS

Reaction	Solvent	k_1			k_2			Reference
		$\Delta H^{\ddagger}$	$\Delta S^{\ddagger}$	$\Delta V^{\ddagger}$	$\Delta H^{\ddagger}$	$\Delta S^{\ddagger}$	$\Delta V^{\ddagger}$	
trans-Pt(Py)$_2$Cl(NO$_2$) + Py	CH$_3$OH	—	—	—	12	-24	-9	6
cis-Pt(Py)$_2$Cl(NO$_2$) + Py	CH$_3$OH	—	—	—	12	-32	-6	6
trans-Pt(PEt$_3$)$_2$Cl$_2$ + Py	CH$_3$OH	—	—	—	14	-25	-14	6
trans-Pt(PEt$_3$)$_2$Cl$_2$ + N$_3^-$	CH$_3$OH	—	—	—	15	-24	—	27
trans-Pt(PEt$_3$)$_2$Br$_2$ + N$_3^-$	CH$_3$OH	—	—	—	13	-24	—	27
trans-Pt(PEt$_3$)$_2$I$_2$ + N$_3^-$	CH$_3$OH	—	—	—	12	-16	—	27
trans-Pt(PEt$_3$)$_2$(2,4,6-Me$_3$C$_6$H$_2$)Br + SC(NH$_2$)$_2$	CH$_3$OH	17	-20	-11	11	-33	-13	28
cis-Pt(PEt$_3$)$_2$(2,4,6-Me$_3$C$_6$H$_2$)Br + I$^-$	CH$_3$OH	20	-14	-16	15	-29	-15	28
cis-Pt(PEt$_3$)$_2$(2,4,6-Me$_3$C$_6$H$_2$)Br + SC(NH$_2$)$_2$	CH$_3$OH	19	-17	-17	14	-29	-13	28
Pt(dien)Cl$^+$ + SCN$^-$	H$_2$O	20	-18	—	10	-25	—	27
Pt(dien)Br$^+$ + SCN$^-$	H$_2$O	19	-17	—	9	-27	—	27
Pt(dien)I$^+$ + SCN$^-$	H$_2$O	—	—	—	10	-25	—	27
Pt(dien)N$_3^+$ + SCN$^-$	H$_2$O	—	—	—	14	-22	—	27
Au(dien)Cl^{+2} + Br$^-$	CH$_3$OH	—	—	—	13	-4	—	27

Other Metal Centers

While most studies of SP substitution rxns have been of Pt(II) complexes a few studies have been accomplished on Pd(II), Ni(II), Au(III), Rh(I) and Ir(I).

$$M(^{13}CN)_4{}^{-n} + {}^{13}CN \longrightarrow \text{exchange measured by line-broadening}$$

As an entering ligand, CN^- is so strong that the rate law showed no k_1 term.

$$\text{rate} = k_2[M(CN)_4{}^{-n}][CN^-]$$

. RATE CONSTANTS AND ACTIVATION PARAMETERS FOR CN^- EXCHANGE WITH $M(CN)_4{}^{-n}$ AT 24°C[29]

Complex	$k_2(M^{-1}s^{-1})$	$\Delta H^{\ddagger}$ (kcal/mole)	$\Delta S^{\ddagger}$ (eu)
$Ni(CN)_4^{2-}$	$>5 \times 10^5$	—	—
$Pd(CN)_4^{2-}$	120	4	−45
$Pt(CN)_4^{2-}$	26	6	−37
$Au(CN)_4^-$	3900	7	−24

The order of reactivity is (Ni(II) > Au(III) > Pd(II) > Pt(II).

Pd(II) Complexes

Analogous Pd(II) complexes react approx. 10^5 times more rapidly than do Pt(II) complexes. The greater reactivity of the Pd(II) complexes has previously been ascribed to a weaker Pd-X bond. A higher effective nuclear charge leads to stronger metal ligand bonds (for ligands that do not accept electron density from the metal) as one proceeds from first row to second row to third row TMs. The mechanism appears to be of the same type with both a ligand attack and a solvent attack term, although the solvent attack term appears to be more important for Pd(II) complexes that it is for Pt(II).

Complex	k_{obs}, M = Pd(II)	k_{obs}, M = Pt(II)	Reference
M(dien)Cl+	fast	3.5×10^{-5}	20
M(dien)I+	3.2×10^{-2}	1.0×10^{-5}	20
M(dien)SCN+	4.3×10^{-2}	3.0×10^{-7}	20
M(dien)NO$_2^+$	3.3×10^{-2}	2.5×10^{-7}	20
trans-M(PEt$_3$)$_2$(o-tolyl)Cl	5.8×10^{-1}	6.7×10^{-6}	7

RATE CONSTANTS FOR THE REACTION
OF THE TETRAHALIDES OF Pt AND Pd WITH
ACETYLACETONATE[30]

Complex	$k_1(s^{-1})$	$k_2(M^{-1}s^{-1})$	$T(°C)$
PdCl$_4^{2-}$	71	2.2	25
PtCl$_4^{2-}$	1.2×10^{-2}	1.2×10^{-3}	55
PdBr$_4^{2-}$	210	1.9	25
PtBr$_4^{2-}$	3.0×10^{-1}	1.1×10^{-3}	55

Substitution of Pd(acac)$_2$ shows the similarity of entering group effects for Pd(II) and Pt(II).

$$Pd(acac)_2 + 4X^- + 2H^+ \longrightarrow PdX_4^{2-} + 2H(acac)$$
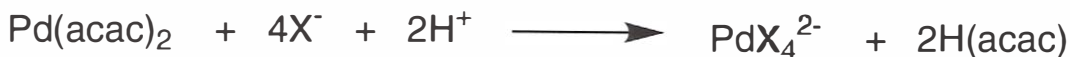
ENTERING GROUP EFFECTS
ON THE RATE OF SUBSTITUTION OF
Pd(acac)$_2$[30]

X	$k(\times 10^2 s^{-1})$
OH$^-$	3.2
Cl$^-$	8.9
Br$^-$	32
I$^-$	fast
SCN$^-$	very fast

Square-planar complexes of Pd show the same characteristics as Pt complexes in their substitution rxns: associate reactions, either attack by solvent or by incoming nucleophile; the *trans* ligand, the leaving group, the entering nucleophile, and the solvent all affect the rate of substitution. The difference is that Pd complexes undergo substitution 10^5 times more rapidly than do Pt complexes.

Ni(II) Complexes

Many Ni(II) complexes ar octahedral. Those that are square planar react very rapidly - $Ni(CN)_4^{2-}$ exchanges CN^- in seconds.

trans-Ni(PEt$_3$)$_2$(*o*-tolyl)Cl   +   Py

$$\longrightarrow \quad \textit{trans-}Ni(PEt_3)_2(\textit{o-}tolyl)Py \quad + \quad Cl^-$$
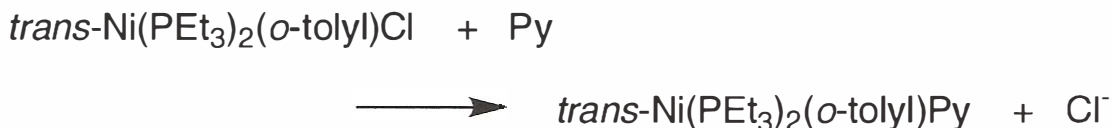
rate = $k_1[Ni(II)] + k_2[Ni(II)][Py]$

The relative rates for the Ni(II), Pd(II) and Pt(II) complexes are 5×10^6, 1×10^5, and 1, respectively.

Au(II) Complexes

Although Au(III) is isoelectronic with Pt(II), studies of Au(III) are much less common. Why?

COMPARISON OF THE RATES
OF SUBSTITUTION REACTIONS OF Au(III)
AND Pt(II) COMPLEXES[32]

Reaction	$k_1(s^{-1})$	$k_2(M^{-1}s^{-1})$
$AuCl_4^- + {}^*Cl^-$	0.006	1.47
$PtCl_4^{2-} + {}^*Cl^-$	3.8×10^{-5}	0
$Au(dien)Cl^{2+} + Br^-$	<0.5	154
$Pt(dien)Cl^+ + Br^-$	8.0×10^{-5}	5.3×10^{-3}

The form of the rate law is the same as for other SP complexes, although the solvent attack term is less important.
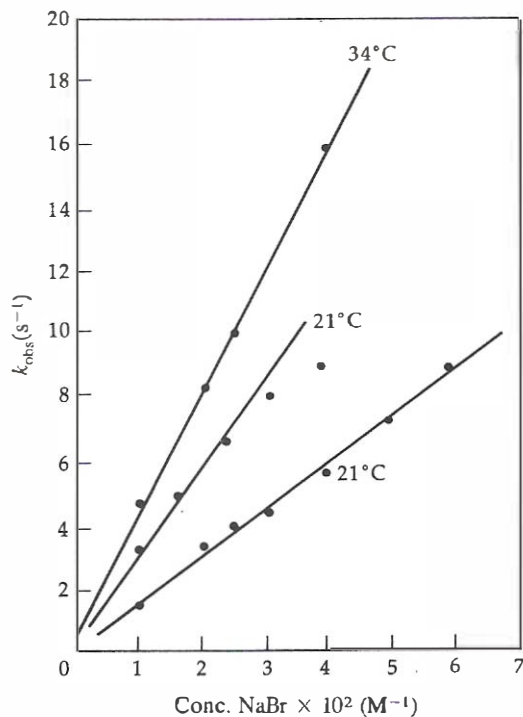
Dependence of k_{obs} on bromide ion concentration for the reaction of $[Au(dien)Cl]^{2+}$ with this reagent. [Reprinted with permission from W. H. Baddley and F. Basolo, *Inorg. Chem.* **3**, 1087 (1964). Copyright 1964 American Chemical Society.]

Summary

Substitution reactions of square planar complexes proceed by nucleophilic attack of an incoming ligand on the square planar complex. The two-term rate law observed includes a term that is dependent on the incoming nucleophile and a term that is independent of the incoming nucleophile; attack on the complex by the entering ligand and the solvent, respectively.

The rate of rxn shows a dependence on the ligand *trans* to the substitution site, on the leaving group, and on the entering nucleophile. The importance of these effects depends on the amount of bond formation or bond breaking in the transition state.

One can consider the rxn as a double-humped potential curve as shown below.

If the first maximum is the TS, then bond formation is more important (a very sharp dependence on the entering nucleophile). If the second maximum is the TS, then bond breaking is more important (leaving-group effects would be very large).

Reactivity of Coordination Compounds

Substitution Reactions of Octahedral Werner-Type Complexes

Kinetics

Not as comprehensively defined as for substitutions on square planar complexes.

Under pseudo first order conditions, the rate is dependent on the concentration of the entering ligand at low ligand concentration and is independent of the concentration of L at high concentration of L. In summary we get the following:

Dissociative First

$$\text{rate} = \frac{k_1 k_2 [M(H_2O)_6][L]}{k_{-1}[H_2O] + k_2[L]}$$

$$M(H_2O)_6 \underset{k_{-1}}{\overset{k_1}{\rightleftharpoons}} M(H_2O)_5 + H_2O$$

$$M(H_2O)_5 + L \xrightarrow{k_2} M(H_2O)_5L$$
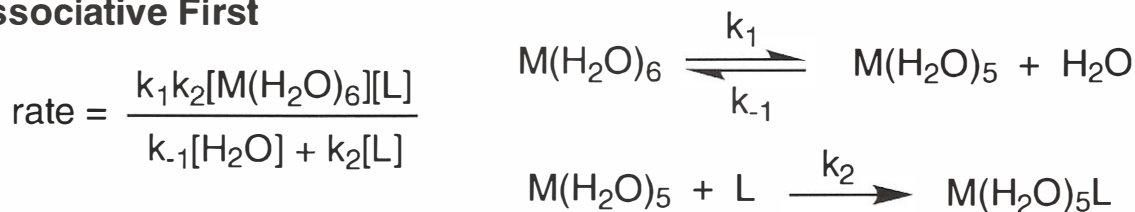
These equations represent a dissociative mechanism.

If $k_2[L] \gg k_{-1}[H_2O]$, this simplifies to

$$\text{rate} = k_1[M(H_2O)_6]$$

indicating a first-order concentration dependence only. If $k_{-1}[H_2O] \sim k_2[L]$, however, then the rate is influenced by both $[M(H_2O)_6]$ and $[L]$.

Associative Second

At the limit of an associative process the TS is actually an intermediate, since it has sufficiently long lifetime to be detected experimentally.

$$M(H_2O)_6 + L \underset{k_{-1}}{\overset{k_1}{\rightleftharpoons}} M(H_2O)_6L$$

$$M(H_2O)_6L \xrightarrow{k_2} M(H_2O)_5L + H_2O$$
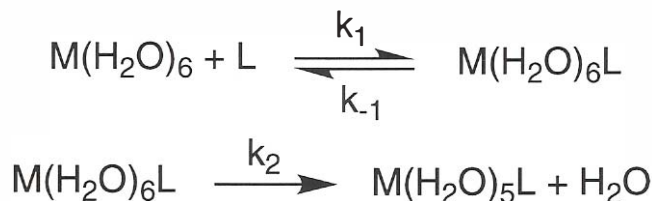
Said in another way, in the above two-step sequence the second step is relatively slow ($k_2 \ll k_1$), so the following expression applies:

$$\text{rate} = k_2[M(H_2O)_6L]$$

However,...

the change in concentration of an intermediate such as $M(H_2O)_6L$ is not usually measurable in kinetic experiments; use *steady-state approximation*, to give as a rate law

$$\text{rate} = \frac{k_1 k_2 [M(H_2O)_6][L]}{k_{-1} + k_2}$$

Thus, an associative process exhibits a rate-dependence on both reactants.

Unfortunately, these two descriptions represent the two extremes of a continuum. Most reactions proceed by processes intermediate between these; that is, the bond forming and bond breaking steps are not completely sequential. A sequence in which bond formation and bond rupture overlap in time is said to be of the *interchange* (I) type.

Interchange mechanisms are divided into I_a, where the transition state is X-ML$_n$···L, with the bond formation leading the bond rupture; and I_d, primarily dissociative activation, with the transition state X···ML$_n$-L and bond rupture leading bond formation.

Substantial evidence can be cited in favor of a dissociative mechanism over an associative mechanism in some rxns:

1. There is often little or no dependence on the entering ligand.
2. An increase in charge on the complex decreases the rate of substitution. An increase in charge would be expected to accelerate an associative rxn with increased attraction for the incoming ligand and more facile acceptance of the negative charge build-up on the metal. A dissociative rxn would be slowed by an increase in charge since the dissociating ligand would be held more tightly; eg. $Cr(en)(H_2O)_2Cl_2$ [2] is 3.1 X 10^{-5} s^{-1} and for $Cr(en)(H_2O)_3Cl^{+}$ [2] [3] is 3.0 X 10^{-7} s^{-1}. [2]
3. Steric crowding increases the rate of substitution rxns. For associative rxns an increase in the crowding around the metal inhibits approach of the incoming ligand and would decrease the rate of rxn. Steric crowding would be relieved by dissociation to yield a five-coordinate intermediate and thus lead to an increase in the rate of dissociation; eg. Cl$^-$ replacement on $Co(NH_3)_5Cl^{2+}$ occurs at a rate of 1.7 X 10^{-6} s^{-1} while Cl$^-$ removal from $Co(NMeH_2)_5Cl^{2+}$ occurs at a rate of 3.7 X 10^{-4}.
4. The rates of different leaving groups correlate with the bond strengths.

Leaving Group and Chelate Effects

As expected for a rxn that proceeds by a dissociative mechanism, the rate is dependent on the nature of the leaving group. A well known example that has been studied confirming this is the aquation of $Co(NH_3)_5X^{2+}$.

$$[Co(NH_3)_5X]^{2+} + H_2O \underset{}{\overset{k_f}{\rightleftharpoons}} [Co(NH_3)_5(H_2O)]^{3+} + X^-$$

X	$k_f (s^{-1})$
NO_3^-	2.7×10^{-5}
I^-	8.3×10^{-6}
Br^-	6.3×10^{-6}
H_2O	5.8×10^{-6}
Cl^-	1.7×10^{-6}
SO_4^{2-}	1.2×10^{-6}
$CH_3CO_2^-$	1.2×10^{-6}
NH_3	10^{-10}
NCS^-	5.0×10^{-10}
N_3^-	2.1×10^{-9}
NO_2^-	slow
OH^-	slow

The order of leaving-group effects ($NO_3^- > I^- ... OH^-$) represents the order of complex stability. Thus the leaving-group order represents the bond-strength order for the ligands.

FYI, the reverse rxn is called an *anation* rxn.

X	$k_r (s^{-1})$
Br^-	2.5×10^{-6}
NO_3^-	2.3×10^{-6}
Cl^-	2.1×10^{-6}
NCS^-	1.3×10^{-6}

Bidentate ligands are substituted more slowly than mondentate ligands, and complexes with chelate ligands are more stable than comparable complexes of mondentate ligands; the "chelate effect."

Kinetics for substitution of bidentate ligands are presented for comparison on the next page.

Complex	$k_1 (s^{-1})$
Ni(py)	38.5
Ni(bipy)	3.8×10^{-4}
Ni(NH₃)	5.8
Ni(en)	0.27

$$M\left(\begin{array}{c}L\\L\end{array}\right) \underset{k_{-1}}{\overset{k_1}{\rightleftharpoons}} M-L-L$$

$$M-L-L \underset{k_{-2}}{\overset{k_2}{\rightleftharpoons}} M + L-L$$
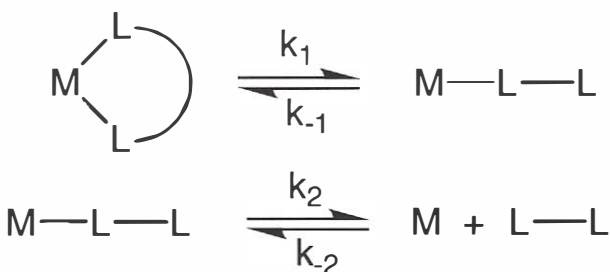
The simplest explanation for the chelate effect is that, after dissociation of one end, there is a very high effective concentration near the metal of that end since the chelate is still bound to the metal. Thus the k_{-1} step is much larger for a chelate than for a related monodentate ligand.
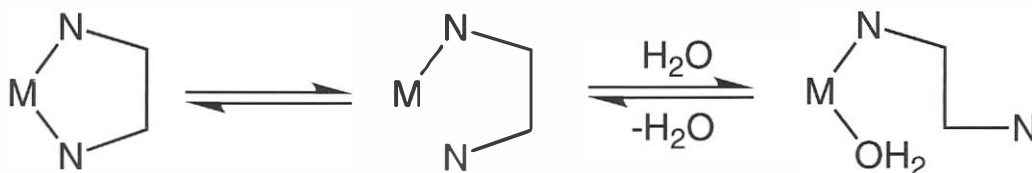
The bond breaking step is slower than for dissociation of a unidentate ligand because angular expansion of the chelate is required to lengthen the M-N distance; large enthalpic term, ΔH.

Effect of the Metal

Some metal complexes are labile regardless of the ligand environment while complexes of other metals are inert.

metal	rate	e⁻ configuration
Cr^{2+}	7×10^9	d^4
Mn^{2+}	3×10^7	d^5
Fe^{2+}	3×10^6	d^6
Co^{2+}	1×10^6	d^7
Ni^{2+}	3×10^4	d^8
Cu^{2+}	8×10^9	d^9
Fe^{3+}	3×10^3	d^5
Cr^{3+}	3×10^{-6}	d^3
Rh^{3+}	4×10^{-8}	d^6

Enormous rate differences due to the nature of the metal. If one looks at bonding, one can see that the bond involves an attraction of the pair of electrons on the ligand to the positive charge on the metal. An increase in the charge on the metal would lead to an increased attraction to the ligand and a decreased rate.

For the 2+ hexaaquo ions of the first row transition metals another explanation is required since the charge would steadily increase across the row and the rate does not correlate with the increasing charge.

Crystal field activation energies (CFAE's) - derived by subtracting the stabilization in the square pyramidal TS from the stabilization for the octahedral ground state

e^- configuration	octahedral CFSE	square pyramidal CFSE	CFAE
d^0	0	0	0
d^1	4	4.6	-0.6
d^2	8	9.1	-1.1
d^3	12	10.0	2
d^4 (sf)	16	14.6	1.4
d^4 (wf)	6	9.1	-3.1
d^5 (sf)	20	19.1	0.9
d^5 (wf)	0	0	0
d^6 (sf)	24	20.0	4
d^6 (wf)	4	4.6	-0.6
d^7 (sf)	18	19.1	-1.1
d^7 (wf)	8	9.1	-1.1
d^8	12	10	2.0
d^9	6	9.1	-3.1
d^{10}	0	0	0

For correlation between CFAE and rate of H_2O exchange is quite good. Note, the contribution from CFAE is only one part of the total activation process and can only be applied for complexes with the same ligands and charge.

From the table we can reason why d^3, d^8 and strong field d^6 configurations, i.e. Cr^{3+}, Ni^{2+} and Co^{3+} complexes are quite inert.

To summarize the effect of metal on reactivity:
1. High oxidation state complexes are less reactive than low oxidation state TM complexes.
2. For analogous complexes the reactivity decreases going down a column.
3. A larger CFAE leads to slower reactions.

Acid-Catalysis

same product

$$Cr(H_2O)_5 X^{2+} + H_3O^+ \xrightarrow{k_1} Cr(H_2O)_6^{3+} + HX \qquad k_1$$

$$Cr(H_2O)_5 X^{2+} + H_2O \xrightarrow{k_0} Cr(H_2O)_6^{3+} + X^- \qquad k_0$$
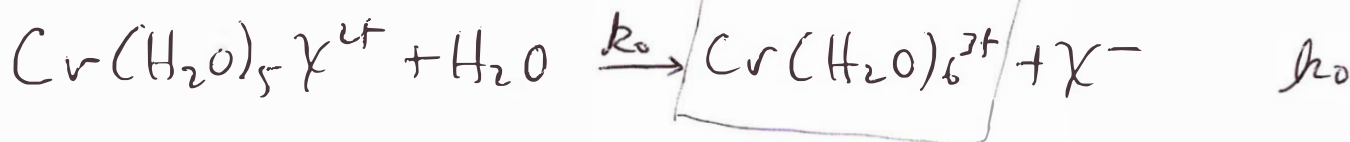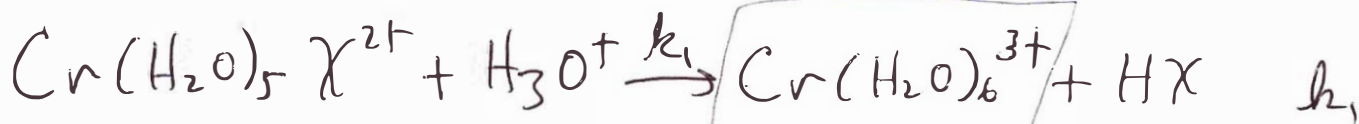
Acid Catalyzed Aquation Rxns of $Cr(H_2O)_5 X^{2+}$

X^-		k_0 slower		k_1 faster
N_3^-	—	2.6×10^{-8}	—	9.3×10^{-7}
F^-	—	6.2×10^{-10}	—	1.4×10^{-8}
CN^-	—	1.1×10^{-5}	—	5.9×10^{-4}
NH_3	—	no acceleration		$\leftarrow$ no e^- pairs

mechanism.

$$\left[(H_2O)_5 Cr - \overset{H^+}{\underset{\ddot{\,}}{F}} \right]^{+2}$$
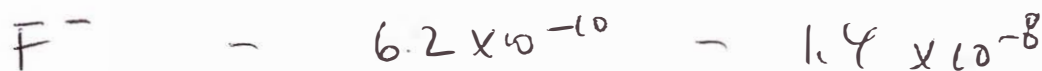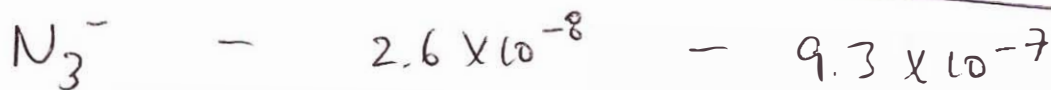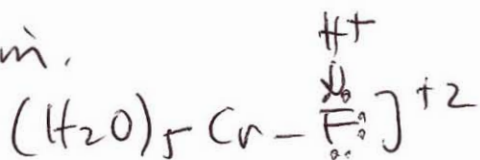
NH_3 ~~~~
removed is not
catalyzed by acid

$$\longrightarrow (H_2O)_5 - Cr - (H_2O)$$
$$+ HF$$

$$Cr \equiv NH_3$$
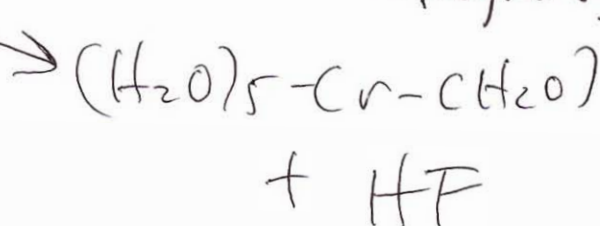
Acid-Catalyzed Chelation

$$Co \overset{O}{\underset{O}{<}} \overset{\cdot O}{C} = O + H_3O^+$$

$$\downarrow$$

$$Co \overset{OH_2}{\underset{O}{<}} - \overset{OH}{\underset{C}{C}}$$

$$\downarrow H_2O$$

$$Co(H_2O)_2 + H_2CO_3$$
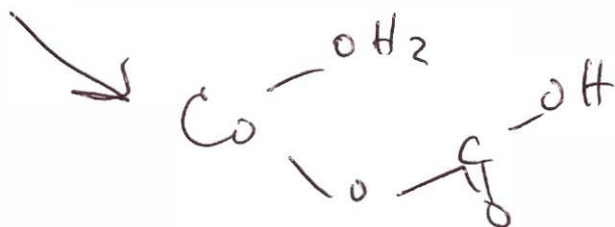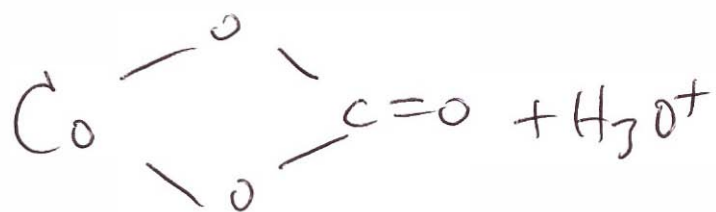
Protonation inhibits the re-formation of the
O—Co bond

Base-Catalysis

1) $Co(NH_3)_5 X^{2+} + OH \underset{\rightleftharpoons}{\overset{k}{}} Co(NH_3)_5 OH^{2+} + X^-$
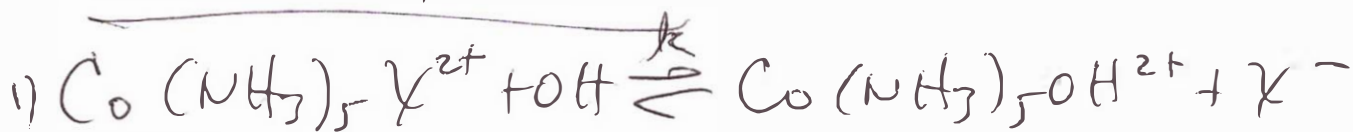
2) $rate = k[Co(NH_3)_5 X^{2+}][OH^-]$

3) Conjugate base mechanism

a) $Co(NH_3)_5 X^{2+} + OH^- \underset{k_{-1}}{\overset{k_1}{\rightleftharpoons}} Co(NH_3)_4(NH_2)X^+ + H_2O$

b) $Co(NH_3)_4(NH_2)X^+ \overset{k_2}{\longrightarrow} Co(NH_3)_4(NH_2)^{2+} + X^-$

c) $Co(NH_3)_4(NH_2)^{2+} + H_2O \overset{fast}{\longrightarrow} Co(NH_3)_5 OH^{2+}$
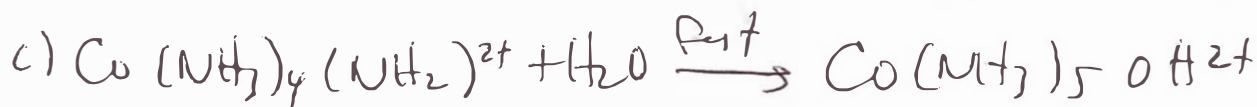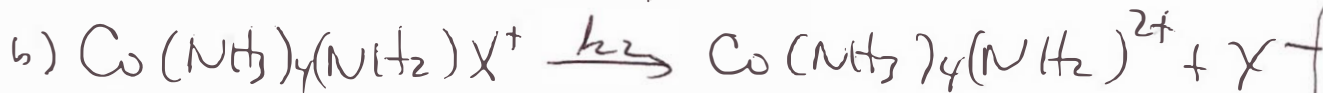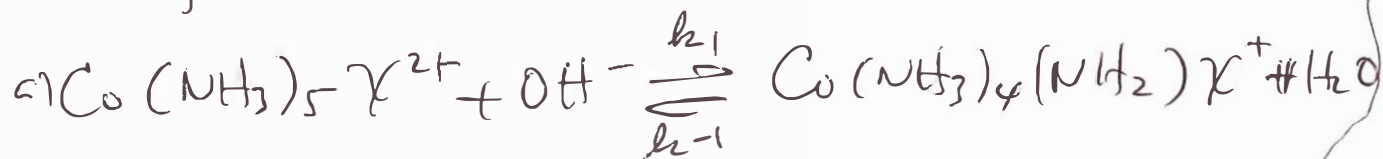
$$rate = \frac{k_1 k_2 [Co(NH_3)_5 X^{2+}][OH^-]}{1 + k_1 [OH^-]}$$

but if $k_1 [OH^-]$ ij < 1 then

Evidence,

1) Different Nu: reacts at similar rates

2) Steric acceleration is observed (Dissociative)

Aquation rxn

$$Co(NH_3)_5 X^{2+} \underset{-H_2O}{\overset{H_2O}{\rightleftharpoons}} Co(NH_3)_5 H_2O^{3+}$$
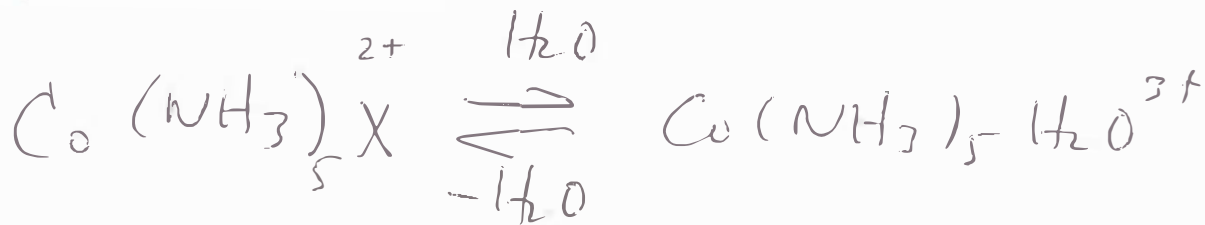
X	$k(s^{-1})$	$K_{eq}(m^{-1})$
NCS^-	4.1×10^{-10}	3.7×10^{-4}
N_3^-	2.1×10^{-9}	1.2×10^{-3}
F^-	8.6×10^{-8}	0.040
Cl^-	1.7×10^{-6}	0.90
Br^-	6.5×10^{-6}	2.9
I^-	8.3×10^{-6}	8.3
NO_3^-	2.7×10^{-5}	12

Activation Parameters

$$\Delta G^{\ddagger} = \Delta H^{\ddagger} - T\Delta S^{\ddagger} \qquad ; \ \Delta H \text{ not very informative}$$

$$\Delta S^{\ddagger}$$

$\Delta S^{\ddagger} < -10 \qquad$ Ass. RXN $\quad mx \xrightarrow{L} mxL$

$\Delta S^{\ddagger} > +10 \qquad$ Diss. RXN $\quad mx \rightarrow m^{\ddagger} + x^{-}$

$$\Delta S = \{ S_{prod} - S_{reac.}$$

$\Delta V^{\ddagger}$ - volume of activation; measure of the compressibility difference between the ground state & T-S.

$\Delta V^{\ddagger} \ (+)$ Diss. RXN

$\Delta V^{\ddagger} \ (-)$ Ass. RXN
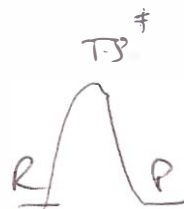
Complex	$\Delta H^{\ddagger}$	$\Delta S^{\ddagger}$	$\Delta V^{\ddagger}$
In (NH$_3$)$_5$(H$_2$O)$^{3+}$	28.1	2.7	-3.2
Co (NH$_3$)$_5$(H$_2$O)$^{3+}$	26.6	67	1.2
Co (NH$_3$)$_5$(NCS)$^{2+}$	30.1	-0.8	-4.0

Associative

$$mL_n + x \underset{k_{-1}}{\overset{k_1}{\rightleftharpoons}} mL_nX \xrightarrow[\text{slow}]{k_2} mL_{n-1}X + L$$
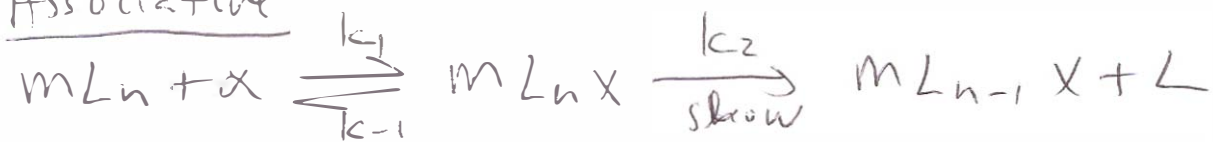
$$\text{Rate} = k_2 [mL_nX] \longleftarrow \quad \text{intermediate is difficult to measure}$$

use a steady state approach (approximation)

$$\frac{d[mL_nX]}{dt} = 0 = k_1[mL_n][X] - k_{-1}[mL_nX] - k_2[mL_nX]$$

$$0 = k_1[mL_n][X] - (k_{-1} + k_2)[mL_nX]$$

$$[mL_nX] = \frac{k_1[mL_n][X]}{k_{-1} + k_2} \quad ; \quad \frac{\text{Rate}}{k_2} = [mL_nX]$$

so,

$$\boxed{\text{Rate} = \frac{k_2 k_1 [mL_n][X]}{k_{-1} + k_2}}$$

Thus, an associative process exhibits a rate dependence in both reactants. $\longleftarrow$

us-a-us

$$\boxed{mL_n \, \& \, X}$$

Dissociative

$$mL_n \underset{k_{-1}}{\overset{k_1}{\rightleftharpoons}} mL_{n-1} + L$$

$$mL_{n-1} + X \xrightarrow[slow]{k_2} mL_{n-1}X$$
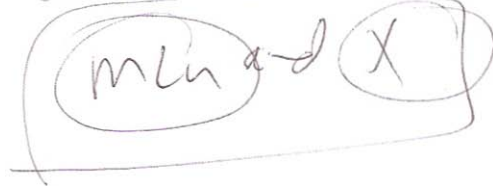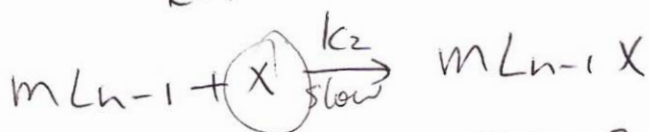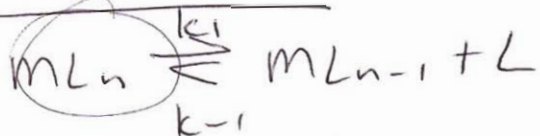
$$Rate = k_2 [mL_{n-1}][X]$$

$$\frac{d[mL_{n-1}]}{dt} = k_1[mL_n] - k_{-1}[mL_{n-1}][L]$$
$$- k_2[mL_{n-1}][X]$$

Steady state approach yields

$$Rate = \frac{k_1 k_2 [mL_n][X]}{k_{-1}[L] + k_2[X]}$$

If $k_2[X] >> k_{-1}[L]$ then

$$Rate = k_1[mL_n]$$

If $k_{-1}[L] \approx k_2[X]$, then the rate law is influenced by both $[mL_n]$ & $[X]$, making it difficult to distinguish between a & d afuetin.

$$\boxed{mL_n \,\&\, X}$$
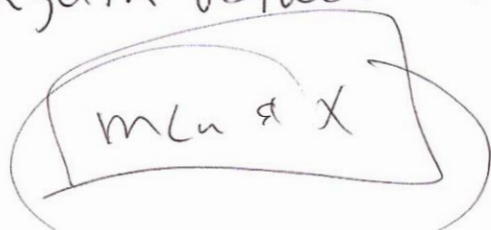
pH Effects: Acid and Base Hydrolysis

The rates of hydrolysis rxns are often accelerated by addition of either acid or base. For example, the rate law for the hydrolysis of the Cr(III) complex $[Cr(H_2O)_5OAc]^{2+}$ contains two independent rate constants:

$$k_{obs} = k_1 + k_2[H^+]$$

This suggests two different rxn pathways. The first-order rate constant k_1 is for "normal behavior. The second term corresponds to a pathway beginning with the protonation of the acetate ligand; this weakens its Lewis basicity and facilitates dissociation.

The base-catalyzed hydrolysis of $[Co(NH_3)_5Cl]^{2+}$ also follows second-order kinetics. Date are consistent with a d-type mechanism. It is generally believed that hydroxide ion serves to deprotonate one of the NH_3 ligands. This promotes dissociation by stabilizing the five-coordinate TS through ligand to metal π donation by NH_2^-:

$$
\left[
\begin{array}{c}
NH_2 \\
\| \\
H_3N\cdots M \cdots NH_3 \\
H_3N \qquad NH_3
\end{array}
\right]^{*}
$$
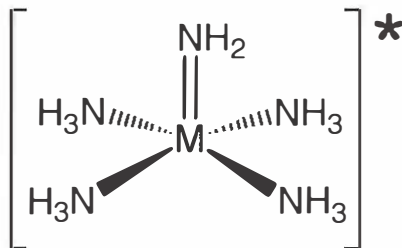
The predominant mechanism of substitution rxns is dissociative or dissociative interchange. The dissociative mechanism persists even for acid- and base-catalyzed substitution rxns. Substitutional reactivity of octahedral complexes depends on (1) the nature of the leaving group, with strongly binding ligands slower and with chelate ligands slower than monodentate ligands; (2) the charge on the metal center, the more highly charged metal undergoing substitution more slowly; (3) wheter the metal is first, second, or third row, the reactivity decreasing in that order; and (4) the d-electron configuration of the metal.

Electron Transfer Reactions

Let us consider the aqueous electron transfer process

$$[Fe^*(H_2O)_6]^{2+} + [Fe(H_2O)_6]^{3+} \rightleftharpoons [Fe^*(H_2O)_6]^{3+} + [Fe(H_2O)_6]^{2+}$$

which can be followed using an isotopically labeled reactant. The rate of electron exchange varies with the pH, being much faster in basic solution. We can write the rate eq as follows:

$$k_{obs} = k_1 + \frac{k_2 K_h}{[H^+]}$$

Here k_1 and k_2 are both second-order rate constants (first order in each reagent), and K_h is the hydrolysis constant for $[Fe(H_2O)_6]^{3+}$. This is evidence for two competing processes. In the first (the *outer sphere* mechanism, with rate constant k_1), electron transfer is believed to occur directly from one metal center to another. The second (*inner sphere*) mechanism involves the formation of the bridged complex $[(H_2O)_5Fe\text{-}OH\text{-}Fe(OH_2)_6]^{4+}$, where a hydroxo ligand is simultaneously bound to both metals.

The reason for the pH dependence is obvious-the formation fo the bridged intermediate requires the deprotonation of $[Fe(H_2O)_6]^{3+}$ to $[Fe(H_2O)_5OH]^{2+}$ (H_2O is not sufficiently basic to bind to two metal ions simultaneously). The transferred electron "hope across the bridge" via the ligand orbitals.

Electron transfer appears to occur by an inner-sphere pathway whenever possible; it is faster, provided that an appropriate bridging ligand is available.

Outer-Sphere Reactions

Outer-sphere rxns are thought to occur through the following sequence:
1. The formation of a *precursor complex*, in which the oxidant and reductant are momentarily trapped within a solvent cage.
2. Activation to some type of excited state.
3. Reorganization to a *successor complex*, in which the metal have acquired new oxidation states.
4. Dissociation of the oxidized and reduced products.

$$1. \quad A + B \rightleftharpoons [A,B]$$

$$2. \quad [A,B] \rightleftharpoons [A,B]^*$$

$$3. \quad [A,B]^* \rightleftharpoons [A^-,B^+]$$

$$4. \quad [A^-,B^+] \rightleftharpoons A^- + B^+$$
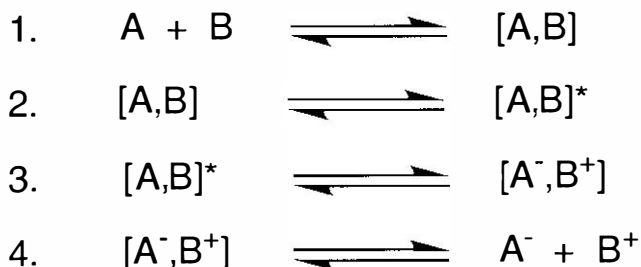
Since outer sphere rxns involve no bond-breaking or bond-making they are amenable to theoretical treatment. In Marcus's interpretation, for a rxn with $\Delta G^o = O$, the free energy of activation is the sum of several contributions.

$$\Delta G^* = RT \ln kT/hZ + \Delta G_a^* + \Delta G_i^* + \Delta G_o^*$$
$$\;\; A \qquad\qquad B \qquad C \qquad D$$

A = allows for the loss of translational and rotational free energy on forming the collision complex from the reactants.
B = free energy change due to electrostatic interaction between the reactants at the separation distance in the activated complex compared to the inter-action at infinite separation.
C = free energy change that is required for rearrangement of the coordination sphere-elongation or contraction of the metal-ligand bonds in the activated complex and perhaps also rearrangement of the ligand.
D = solvent sphere rearrangement.

ΔG_o^* can be quite different for different ligand systems. In complexes that do not differ greatly in oxidation state or ligands, differences in outer sphere reactivity cannot arise from ΔG_a^* or ΔG_o^* and so must arise from changes in ΔG_i^*; simply said, the metal-ligand bond distance changes.

Changes in Metal-Ligand Bond Distances as the Oxidation State Changes.

M	L	M(II)-L	M(III)-L
Ru	NH_3	2.144	2.104
Ru	H_2O	2.122	2.029
Co	NH_3	2.114	1.936
Fe	bipy	1.97	1.963
Co	bipy	2.128	1.93

Ann. Rev. Phys. Chem. **1964**, *15*, 155.

$$(NH_3)_6^{2+} + [Co(NH_3)_6]^{2+} \rightleftharpoons [Co(NH_3)_6]^{3+} + Co(NH_3)_6^{3+}$$

$k_2 = 10^{12} \ m^{-1} s^{-1}$

very slow

$$\underset{\alpha s}{([Fe(CN)_6]^{3-})} + \underset{\underset{\alpha b}{M}}{([Fe(CN)_6]^{4-})} \;\rightleftharpoons\; ([Fe(CN)_6]^{4-}) + ([Fe(CN)_6]^{3-})$$

$3 \quad - \quad - \quad - \quad -$

$E_{is}, \; H, \; H, \; H, \; H, \; H, \; H, \; H, \; H$ — no change $i = \int n$ —

$\sim (log \ outplut \ valle)$

$$(H_2O)_6]^{2+} + [Cr^*(H_2O)_6]^{3+} \rightleftharpoons (Cr(H_2O)_6)^{3+} + (Cr^*(H_2O)_6)^{2+}$$

d^4 $\qquad$ d^3

e_g

antibonding

non-bonding

t_{2g}

Δ_o $\qquad$ e_g

t_{2g}

MX_6^{n-6} $\qquad$ X^- ligands
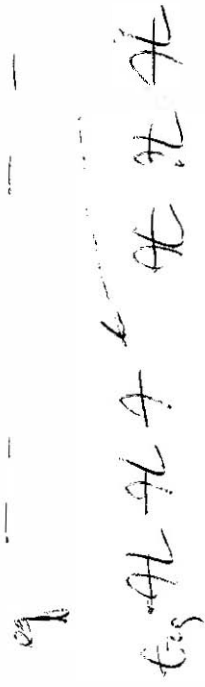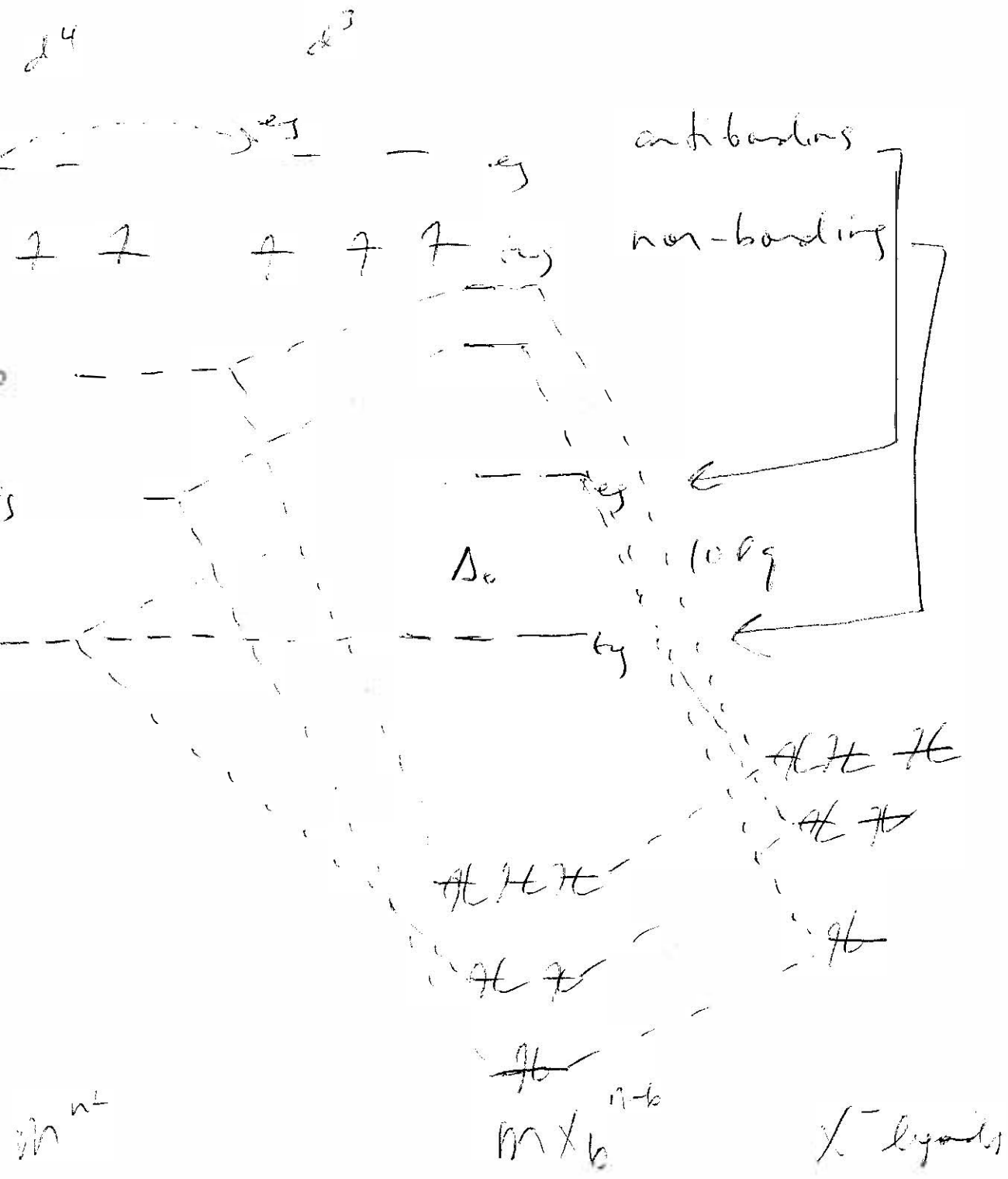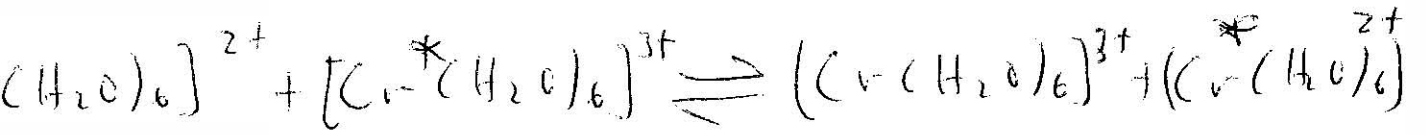
Let us examine the following rxn:

$$[Cr(H_2O)_6]^{2+} + [Cr^*(H_2O)_6]^{3+} \rightleftharpoons [Cr(H_2O)_6]^{3+} + [Cr^*(H_2O)_6]^{2+}$$

The precursor complex can be thought of as a loosely bound unit in which the oxidant is in the second coordination sphere of the reductant, and vice versa. next, activation is required. The Cr-O equilibrium bond lengths are unequal in the two reactants (Cr(II) is larger than Cr(III)), and these distances must change before the electron can be transferred. The TS presumably contains equal bond distances, since that represents the greatest degree of distortion necessary. After the electron is transferred, the bonds of the successor complex readjust to the new equilibrium distances. This is followed by separation (diffusion into the solution) of the oxidized and reduced products.

oxidant	reductant	k, L/mol·s
$[V(H_2O)_6]^{3+}$	$[V(H_2O)_6]^{2+}$	0.01
✳ $[Cr(H_2O)_6]^{3+}$	$[Cr(H_2O)_6]^{2+}$	$<2 \times 10^{-5}$
MnO_4^-	MnO_4^{2-}	3.6×10^{-3}
$[Fe(H_2O)_6]^{3+}$	$[Fe(H_2O)_6]^{2+}$	4.0
ⱥ $[Fe(CN)]^{3-}$	$[Fe(CN)]^{4-}$	7.4×10^2
$[Fe(phen)_3]^{3+}$	$[Fe(phen)_3]^{2+}$	3×10^7
$[Co(NH_3)_6]^{3+}$	$[Co(NH_3)_6]^{2+}$	3×10^{-12}

Two observations can be made relevant to the above data:
1. The most rapid ~~slowest~~ outer-sphere transfers occur when the electron in question originates from and enters an e_g^*, rather than t_{2g} molecular orbital, because the e_g^* orbitals are the more accessible of the two types. They are partly ligand in character, and therefore extend further into space than the σ nonbonding t_{2g} orbitals.
2. The ligands affect the rate of electron transfer. Ligands might be involved in the transfer inany of at least three ways: *chemical exchange,* in which the ligand is temporarily reduced and then reoxidized; *double exchange,* in which the ligand accepts one electron from the reducing agent and then donates a different electron to the oxidizing agent; or (for ligands with π systems) *superexchange,* in which a vacant $π^*$ ligand orbital serves as a temporary repository for the electron.

Inner-Sphere Reactions

Inner sphere mechanisms are characterized by the formation of a binuclear TS/intermediate during the electron transfer rxn. As stated earlier, a very important facet of the inner sphere process is the bridging ligand that forms part of the coordination spheres of both the oxidizing and the reducing metal ions. The bridging ligand must fxn as a Lewis base toward both metal centers-it must have two pairs of electrons that can be donated to different metal centers.

$$M(II) + L\text{-}N(III) \rightleftharpoons M(II), L\text{-}N(III) \qquad collision$$

$$M(II), L\text{-}N(III) \rightleftharpoons M(II)\text{-}L\text{-}N(III) \qquad precursor$$

$$M(II)\text{-}L\text{-}N(III) \rightleftharpoons M(III)\text{-}L\text{-}N(II) \qquad successor$$

$$M(III)\text{-}L\text{-}N(II) \rightleftharpoons M(III)\text{-}L + N(II) \qquad product$$
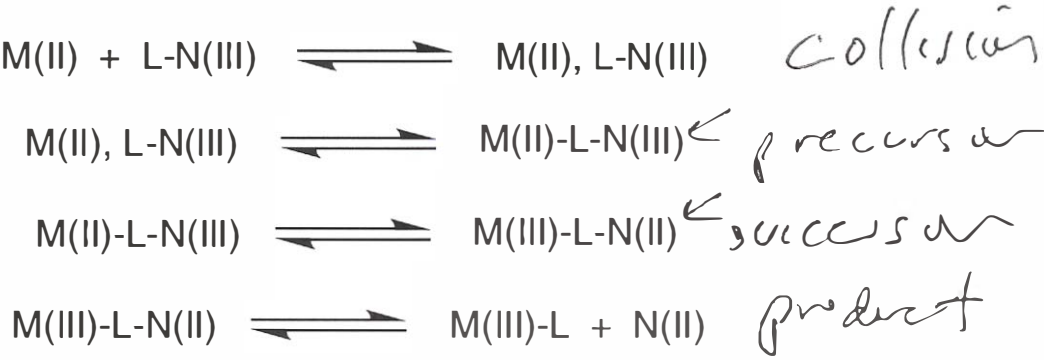
The first rxn is the diffusion-controlled formation of a collision complex. The second rxn is the formation of the precursor complex in which the ligand bridges the two metal centers but the electron has not been transferred. The third rxn is the electron transfer leading to the successor complex. The last rxn is the dissociation of the successor complex to the products.

Any of these rxns may be rate determining as shown below:
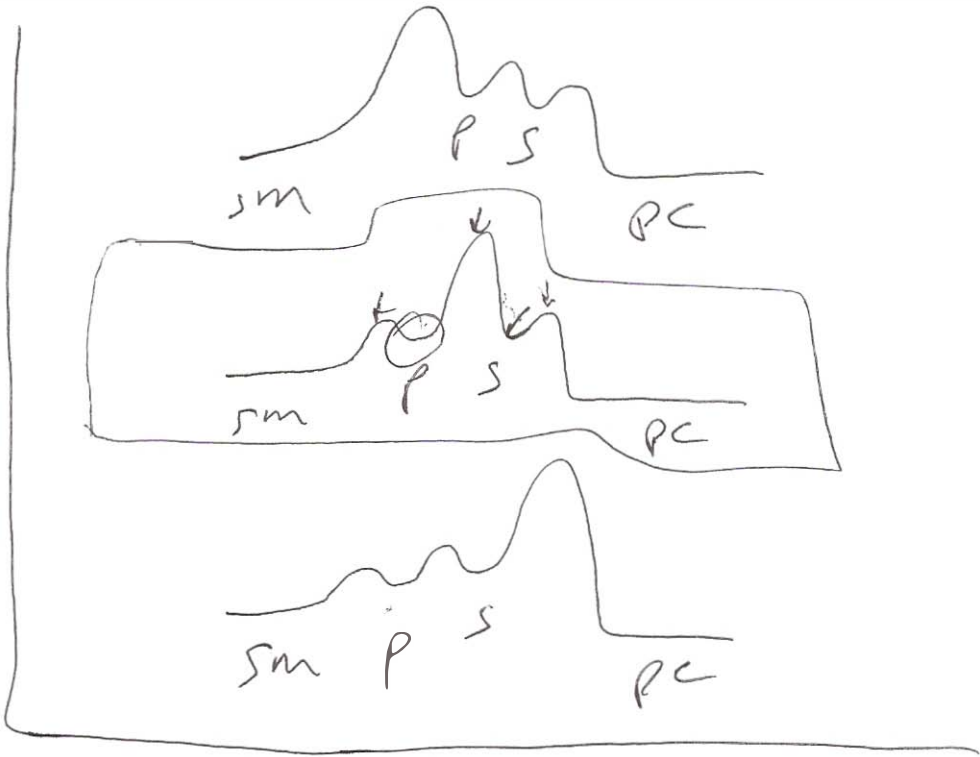
The first unequivocal example of an inner-sphere process was provided by Taube and co-workers (*J. Am. Chem. Soc.* **1954**, *76*, 2103.) and involved the following rxn:

$$[Co(NH_3)_5Cl]^{2+} + [Cr(H_2O)_6]^{2+} \longrightarrow [Cr(H_2O)_5Cl]^{2+} + [Co(H_2O)_6]^{2+}$$
$$+ 5NH_4^+$$
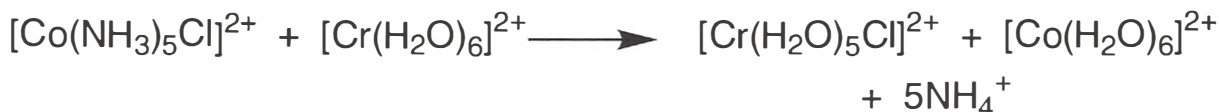
The chromium(II) complex is labile, and the precursor complex can easily be formed. The electron transfer occurs readily. In the successor complex the Cr(III) center is the more inert and the chloride-chromium bond remains while the labile Co(II) loses chloride.

oxidant	reductant	k, L/mol·s
$[Cr(H_2O)_5OH]^{2+}$	$[Cr(H_2O)_6]^{2+}$	0.7
$[Cr(H_2O)_5F]^{2+}$	$[Cr(H_2O)_6]^{2+}$	2.7×10^{-4}
$[Cr(H_2O)_5Cl]^{2+}$	$[Cr(H_2O)_6]^{2+}$	5.1×10^{-2}
$[Cr(H_2O)_5CN]^{2+}$	$[Cr(H_2O)_6]^{2+}$	7.7×10^{-2}
$[Fe(H_2O)_5F]^{2+}$	$[Fe(H_2O)_6]^{2+}$	9.7
$[Fe(H_2O)_5Br]^{2+}$	$[Fe(H_2O)_6]^{2+}$	4.9
$[Fe(H_2O)_5N_3]^{2+}$	$[Fe(H_2O)_6]^{2+}$	1.9×10^3

Nature of the Bridging Ligand

The bridging ligand can be very important in inner sphere rxns.

Rate Constants for Reduction of $Co(NH_3)_5^{3+}$ by $Cr(H_2O)_6^{2+}$.

L	k
NH_3^-	8.0×10^{-5}
F^-	2.5×10^5
Cl^-	6.0×10^5
Br^-	1.4×10^6
I^-	3.0×10^6
N_3^-	3.0×10^5
OH^-	1.5×10^6
NCS^-	19
SCN^-	1.9×10^5
H_2O	~0.1

The order observed for the halides represents the ability of the ligand to donate to two metal centers.

The ability of a ligand to mediate an electron transfer has been ascribed to a matching of the symmetry of metal and ligand orbitals. If symmetries of the orbitals of the metal ions that donate and accept the electron are the same, ligands with orbitals of matching symmetry may provide a lower energy pathway for electron transfer.

Thus if the reductant donates an e_g electron to an e_g orbital, a ligand such as Cl^- (a sigma carrier) would be a better bridging ligand than N_3^- or OAc. Electron transfer involving a t_{2g} orbital would be better accomodated by an N_3^- or an OAc because of better overlap of the t_{2g} orbital with the π system of N_3^- or OAc.

Summary

Electron transfer is one of the primary rxns of TM complexes. Its rate depends on the concentration of the oxidant and the reductant. Electron transfer mechanisms are of two basic types: an outer sphere mechanism between metal centers with intact coordination spheres and an inner sphere mechanism in which a ligand bridges the two metal centers. In either case a primary consideration in the rate is the changes in the bond lengths and angles necessary before electron transfer can occur. Outer sphere rxns can be adequately described by theoretical methods. The nature of the bridging ligand is important for inner sphere rxns. Conjugation in a bridging ligand aids electron transfer, although electron transfer can occur over very long distances even in the absence of conjugation.

Organometallic Chemistry

Organometallic chemistry (OC) is the chemistry of compounds containing metal-carbon bonds. Main-group metals and transition metals (TM's), as well as lanthanides and actinides, form bonds to C.

First organometallic compound discovered in 1827 - Zeise's salt.
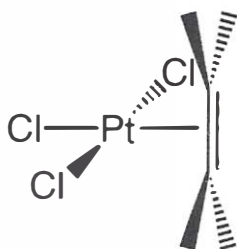
Zeise, W. C. *Ann. Phys.* **1827**, *9*, 932.

Much interest centers on OC because of its importance in catalysis. Transformations in organic molecules on laboratory and industrial scales often involve catalysis by metals.

$$Ni(CN)_2$$
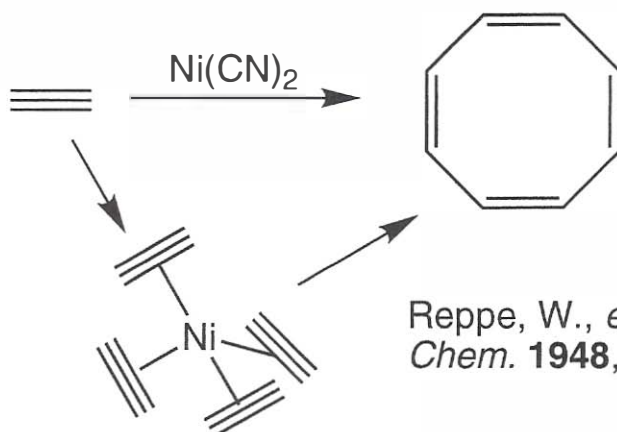
Reppe, W., *et al. Leibig. Ann. Chem.* **1948**, *560*, 104.

Renaissance in the last 40 years.
1. catalysis in organic sythesis
2. biochemistry
3. solid-state materials

Investigation of the fundamental chemistry of organometallic complexes has uncovered a tremendous number of intriguing rxns and modes of ligand attachment. The results have been applied to improving product yield and selectivity of catalyzed rxns. A variety of novel and synthetically useful stoichiometric rxns have been developed.

Organometallic compounds can be loosely divided into two types, depending on whether the M-C bonds are of the σ or π variety.

Some Organometallic Landmarks and Homework

1. Wengrovius, J. H.; Sancho, J.; Schrock, R. R. *J. Am. Chem. Soc.* **1981**, *103*, 3932.

2. Fischer, E. O.; Kreis, G.; Kreiter, C. G.; Muller, J.; Huttner, G.; Lorenz, H. *Angew. Chem. Int. Ed. Engl.* **1973**, *12*, 564.

3. Fischer, E. O.; Maasbol, A. *Angew. Chem. Int. Ed. Engl.* **1964**, *3*, 580.

4. Vaska, L.; Diluzio, J. W. *J. Am. Chem. Soc.* **1962**, *84*, 679.

5. Janowicz, A. H.; Bergman, R. G. *J. Am. Chem. Soc.* **1982**, *104*, 352.

6. Tebbe, F. N.; Parshall, G. W.; Reddy, G. S. *J. Am. Chem. Soc.* **1978**, *100*, 3611.

7. Kealy, T. J.; Pauson, P. J. *Nature (London)* **1951**, *168*, 1039.

8. Brookhart, M.; Green, M. L. H. *J. Organomet. Chem.* **1983**, *250*, 395.

9. Whitesides, G. M.; Boschetto, D. J. *J. Am.. Chem. Soc.* **1969**, *91*, 4313.

10. Longuet-Higgins, H. C.; Orgel, L. E. *J. Chem. Soc.* **1956**, 1969.

11. Brown, J. M.; Chaloner, P. A. *J. Chem. Soc., Chem. Commun.* **1980**, 344.

12. Chatt, J.; Shaw, B. L. *J. Chem. Soc.* **1959**, 4020.
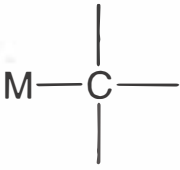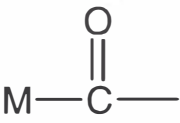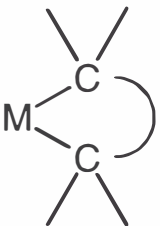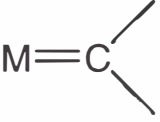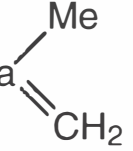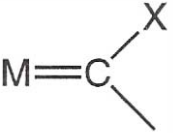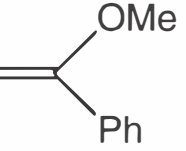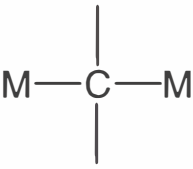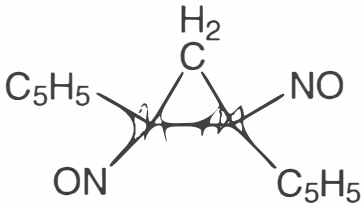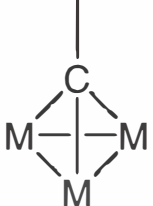
Some Synthetic Applications of Transition Metal Chemistry
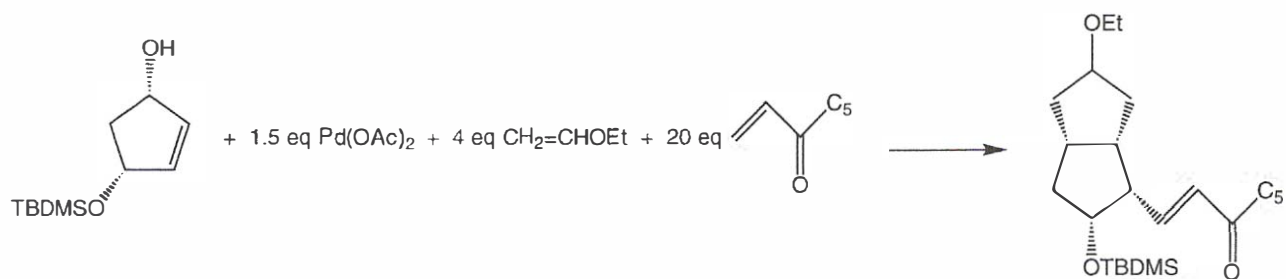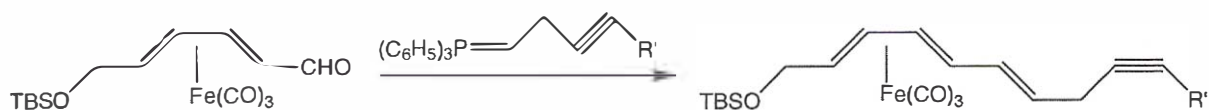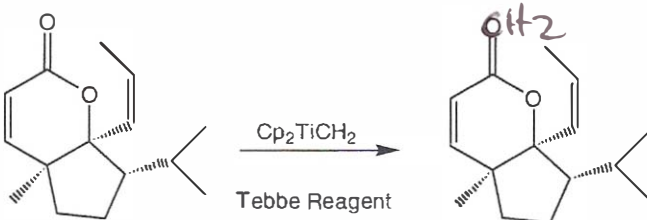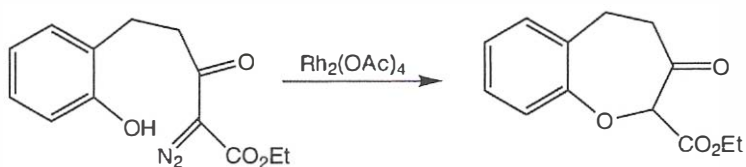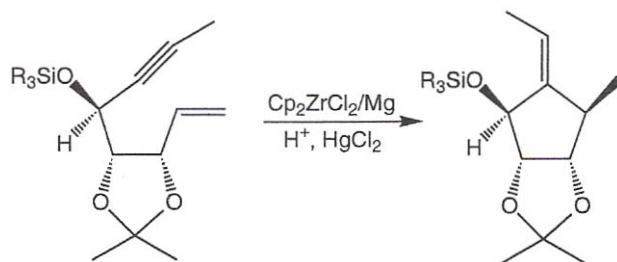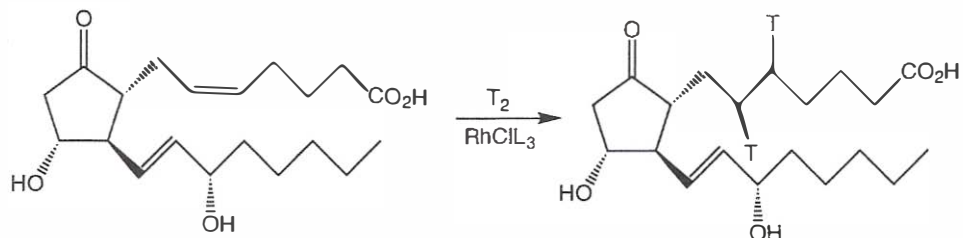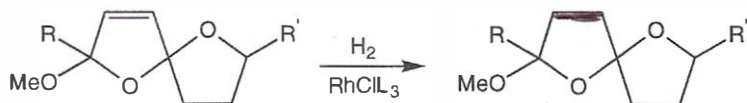
Of course, the bonds to ligands such as CO and CN⁻ have both components—the ligands donate σ electron pairs via C, and are also π acceptors.

Compounds Containing Metal-Carbon σ Bonds

Considerable variation occurs in the structures and bonding of species having M-C σ linkages.

Linkage	Name	Example
	Alkyl	$EtHgBr$, $Sc(C_6H_5)_3$, WMe_6
	Acyl	$MeC(O)Co(CO)_3$
	Metallacyle	
	Alkylidene (Schrock carbene)	
	Carbene	
$M{\equiv}C{-}$	Carbyne (alkylidyne)	$(OC)_4IW{\equiv}{-}Ph$
$M{-}C{-}M$	μ-Alkylidene	
	μ³-Alkylidyne	$[(CO)_3Co]_3CMe$

Modes of Metal-Carbon σ Bond Formation

TM alkyls and their derivatives can be synthesized by many of the same types of rxns as the main group organometallics. Let's describe six of the most general methods.

1. Insertion of metal Atoms

Many TM's react with alkyl halides at or above room temperature.

$$2Zn + 2\ EtI \xrightarrow{\ \Delta\ } [2EtZnI] \longrightarrow ZnEt_2 + ZnI_2$$

$$Pd + CF_3COCl \longrightarrow CF_3C(O)PdCl$$

2. Metal-Metal Exchange

Recall the tendency for bonds to form between elements having large differences in electronegativity.

$$4MeMgCl + TiCl_4 \longrightarrow TiMe_4 + 4MgCl_2$$

$$WCl_6 + 6MeLi \longrightarrow WMe_6 + 6LiCl$$

$$Et_3PAuBr + C_6H_5Li \longrightarrow Et_3PAuC_6H_5 + LiBr$$
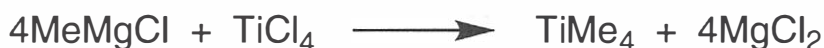
3. Addition Across Carbon-Carbon Multiple Bonds

Metal hydrides often can be induced to add to alkenes.

(actually reversible)
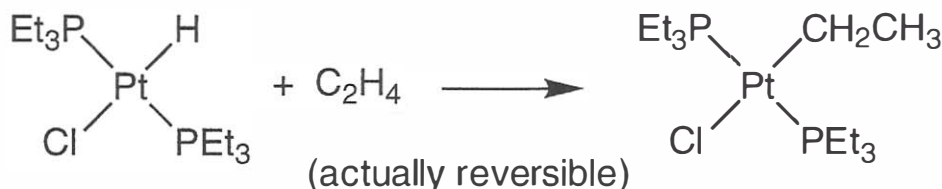
Addition across carbon-carbon triple bonds is also known.

$$AgF + F_3CC\equiv CCF_3 \longrightarrow F_3CC(Ag)=C(F)CH_3$$

$$HRh(PPh_3)_2CL_2 + C_2H_2 \longrightarrow H_2C=CHRh(PPh_3)_2CL_2$$

4. Reactions of Anionic Complexes with Alkyl and Aryl Halides

Metals in low oxidation states sometimes behave as nucleophiles. For example, many metal carbonyl anions (carbonylates) react with methyl iodide:

$$Na^+[M(CO)_n]^- + CH_3I \longrightarrow CH_3M(CO)_n + NaI$$

Similarly, a series of symmetric bis(iron) complexes can be obtained from rxns between $[Fe(C_5H_5)(CO)_2]^-$ and dibromoalkanes.

$$2Na^+[Fe(C_6H_5)(CO)_2]^- + Br(CH_2)_nBr$$

-2NaBr

$$(C_6H_5)(CO)_2Fe\text{-}(CH_2)_n\text{-}Fe(CO)_2C_5H_5$$
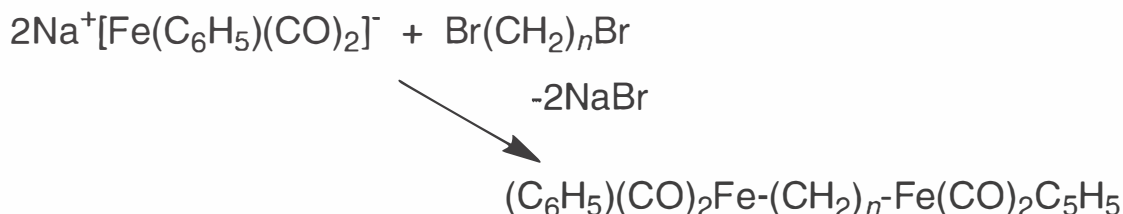
5. Oxidative Addition

Akyl halides undergo oxidative addition rxns with certain square planar complexes to produce octahedral products. Related rxns are possible for other geometries as well.

$$Ru(PPh_3)_2(CO)_3 + CH_3I \xrightarrow{-CO}$$
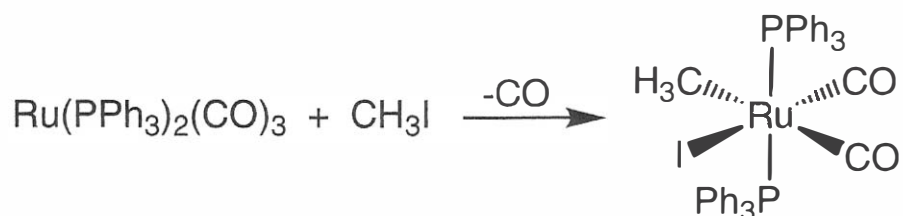
Less commonly, it is possible to oxidatively add to molecules containing C=C or C≡C bonds, producting metallacycles.

$$Fe(CO)_5 + 2F_2C=CF_2 \xrightarrow{-CO}$$
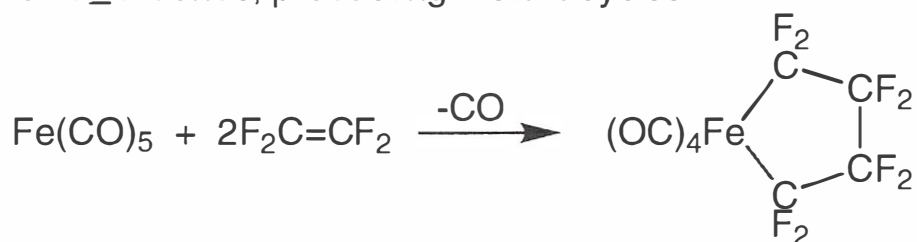
Intramolecular examples of such *cyclometallation* rxns are also known. This typically requires C-H bond rupture within a ligand such as Ph_3P.

$$Ir(PPh_3)_3Cl \longrightarrow$$

55
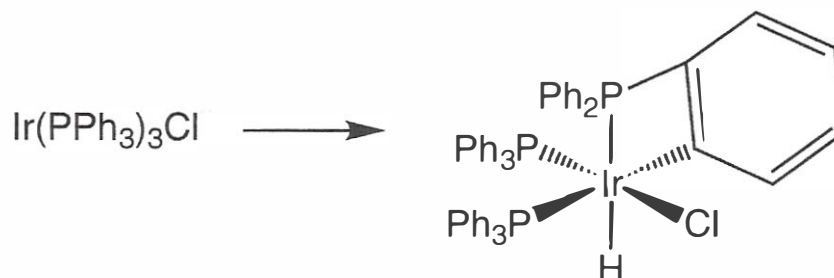
6. Elimination

The heating of acyls and related species may result in the elimination of a small molecule and the formation of a new M-C bond.

$$H_3CC(O)Mn(CO)_5 \xrightarrow[\Delta]{-CO} H_3CMn(CO)_5$$

$$\underset{RO_2C}{\overset{Ph_3P\text{\textit{\textquotedbl}}}{}}Rh\overset{\text{\textbackslash}CO}{\underset{PPh_3}{}} \xrightarrow[\Delta]{-CO_2} \underset{R}{\overset{Ph_3P\text{\textit{\textquotedbl}}}{}}Rh\overset{\text{\textbackslash}CO}{\underset{PPh_3}{}}$$
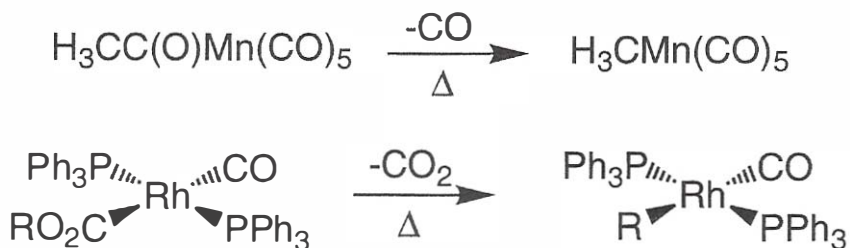
Stabilities and Modes of Decomposition of Metal Alkyls

Stable compounds can be highly reactive-in fact, high reactivity is a common problem in OC. Many species containing metal-carbon bonds are reactive toward components of the atmosphere [ie, are readily oxidized by O_2 and/or $H_2O(g)$].

$$(CH_3)_2Zn + 4O_2 \longrightarrow ZnO + 2CO_2 + 3H_2O$$

Three common modes of decomposition for compounds containing metal-carbon σ bonds are reductive elimination, α-rearrangement, and β-hydride elimination.

Reductive elimination may occur by either an intermolecular or intramolecular pathway.

$$\underset{Ph_3P}{\overset{Ph_3P\text{\textit{\textquotedbl}}}{}}Pt\overset{\text{\textbackslash}H}{\underset{CH_3}{}} \xrightarrow{\Delta} Pt(PPh_3)_2 + CH_4$$
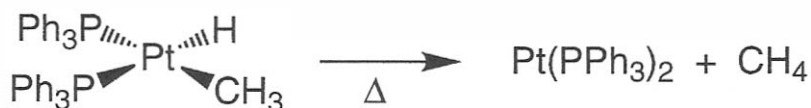
Isotopic labeling studies show that the elimination of CH_4 from $Os(CO)_4(H)Me$ is bimolecular:

$$2Os(CO)_4(H)Me \xrightarrow{50^\circ C} (CO)_4(H)Os\text{-}Os(Me)(CO)_4 + CH_4$$

For compounds in which the metal-bonded carbon is a carbonyl, α *rearrangement* to produce a dative M <---CO interactions may occur:

$$M-\underset{\underset{R}{|}}{C}=O \longrightarrow R-M-C\equiv O:$$

$$H_3CC(O)Co(CO)_3 \rightleftharpoons H_3CCo(CO)_4$$
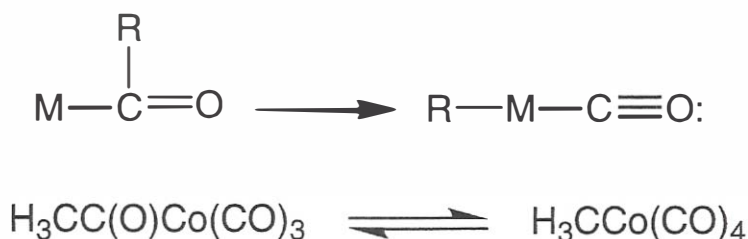
A general scheme for β-*insertion* elimination is

$$M\text{-}H + R_2C{=}CR'_2$$
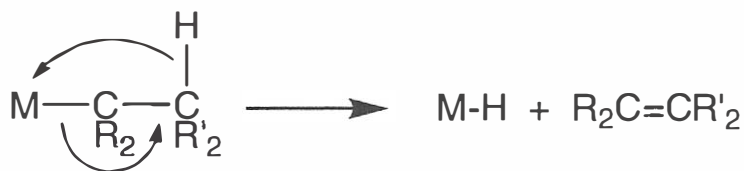
This is the reverse of M-H addition to carbon-carbon double bonds. Being an intramolecular process, it requires an approximately coplanar arrangement to bring the hydrogen close to the metal:

Species for which such an orientation is impossible are often stabilized; for example, the metallacycle
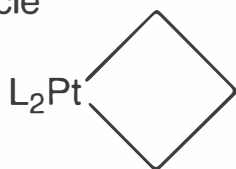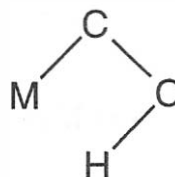
$$L_2Pt\diagdown$$

undergoes elimination of alkene very slowly in comparison to its acyclic analogue L_2PtEt_2.

Multiple Bonding Between TM's and Carbon

In recent years, an astonishing number of species have been prepared and studied that contain double or triple bonds between a TM and carbon. The synthesis of such compounds is usually accomplished through elimination rxns. For example, consider the rxn

$$Ta(Cl)_2R_3 + 2RLi \longrightarrow TaR_5 + 2LiCl$$

When R = Me, the homoleptic product is obtained as indicated. If R is a large group such as neopentyl the considerable steric hindrance causes decomposition via what is believed to be intramolecular elimination from one of the α carbons:

$$R_3Ta{=}CHCMe_3 + CMe_4$$
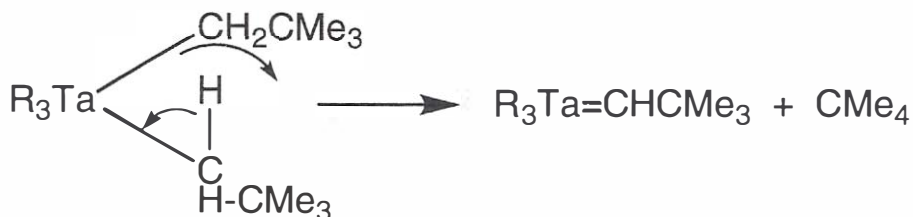
The product is an *alkylidene* (or *Schrock carbene*).

The evidence for multiple bonding includes shortened M-C bond distances, planarity at carbon, and ^{13}C NMR chemical shifts characteristic of sp^2 hybridization. Many alkylidenes have been reported in recent years. It is also possible to prepare bis(alkylidenes) by rxn such as

$$Nb(CH_2CMe_3)_4Cl \xrightarrow[-2CMe_4]{+2PMe_3} \underset{\underset{PMe_3}{|}}{\overset{\overset{PMe_3}{|}}{Cl-Nb}} \begin{matrix} CHCMe_3 \\ CHCMe_3 \end{matrix}$$
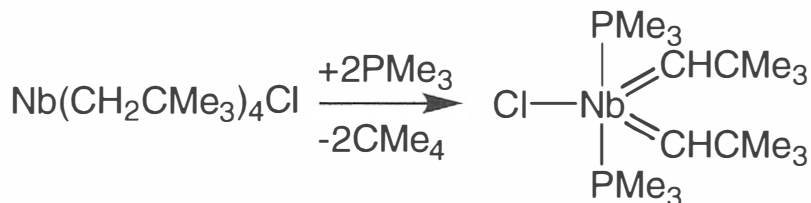
If one of the substituents on carbon contains a lone pair (ie, $L_xM=C(R)X:$), then the species is referred to as a metal *carbene* (or *Fischer carbene*). The first carbene to be reported resulted from the rxn of phenyllithium with $W(CO)_6$.

$$W(CO)_6 + Li^+C_6H_5^- \longrightarrow Li^+ \left[(OC)_5W-C \underset{C_6H_5}{\overset{O}{\diagup}} \right]^-$$
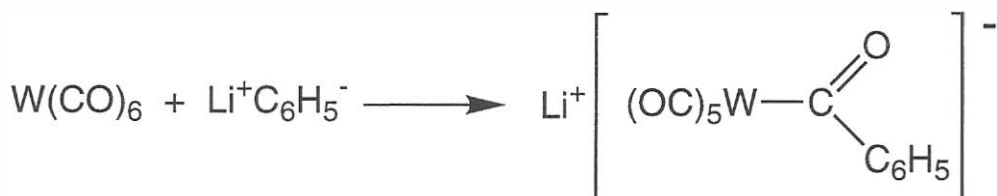
Addition of a methylating agent then yields the carbene:

$$\left[(OC)_5W-C \underset{C_6H_5}{\overset{O}{\diagup}} \right]^- \xrightarrow{Me_3O^+BF_4^-} (OC)_5W=C \underset{C_6H_5}{\overset{OMe}{\diagup}}$$
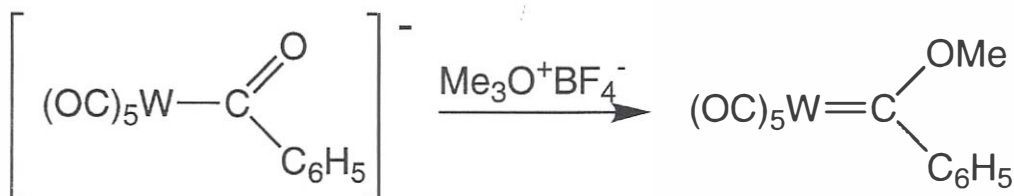
The reason for differentiating between alkylidenes and carbenes is that the latter exhibit resonance:

$$L_nM=C \underset{R}{\overset{OMe}{\diagup}} \longleftrightarrow L_nM-C \underset{R}{\overset{OMe}{\diagup}}$$
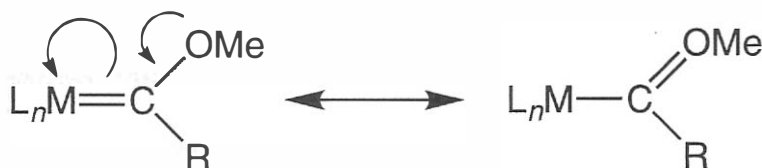
This resonance weakens the metal-carbon bond, as exhibited by an increased bond distance. In fact, in $(CO)_5W=C(C_6H_5)OMe$, the $W=C$ bond distance is 205 pm, about 8% longer than the average of the M-CO bonds. Conversely, there is significant shortening of the $M=C$ linkage(s) in alkylidenes. Bond distances provide a useful measure of the extent of M-C multiple bonding (see Table).

Tungsten-carbon bond distances as a function of bond order for selected compounds (pm).

Compound	d(W-CO)	d(W-C)	d(W=C)	d(W≡C)
$W(CO)_6$	206			
$[(OC)_5W-CH(OMe)(C_6H_5)]^-$		234		
$(OC)_5W=C(OMe)(C_6H_5)$	189		205	
$(OC)_5W\equiv C(C_6H_5)_2$	202			214
$I(OC)_4W\equiv CC_6H_5$	214			188
$Me_3C-CH_2\ / \ Me_3C-CH= W\equiv C-CMe_3$		226	194	176
$Cl(X)(CO)(py)_2W\equiv CC_6H_5$	203			180

Metal Carbonyls and Their Derivatives

The most common of all carbon donor ligands is CO, and thousands of complexes are known that contain carbonyl groups.

$$^-M—C≡O:^+ \longleftrightarrow M=C=O$$

I have supplied you a list of homoleptic carbonyl species. One finds that metals near the center of each transition series produce the most stable species. The remaining metals form carbonyl-containing complexes, but only as anions or in the presence of other ligands.

If we can go back to a little MO theory we can see that the electron pair in the MO localized on C is more loosely bound and is the one available for electron donation to a metal.
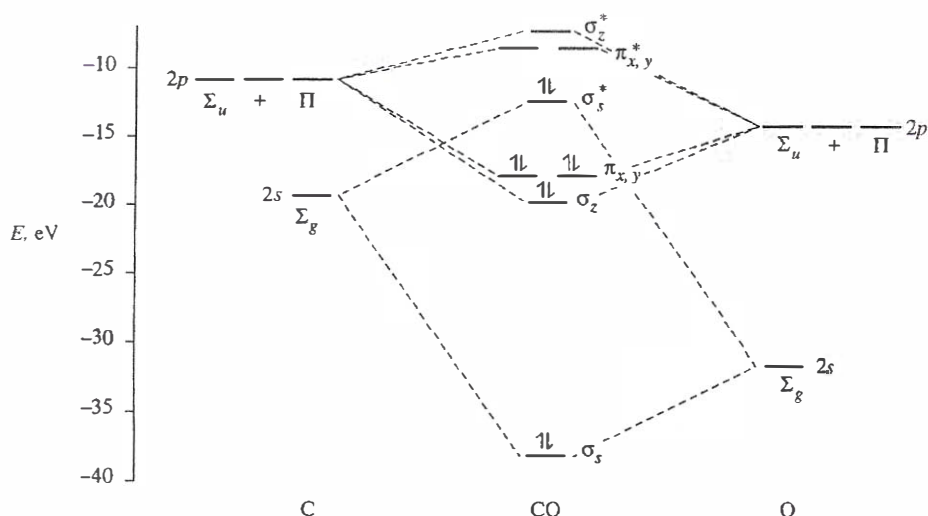
Figure 3.13 Molecular orbitals and their approximate energies for carbon monoxide, CO. The HOMO is the σ_s^* orbital, which is predominantly carbon in character.

The bottom figure show the bonding resulting from overlap of the filled C σ orbital and an empty metal s orbital. CO also has a pair of empty, mutually perpendicular π* orbitals that overlap with filled metal orbitals of π symmetry and help to drain excess negative charge from the metal onto the ligands. Because ligands (in this case, CO) containing empty π* orbitals accept electrons, they are Lewis acids and are called π **acids**. Metal-to-ligand electron donation is referred to, as you know, as **back-bonding**.

(a) ligand-to-metal
σ-bonding

(b) Metal to ligand π* back bonding
(one of a mutually perpendicular
set shown)
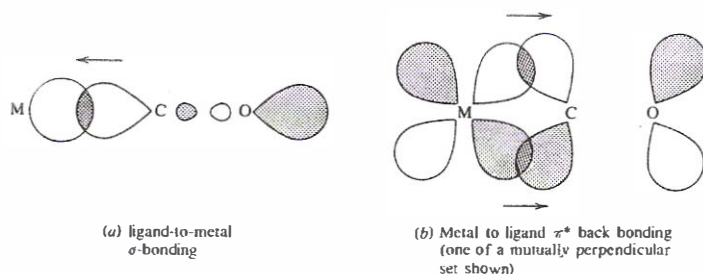
Figure 12.1 Orbital overlap in M—CO bonding. Arrows show direction of electron flow. (a) Ligand-to-metal σ bonding. (b) Metal-to-ligand π* back-bonding (one of a mutually perpendicular set shown).

60

Energetically, the most important bonding component is σ L-->M donation. Backbonding (the π component) assumes greater relative importance when the metal has many electrons to dissipate; thus, low oxidation states are stabilized by π-acid ligands.

σ- and π-bonding reinforce each other: The greater the electron donation from a filled ligand σ orbital, the greater the partial positive charge on the ligand and the more stable the π^* orbitals become, making them better acceptors. This mutual reinforcement is called **synergism**. The importance of synergic bonding is indicated by the fact that CO forms a very large number of complexes with TM's in low oxidation states, even though it is an extremely poor Lewis base toward other species.

CN^-, isocyanides (:CNR), carbenes (:C(X)(Y), NO^+, phosphines (R_3P), arsines (R_3As), stibines (R_3Sb), bipyridine (bipy), and phenanthroline (phen)

Trends in M-CO bond dissociation energies are of interest. There is a general increase in average bond energy going across the first transition series, with a maximum reached at nickel. (The homoleptics of Sc, Ti, V, Cu, and Zn are too unstable to permit measurement). Bond strength appears to increase going down a family. This is thought to be a reflection of enhanced σ interaction, since back-bonding is greater for the $3d$ elements than for their heavier congeners.

Table 18.5   Average M–CO bond dissociation energies for selected homoleptic carbonyls

Compound	$\bar{D}$, kJ/mol	Compound	$\bar{D}$, kJ/mol
$Cr(CO)_6$	108	$Re(CO)_5$	182
$Mo(CO)_6$	152	$Fe(CO)_5$	117
$W(CO)_6$	178	$Co(CO)_4$	136
$Mn(CO)_5$	99	$Ni(CO)_4$	147

Source: Taken from data compiled by Conner, J. A. Top. Curr Chem. 1977, 71, 71.

Synthesis of Carbonyls

A few metal carbonlyls, the best-known being $Ni(CO)_4$ and $Fe(CO)_5$, can be prepared by simply heating the metal under a high pressure of CO. More commonly, chemical reduction is carried out in the presence of excess CO:

$$CrCl_3 + Al + 6CO \xrightarrow[140^\circ C]{150\ atm} Cr(CO)_6 + AlCl_3$$

$$2CoCO_3 + 8CO + 2H_2 \xrightarrow{\Delta} Co_2(CO)_8 + 2H_2O + 2CO_2$$
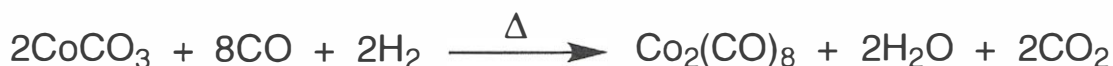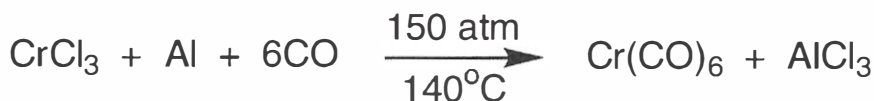
It is sometimes possible to use CO as the reducing agent (also known as **reductive carbonylation**):

$$Re_2O_7 + 17CO \xrightarrow{\Delta} Re_2(CO)_{10} + 7CO_2$$

Higher nuclearity carbonlys (those containing more metals) result from thermolysis of lower ones. Metal-CO bond cleavage produces unsaturated fragments which combine. In some case, such as $Os(CO)_5$, the lower carbonyl is unstable even at ambient temperature:

$$2Os(CO)_5 \xrightarrow{\Delta} Os_3(CO)_{12} + 3CO$$

Photochemical bond cleavage also occurs, as in the synthesis of the diiron complex shown below.

$$2Fe(CO)_5 \xrightarrow{hv} Fe_2(CO)_9 + CO$$

The 18-Electron Rule

The first carbonyls discovered were $Ni(CO)_4$, $Fe(CO)_5$, and $Co_2(CO)_8$. Their formulas, as well as the formulas of carbonyls discovered later, were suggestive to N.V. Sidgwick of a stable 18-electron (pseudo-noble-gas) valence shell configuration around the metal, comparable to the stable octet for the lighter elements suggested by Lewis.

A very large number of metal carbonyls-including many anionic and cationic species, nitrosyl-, hydrogen-, and halogen-substituted metal carbonyls, and small metal cluster carbonyls-conform to the 18-electron rule.

This rule can be formulated in terms of the total number of electrons around the metal-in which case this number is usually found to be 36, 54, or 86, corresponding to the atomic numbers of the noble gases Kr, Xe, and Rn. The metals are then said to have the effective atomic number of the noble gases, or to obey the **EAN rule**.

Some Rules

1. Count two electrons for each CO.
2. Count one electron for each metal-metal bond.
3. Find the number of electrons that formally belong to the metal atom alone by (a) adding up the charges on the ligands and changing the sign, (b) finding the metal oxidation number by adding this number to the total charge on the complex, and (c) subtracting the oxidation number from the valence electron count of the neutral metal.
4. Add together the counts from steps 1-3.

Bridging Carbonyl Groups

The geometry of $Co_2(CO)_8$ has been a subject of considerable study. The 18-electron rule is satisfied by a framework in which each cobalt bond to four CO groups, with a metal-metal bond:

Per Co: $9(Co) + (4 \times 2)(CO) + 1(Co\text{-}Co) = 18$ electrons

Molecule is fluxional and there is evidence for a structure in which two CO groups form bridges between the metal centers.
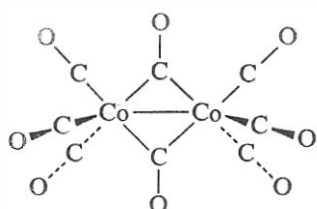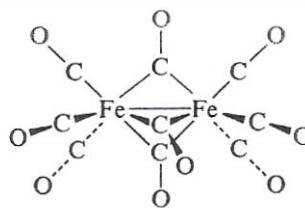
(a) $Co_2(CO)_8$ (b) $Fe_2(CO)_9$

An important resonance structure for the bridged fragment is
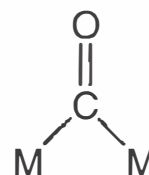
Bridging reduces the strength of the C-O bond. As a result, terminal and bridging CO groups are readily differentiated by their different C-O streching frequencies in infrared spectra.

Higher carbonyls (especially those of the 3d elements) often have bridged structures, even though the bonding requirements could be satisfied by a combination of only metal-metal bonds and terminal CO's

For example

$$\begin{array}{c} (CO)_4 \\ M \\ \diagup \diagdown \\ (CO)_4M\!-\!M(CO)_4 \end{array}$$
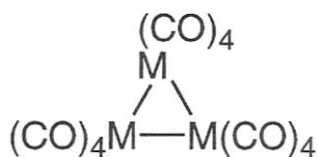
No.   Yes.

Per Fe: $8(Fe) + (3 \times 2)(CO_{terminal}) + (2 \times 1)(CO_{bridge}) + (2 \times 1)(Fe\text{-}Fe) = 18\ e^-$

Carbonyls of the 4d and 5d elements prefer nonbridged structures; $Ru_3(CO)_{12}$ and $Os_3(CO)_{12}$ both have the triangular D_{3h} geometry. But, $Os_3(CO)_{12}$ has only one bridging carbonlyl ligand. This is because the greater size of the 5d metal destabilizes M-C-M bridge bonding. The average M-M bond distances are 288 pm in $Os_3(CO)_{12}$, but only 256 pm between the bridged ions in $Fe_3(CO)_{12}$.

63

It is possible to prepare very large compounds and anions that contain only metals and CO. Compounds having four through six metal atoms, such as $M_4(CO)_{12}$ (M = Co, Rh, and Ir), $M_5(CO)_{16}$ (M = Os), and $M_6(CO)_{16}$ (M = Co, Rh, and Ir), are well established.

More dramatic examples include the anions $[Rh_{14}(CO)_{25}]^{4-}$ and $[Rh_{22}(CO)_{37}]^{4-}$. Covalent and metallic models being to merge in these very large clusters.

Carbonyl Anions, Hydrides, and Other Derivatives

Many carboxylate anions have been prepared and studied. These species are usually made by reacting metal carbonyls with bases, alkali metals, or other reducing agents.

$$Fe(CO)_5 \xrightarrow{+3OH^-} [Fe(CO)_4]^{2-} + H_2O + HCO_3^-$$

$$Co_2(CO)_8 + 2LiBHEt_3 \longrightarrow 2Li^+[Co(CO)_4]^- + H_2 + 2BEt_3$$
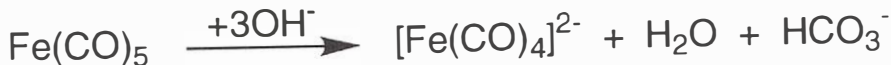
The first titanium and zirconium carbonlylates were prepared by reduction, using potassium naphthalide in the presence of a crown ether or cryptand:

$$TiCl_4(DME) + 6CO \xrightarrow{+4K^+C_{10}H_8^-} [Ti(CO)_6]^{2-}$$

$$ZrCl_4(THF)_2 + 6CO \xrightarrow{+4K^+C_{10}H_8^-} [Zr(CO)_6]^{2-}$$
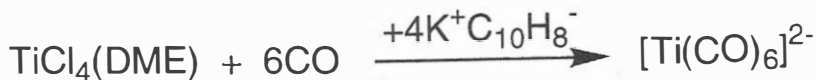
Table 18.7 Some well-characterized carbonyl hydrides and carbonylate ions of the 3d metals

| | Number of Metal Atoms | | |
1	2	3	4
$[Ti(CO)_6]^{2-}$			
$[Zr(CO)_6]^{2-}$			
$HV(CO)_6$			
$[V(CO)_6]^-$			
$[V(CO)_5]^{3-}$			
$H_2Cr(CO)_5$			
$[HCr(CO)_5]^-$	$[HCr_2(CO)_{10}]^-$		
$[Cr(CO)_5]^{2-}$	$[Cr_2(CO)_{10}]^{2-}$		
$HMn(CO)_5$			
$[Mn(CO)_5]^-$			
$[Mn(CO)_4]^{3-}$			
$H_2Fe(CO)_4$		$H_2Fe_3(CO)_{11}$	
$[HFe(CO)_4]^-$	$[HFe_2(CO)_8]^-$	$[HFe_3(CO)_{11}]^-$	$HFe_4(CO)_{13}^-$
$[Fe(CO)_4]^{2-}$	$[Fe_2(CO)_8]^{2-}$	$[Fe_3(CO)_{11}]^{2-}$	
$HCo(CO)_4$			
$[Co(CO)_4]^-$			$[HCo_6(CO)_{15}]^-$
$[Ni(CO)_4]^{2-}$	$[Ni_2(CO)_6]^{2-}$		$[Ni_5(CO)_{16}]^{2-}$
			$[Ni_6(CO)_{12}]^{2-}$

The protonation of reduction of homoleptic carbonyls can be used to prepare certain carbonyl hydrides:

$$[V(CO)_6]^- + H^+ \longrightarrow HV(CO)_6$$

$$Co_2(CO)_8 + H_2 \longrightarrow 2HCo(CO)_4$$

Alkylation and acylation rxns are often facile as well:

$$[Mn(CO)_5]^- + CH_3I \xrightarrow{-I^-} CH_3Mn(CO)_5$$

$$[Mn(CO)_5]^- + CH_3C(O)Cl \xrightarrow{-Cl^-} CH_3C(O)Mn(CO)_5$$

It is also possible to incorporate halogens into metal carbonyl frameworks. Such rxns may or may not involve the elimination of carbon monoxide:

$$Mn_2(CO)_{10} + Br_2 \longrightarrow 2Mn(CO)_5Br$$

$$Fe(CO)_5 + Br_2 \longrightarrow Fe(CO)_4Br_2 + CO$$
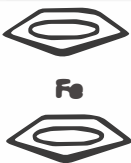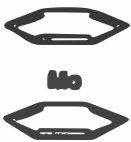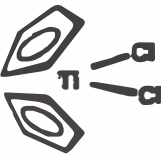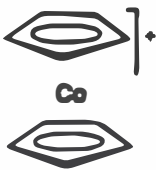
You should be able to verify that all the metal-containing products of the above equations conform to the 18-electron rule.

Nitrosyl Complexes

NO contains one more electron than CO which resides in a π^* MO of predominantly nitrogen character; it is therefore not surprising that NO is both similar to and different from CO as a ligand. Like CO, it generally binds to metals through its less electronegative element, and has an affinity for metals in low oxidation states. However, NO usually behaves as either a one- or three-electron donor. One way to rationalize this is to first assume the transfer of the antibonding electron of NO to the metal; the NO^+ group that results is isoelectronic with CO, and may donate two additional e⁻'s.

The stable homoleptic nitrosyls and mixed nitrosyl-carbonyls have molecular formulas consitent with the 18-electron rule.

$Cr(NO)_4$

$Mn(CO)(NO)_3$

Ionic Model			Covalent Model	

Ionic Model					Covalent Model	
$C_5H_5^-$	6e				$C_5H_5 \cdot$	5e
$C_5H_5^-$	6e		**Fe**		$C_5H_5 \cdot$	5e
Fe^{2+}	6e				Fe	8e
	18e					18e
			2.7			
Mo^{4+}	2e		$MoH_4(PR_3)_4$		Mo	6e
$4 \times H^-$	8e		**2.8**		$4 \times H \cdot$	4e
$4 \times PR_3$	8e				$4 \times PR_3$	8e
	18e					18e
Ni^{2+}	8e		**Ni**		Ni	10e
$2 \times C_3H_5^-$	8e				$2 \times C_3H_5 \cdot$	6e
	16e		**2.9**			16e
Mo	6e		**Mo**		Mo	6e
$2 \times C_6H_6$	12e				$2 \times C_6H_6$	12e
	18e		**2.10**			18e
$2 \times Cl^-$	4e		Cl		$2 \times Cl$	2e
Ti^{4-}	0e		**Ti** Cl		Ti	4e
$2 \times C_5H_5^-$	12e				$2 \times C_5H_5 \cdot$	10e
	16e		**2.11**			16e
Co^{3+}	6e		$]^+$		Co	9e
$2 \times C_5H_5^-$	12e		**Co**		$2 \times C_5H_5 \cdot$	10e
	18e				Positive charge[c]	$-1e$
			2.12			18e

[c] To account for the positive ionic charge on the complex as a whole; for anions, the net charge is added to the total.

FIGURE 2.1   Electron counting on the covalent and ionic models.
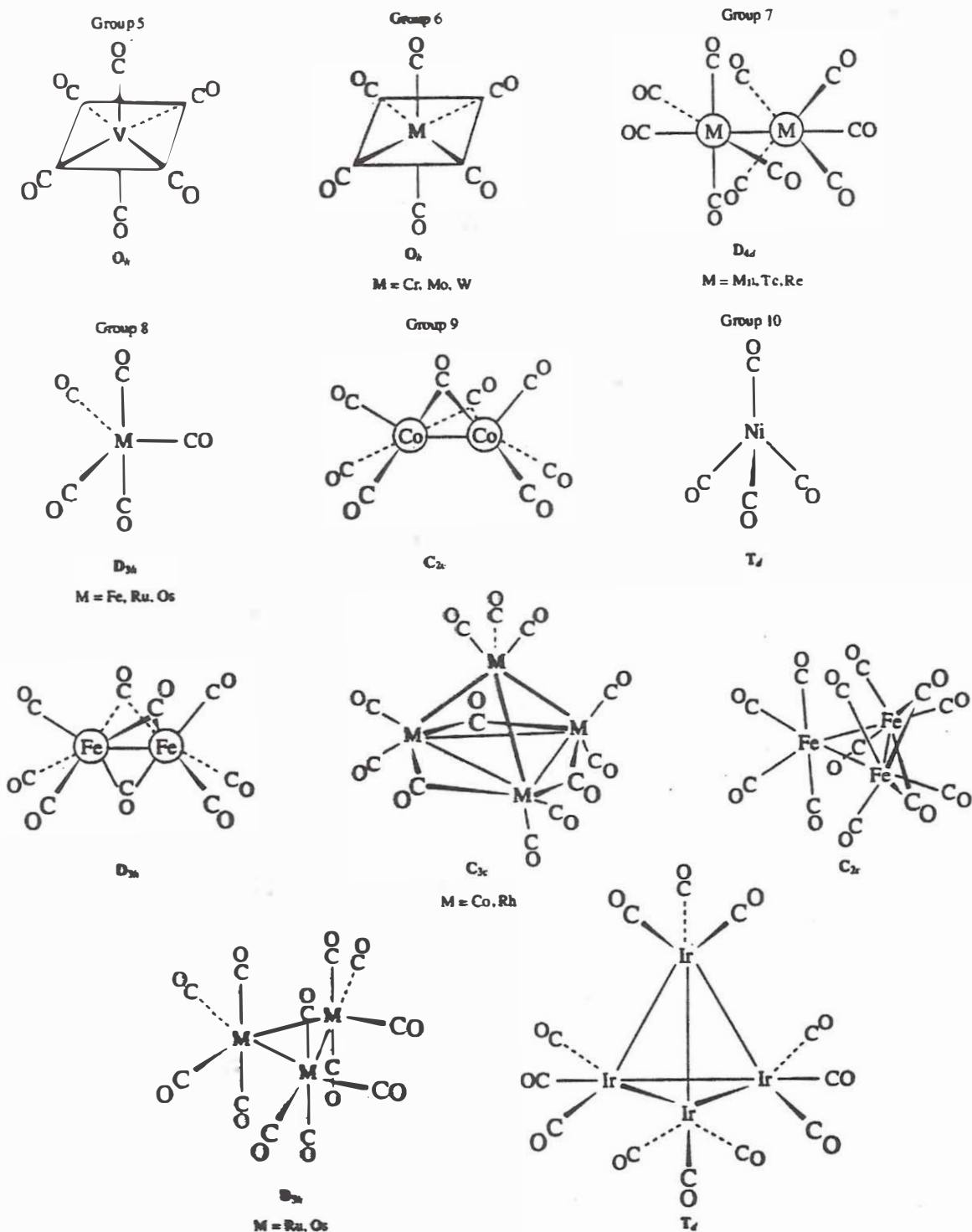
Figure 12.2   Solid-state structures of some neutral binary metal carbonyls.

Table 18.6   Classification of the common geometries of carbonyls having 1–4 metal atoms

Formula	Point Group	Description	
$M(CO)_4$ M = Ni	T_d	Tetrahedral	
$M(CO)_5$ M = Fe, Ru, Os	D_{3h}	Trigonal bipyramidal	
$M(CO)_6$ M = V, Cr, Mo, W	O_h	Octahedral	
$M_2(CO)_8$ M = Rh, Ir	D_{3d}	Pseudo-trigonal bipyramidal	
$M_2(CO)_8$ M = Co	C_{2v}	Doubly bridged	
$M_2(CO)_9$ M = Ru, Os	C_{2v}	Singly bridged	
$M_2(CO)_9$ M = Fe	D_{3h}	Triply bridged	
$M_2(CO)_{10}$ M = Mn, Tc, Re	D_{4d}	Pseudo-octahedral	
$M_3(CO)_{12}$ M = Ru, Os	D_{3h}	Triangular (pseudo-octahedral)	
$M_3(CO)_{12}$ M = Fe	C_{2v}	Doubly bridged	
$M_4(CO)_{12}$ M = Ir	T_d	Tetrahedral (pseudo-octahedral)	
$M_4(CO)_{12}$ M = Co, Rh	C_{3v}	Triply bridged	

Donors Containing Localized π Bonds

C$_2$H$_4$ and Derivatives as Ligands

There are a large number of complexes in which ethylene or some other olefin acts as a donor group.

Ziese's salt

A

Yes.

B

No.
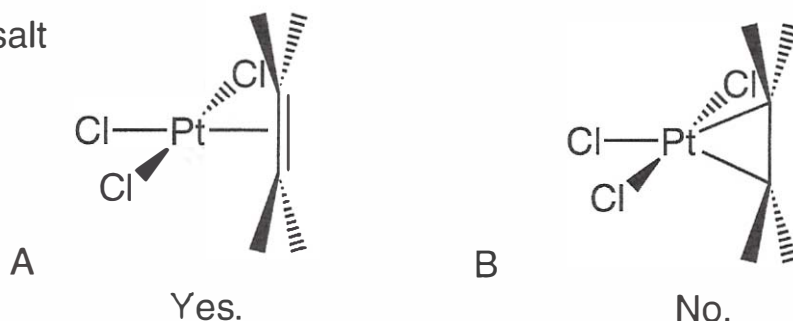
It was first thought that B was correct; a metallacyle-a three-membered C$_2$Pt ring held together by σ bonds. However, this view is not compatible with the C-C bond distance. If only σ bonds were present, the d(C-C) should be close to the single-bond value of 154 pm; however, it is just 138 pm-only slightly longer than the double bond in ethylene (134 pm).

A scheme more consistent with the observed bond distance and other experimental data is the Dewar-Chatt-Duncanson model. The donated electrons are thought to originate from the π-type HOMO of C$_2$H$_4$, which overlaps with σ-type metal d orbitals. This π—>σ interaction is augmented, in the same manner as metal-carbonyl bonds, by back-bonding.

(a)   (b)
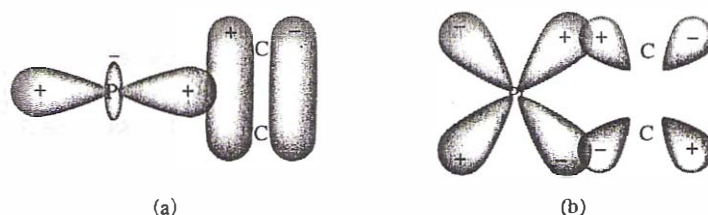
Figure 18.7 Orbital overlap in the [Pt(C$_2$H$_4$)Cl$_3$]$^-$ anion according to the Dewar–Chatt–Duncanson model: (a) dative overlap from the π orbital of C$_2$H$_4$ to a σ-type d_{z^2} metal orbital; (b) π back-bonding from the platinum d_{xz} to the π* orbital of C$_2$H$_4$.

The interactions can be viewed via two resonance structures.

66
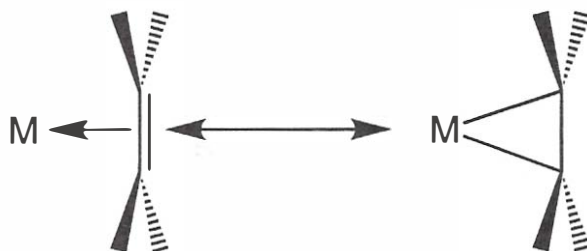
The C-C bond strength is between single and double, and the carbon atoms have hybridizations between sp^2 and sp^3. The relative contributions of the two stuctures (opposite page) appear to vary with the nature of both the metal and the substituents on the carbons.

This bonding scheme is supported by experimental evidence other than bond lengths, including the following:

1. There is a decrease in the vibrational frequency of the C=C bond upon co-ordination from about 1620 cm^{-1} in ethylene to 1525 cm^{-1} in $[Pt(C_2H_4)Cl_3]^-$.
2. The H-C-H bond angles in Zeise's salt ae about 115°, intermediate between the ideal values for sp^2 and sp^3 hybridization.
3. There is a significant trans influence (the *cis* and *trans* Pt-Cl bond distances are 230 and 234 pm, respectively), as would be expected if C_2H_4 behaves as a π acceptor ligand.
4. The carbon atoms exhibit electrophilic character (reflection of the second resonance structure). Thus, nucleophiles such R_2N^- and CN^- attack at carbon rather than at the metal:
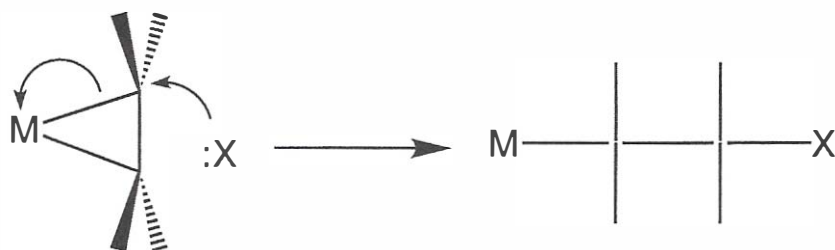
This characteristic makes Zeise's salt and its palladium analogue useful catalysts for the conversion of ethylene to acetaldehyde (the Wacker process).

Metal-olefin bonds can be formed by direct rxn with a free metal (usually using a metal-vapor technique), by addition to a square planar complex, by ligand replacement, or by abstractio of a β hydrogen from an alkyl:

$$Ni + 3C_2H_4 \xrightarrow{\Delta} Ni(C_2H_4)_3$$
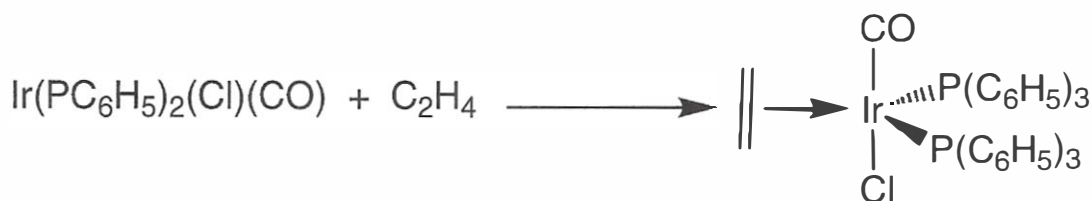
Complexes with Cyclic π Donors

Ferrocene

$C_5H_5^-$ - cyclopentadienide anion; much used as a reagent for the synthesis of a large number of complexes.

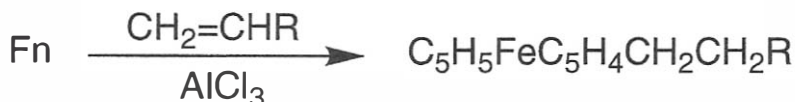Most famous is ferrocene (a.k.a. bis(cyclopentadienyl)iron)

$$FeCl_2 + 2Na^+C_5H_5^- \longrightarrow Fe(C_5H_5)_2 + 2NaCl$$
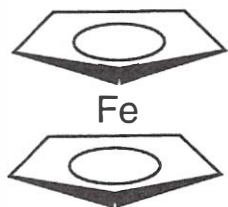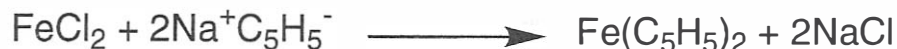
All ten Fe-C bond distances are equal; the two rings are rotated by 9° with respect to one another (ie. not quite eclipsed).

The ligands are pentahapto. The oxidation state is sometimes ambiguous. Let us look upon is as -1 and donating 6 electrons; so,

$Fe^{+2} / C_5H_5^-$, $6(Fe) + (2 \times 6)^f (C_5H_5^-) = 18$ electrons
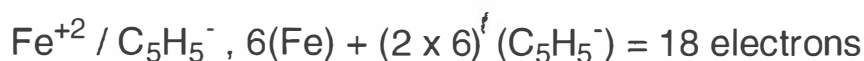
Reactions

Ferrocene (Fn) undergoes a remarkable number of chemical reactions.

$$Fn \xrightarrow[\text{AlCl}_3]{\text{CH}_3\text{C(O)Cl}} C_5H_5FeC_5H_4C(O)Me$$

$$Fn \xrightarrow[\text{AlCl}_3]{\text{CH}_2=\text{CHR}} C_5H_5FeC_5H_4CH_2CH_2R$$

$$Fn \xrightarrow[\text{HF}]{\text{HCHO}} C_5H_5FeC_5H_4CH_2OH$$

$$Fn + n\text{-BuLi} \xrightarrow{-C_4H_{10}} C_5H_5FeC_5H_4C(O)Me$$

Other Metallocenes

Nearly all of the d-block elements form complexes in which one or more C_5H_5 ligands are present.

For example, chromocene (16 e$^-$)

extremely reactive
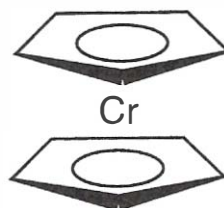
Table 12.4   Electron counting for π-donor ligands *(Continued)*
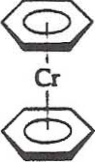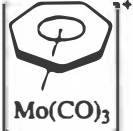
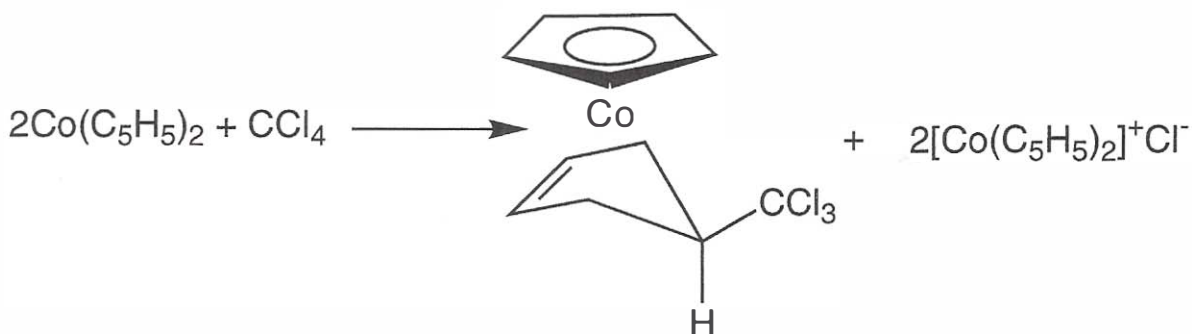| Electrons contributed	Ligand	Structure	Example
6	$\eta^5\text{-}C_5H_6^-$ η^5-pentadienyl		Fe(CO)₃ tricarbonyl(η^5-pentadienyl)iron (1+)
6	$\eta^6\text{-}C_6H_6$ η^6-benzene		Cr bis(benzene)chromium
6	$\eta^7\text{-}C_7H_7^+$ η^7-tropylium		Mo(CO)₃ tricarbonyl(η^7-tropylium)-molybdenum(1+)
6	$\eta^6\text{-}C_7H_8$ η^6-cycloheptatriene		Mo(CO)₃ tricarbonyl(η^6-cycloheptatriene)-molybdenum
6	$\eta^6\text{-}C_8H_8$ η^6-cyclooctatetraene (cot)		Cr(CO)₃ tricarbonyl(η^6-cyclooctatetraene)-chromium

Table 12.5 Some bis(cyclopentadienyl) complexes of transition metals

Compound	Color	mp (°C)	Number of unpaired electrons	Structure and comments
"Cp_2Ti"	Dark green	Dec. 200	0	Dimer with μ-H; structure **A**
	Gray-black		>0	Dimer containing M—M bond; structure **B**
	Purple		0	Dimer with antiferromagnetic spin coupling; structure **C**
$(Me_5C_5)_2Ti$	Yellow-orange	Dec. 60	2	Monomer, tilted rings
"Cp_2Zr"	Purple-black	Dec. 300	0	Str. similar to Ti μ-H dimer A or C
Cp_2V	Purple	167–168	3	Air-sensitive; reacts with CO, X_2, RX
Cp_2Nb			>0	Thermally unstable
"Cp_2Nb"	Yellow		0	Dimer; structure **C**
"Cp_2Ta"			0	Isomorphous with "Cp_2Nb" C
Cp_2V^-	Red		2?	Prepared by K reduction of Cp_2V
Cp_2Cr	Scarlet crystals	172–173	2	Air-sensitive;
Cp_2Mo	Yellow		2	Thermally unstable; very reactive; observed in lo-temperature matrix
"Cp_2Mo"	Yellow (E); green (G)		0	Dimers; structures E, F, and G
Cp_2W			2	Thermally unstable; very reactive intermediate; observed in lo-temperature matrix
"Cp_2W"	Yellow			Dimer; same structure as F
Cp_2Cr^+	Brown-black ($CpCr(CO)_3^-$ salt)		3	Prepared by oxidation of Cp_2Cr ($Cp_2Cr^+ + e \rightarrow Cp_2Cr$, $E° = -0.67\ V$ vs. S.C.E.)
Cp_2Cr^-				Very reactive. $Cp_2Cr + e^- \rightarrow Cp_2Cr^-$, $E° = -2.30\ V$ vs. S.C.E.
Cp_2Mn	Amber		5	Stable form $\leq 159°C$, chain structure
	Pale pink	172–173	5	Stable form $> 159°C$
$(Me_5C_5)_2Mn$	Orange		1	Monomer; Jahn–Teller distorted in solid
Cp_2Re		Dec. ≥ 20 K	1	Thermally unstable
$(Me_5C_5)_2Re$	Deep-purple		1	Planar, eclipsed rings in solid
"Cp_2Re"	Purple-black	Dec. 60	0	Dimer; structure **H**
$(Me_5C_5)_2Re^-$	Orange (K^+ salt)		0	
Cp_2Fe	Orange	173	0	Staggered configuration in solid, eclipsed in gas phase; air-stable, stable > 500°C
Cp_2Ru	Light yellow	199–201	0	Eclipsed configuration in solid; most thermally stable metallocene (>600°C)
Cp_2Os	Colorless	229–230	0	Eclipsed configuration in solid
Cp_2Fe^+	Blue (PF_6^- salt) Dichroic in aq. sol'n. (blue-green to blood red)		1	Prepared by oxidation of Cp_2Fe ($Cp_2Fe^+ + e \rightarrow Cp_2Fe$, $E° = -0.34\ V$ vs. S.C.E.)
"Cp_2Os"$^+$	Green-black		0	Product of oxidation of Cp_2Os; structure H with halves rotated by 90°
Cp_2Co	Purple-black	173–174	1	19-e species; easily oxidized by air to Cp_2Co^+
Cp_2Rh	Brown-black		>0·	19-e species; monomeric $\leq\ -196°$

583

Mo and W conform to the 18 e⁻ rule in the dihydrides $H_2M(C_5H_5)_2$. In these molecules, the Cp rings are tilted.
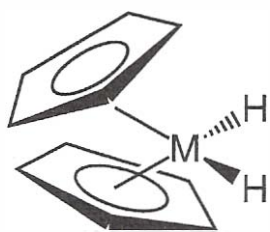
Cobaltocene (19 e⁻), undergoes several types of reactions that produce 18 e⁻ products.

$$2Co(C_5H_5)_2 + Br_2 \longrightarrow 2[Co(C_5H_5)_2]^+Br^-$$

$$2Co(C_5H_5)_2 + CCl_4 \longrightarrow \quad + \quad 2[Co(C_5H_5)_2]^+Cl^-$$

Like $Co(C_5H_5)_2$, nickelocene readily undergoes one electron oxidation; the removal of a second electron can be accomplished electrochemically, but the dication undergoes rapid degradation.

An interesting variation is the "triple-decker (club?) sandwich" cation: $[Ni_2(C_5H_5)_3]^+$, which is obtained from reaction of nickelocene with Lewis acids.

All of the carbon atoms of Cp-like units do not necessarily coordinate to the metal.

$Hg(C_5H_5)_2$
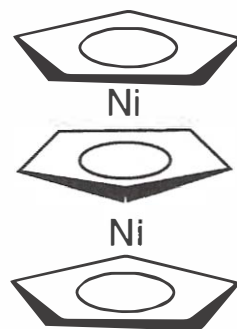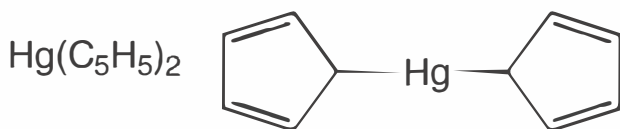
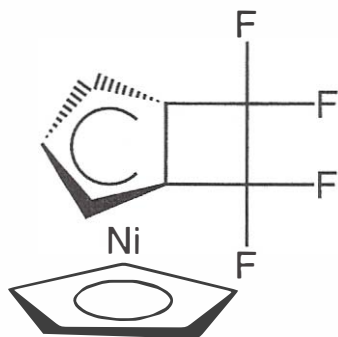$C_5H_5Ni(C_5H_3C_2F_4)$: contains an allyl-like trihapto group

Table 12.4 Electron counting for π-donor ligands

| Electrons contributed	Ligand	Structure	Example
2	η^2-C_2H_4	$H_2C{=}CH_2$	$[PtCl_3(C_2H_4)]^-$ trichloro(ethylene)platinate(I−)
4	η^3-$C_3H_5^-$ η^3-allyl		bis(η^3-ally)di-μ-bromodipalladium
4	η^4-C_4H_8 η^4-butadiene		η^4-butadienetricarbonyliron
4	η^4-C_5H_6 η^4-~~cyclopentadiene~~		dicarbonylbis(η^4-cyclopentadiene)-molybdenum
4	η^4-C_8H_8 η^4-cyclooctatetraene (cot)		$(1, 2, 5, 6$-η^4-cyclooctatetraene)(η^5-cyclopentadienyl)cobalt
6	η^4-$C_4H_4^{2-}$ η^4 cyclobutadiene		tricarbonyl(η^4-cyclobutadiene)iron
6	η^5-$C_5H_5^-$ η^5-cyclopentadienyl (Cp)		tricarbonylchloro(η^5-cyclopentadienyl)molybdenum
	η^5-$Me_5C_5^-$ ~~pentamethyl~~cyclopentadienyl (Cp*)		

Table 12.5   Some bis(cyclopentadienyl) complexes of transition metals (Continued)

| Compound	Color	mp (°C)	Number of unpaired electrons	Structure and comments
"Cp$_2$Rh"	Yellow-orange	Dec. 140	0	Dimer linked through rings; structure I
Cp$_2$Ir	Colorless		>0	19-e species; monomeric ≤ − 196°
"Cp$_2$Ir"	Yellow	Dec. 230	0	Same structure as Rh dimer I
Cp$_2$Co$^+$	Yellow (colorless anion)		0	Prepared by oxidation of Cp$_2$Co or directly from Co halide + Cp$^-$
Cp$_2$Co$^-$	Brown-orange		0?	Prepared by electrochemical reduction in solution
Cp$_2$Rh$^+$	Colorless		0	Prepared directly from RhCl$_3$ + Cp$^-$
Cp$_2$Ir$^+$	Yellow (PF$_6^-$ salt)		0	Prepared directly from IrCl$_3$ + Cp$^-$
Cp$_2$Ni	Dark green	Dec. 173–174	2	20-e species; toxic
Cp$_2$Ni$^+$	Yellow-orange (colorless anion)		1	(Cp$_2$Ni$^+$ + e → Cp$_2$Ni, $E°$ = −0.09 V vs. S.C.E.)
Cp$_2$Ni^{2+}			0	(Cp$_2$Ni^{2+} + e^- → Cp$_2$Ni$^+$, $E°$ = +0.74 V vs. S.C.E.)
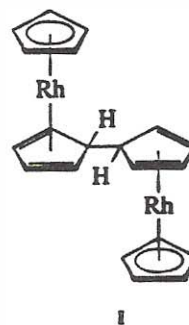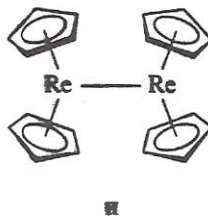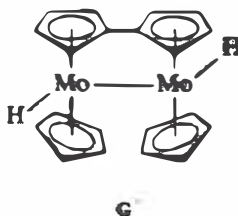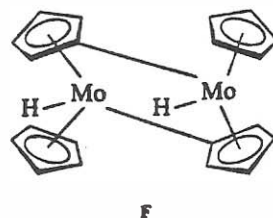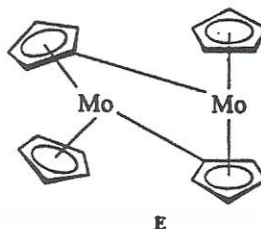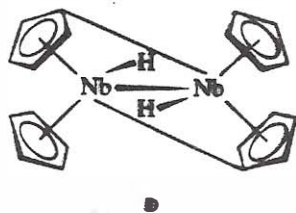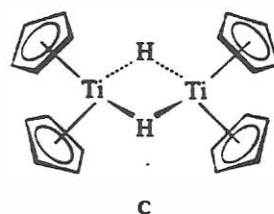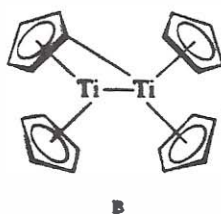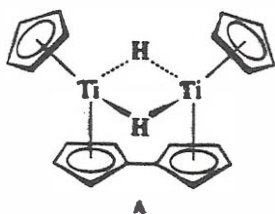
Inorganic Rings, Cages, and Clusters

Multicentered, 3-D aggregates having 3-12 framework atoms-provide a link between discrete molecules and macroscopic matter, so they are of great theoretical and practical importance.

The terms *cage* and *cluster* are used to describe these species, depending on whether localized or delocalized covalent bonding is evidenced.

eg.

X = Pb or BH
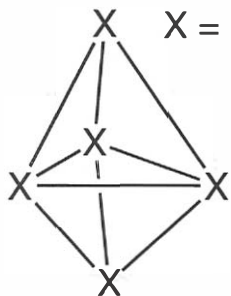
A reasonable bonding model for Pb_5^{2-} can be developed by assuming that there is a covalent Pb-Pb bond along each of the nine edges of the polyhedra; requires 18 of the 22 valence electrons. Remining e^- are nonbonded lone pairs, one on each apical atom.

A Lewis structure therefore can be drawn in which all five Pb atoms have valence octets. Because of the e^--precise bonding (each line = $2e^-$), Pb_5^{2-} may be considered a *cage* anion.

For $B_5H_5^{2-}$, there are again 22 valence e^-'s; however, 10 of them are needed to form the five localized B-H bonds. Only 12 e^-'s remain-too few for the nine B-B nearest-neighbor interactions to be normal 2-e^- bonds. These e^- are delocalized into multicentered MO's; thus $B_5H_5^{2-}$ is a *cluster* anion.

The polyhedra of greatest importance in this are of chemistry are shown below:

(a) Tetrahedron*

(b) Trigonal bipyramid*

(c) Octahedron*

(d) Trigonal prism

(e) Pentagonal bipyramid*

(f) Dodecahedron

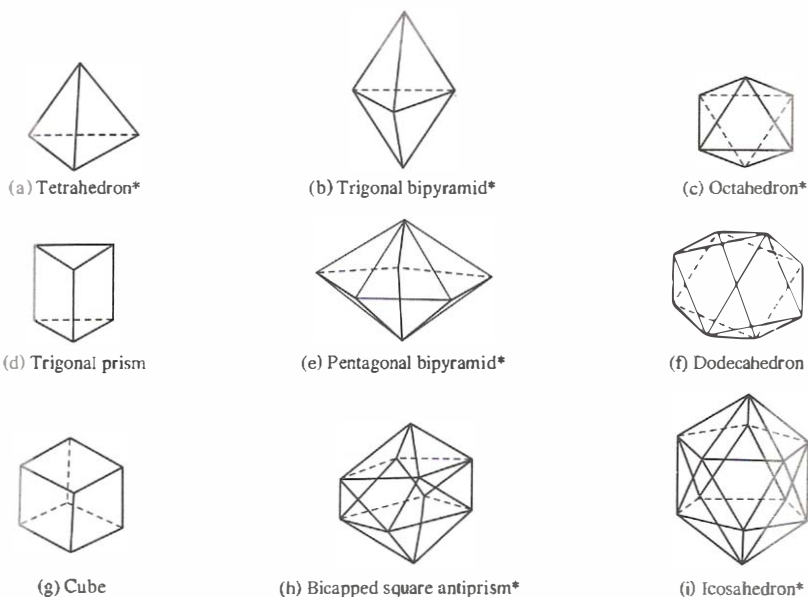(g) Cube

(h) Bicapped square antiprism*

(i) Icosahedron*

Figure 19.1
Common polyhedral frameworks for cage and cluster compounds
(* = deltahedron).

They can be divided into two types-those that are *deltehedral* ("closed" structures in which all the faces are triangular) and those that are not. The tetrahedron, pentagonal bipyramid, bicapped square antiprism, and icosahedron, with 4, 5, 6, 7, 10, and 12 vertices, respectively, are all deltahedral.

The 6n-12 (Deltahedral Cage) Rule

The distinction between deltahedra and other polyhedra is important from the standpoint of chemical bonding. Since the nearest neighbors define the edges of any polyhedron, the maximum possible number of localized two-electron bonds is equal to the number of edges. There is a specific relationship between the number of vertices, n, and the number of edges of deltahedra:

Number of edges $= 3n - 6$

As a result, a total of $6n - 12$ valence e⁻'s maximizes the stability of a deltahedral framework.

eg. P_4

Twelve of the 20 valence e⁻'s are bonding (the others being lone pairs), which is exactly the number required for the framework linkages
($6 \times 4 - 12 = 12$).

Let's change the geometry: P_4 to $P_4(NR_2)_2$ ($R = SiMe_3$). This has the effect of adding 2 valence e⁻'s to the cage system, since one framework P-P bond is converted to two exo-cage P-N bonds:
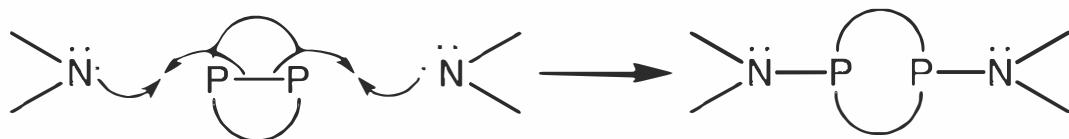
The rupture of the P-P bond causes the involved phosphorus atoms to separate, opening the framework.
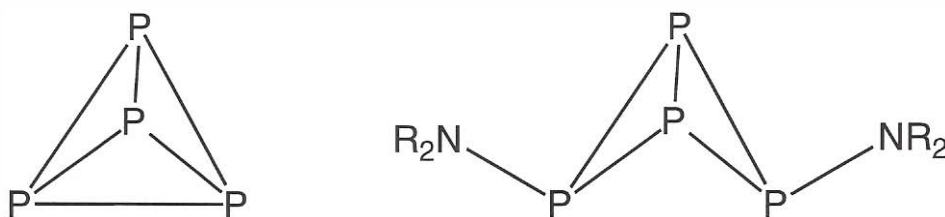
Electron count predictions based on the number of polyhedral edges for cages are summarized on the following page.

**Table 19.1** Number of vertices and edges, and ideal number of electrons for localized bonding in some common three-dimensional frameworks

Structure	Vertices	Edges	Ideal Number of Electrons
Triangle	3	3	6
Tetrahedron	4	6	12
Trigonal bipyramid	5	9	18
Trigonal prism	6	9	18
Octahedron	6	12	24
Pentagonal bipyramid	7	15	30
Cube	8	12	24
Square antiprism	8	16	32
Pentagonal dodecahedron	8	30	60
Tricapped trigonal prism	9	18	36
Monocapped square antiprism	9	20	40
Bicapped square antiprism	10	24	48
Icosahedron	12	30	60

Triangular Arrays

Although not deltahedral, many 3-vertex, triangular "cages" are known that conform to the $6n - 12$ rule: eg. cyclopropane, C_3H_6. Twelve of the 18 valence e⁻'s are used to form the C-H bonds, leaving 6 for the three 2-e⁻ C-C bonds along the edges of the triangle. As in P_4, the addition of e⁻'s causes the structure to open realizing a chain.

eg. $Ru_3(CO)_{12}$
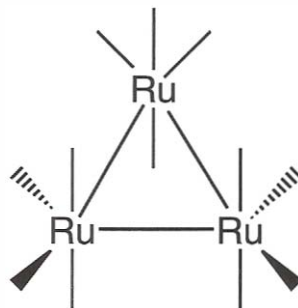
Ru-CO linkages are dative

$Ru = s^2 d^6$

Assume three filled σ nonbonding t_{2g}-type orbitals, so $24 - 3 \times 6 = 6$ e⁻'s available for the three Ru-Ru bonds.

Thus, like the 18 e⁻ rule, this model predicts $Ru_3(CO)_{12}$, its Fe and Os analogues, and valence isoelectronic species such as $H_2Os_3(CO)_{11}$ to be stable.

Another example: Re_3Cl_9.

Each Re(III) has 4 valence e⁻'s; total 12.

Re-Cl interactions are assumed to be dative.

Insufficient to enable occupancy of the t_{2g} subsets. Recall, however, that while these orbitals are σ nonbonding, they do engage in π interactions under the proper circumstances.

In Re_3Cl_9, then, the 12 metal e⁻'s allow for three Re=Re double bonds.

Evidence: Re-Re bond distances = 249 pm (unusually short).
Free element = 275 pm
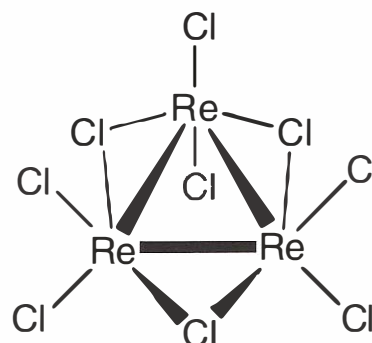
Triosmium Clusters

An important group of three-atom clusters have a core of three Os atoms. Their chemistry is characteristic of that observed for cluster systems, and can therefore be used as a model.

The structures of the parent compound, $Os_3(CO)_{12}$, and three of its hydrido derivatives, $H_2Os_3(CO)_n$ (n - 10-12), are of special interest. Like $Ru_3(CO)_{12}$, triosmium dodecarbonyl consists of three $Os(CO)_4$ units connected by metal-metal bonds conforming to the 18-e⁻ rule.
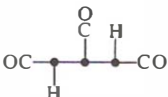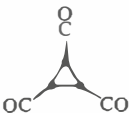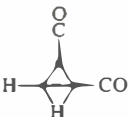
$Os_3(CO)_{12}$ = 48 valence e⁻ (24 from the metals plus 2 from each ligand). Adding 6 shared e⁻'s (three Os-Os bonds) gives 54-exactly 18 per metal atom.

Convert $Os_3(CO)_{12}$ to $H_2Os_3(CO)_{12}$ increases the number of valence e⁻'s from 48 to 50 and what happens?

Next, consider the removal of a carbonyl ligand from $H_2Os_3(CO)_{12}$ to give $H_2Os_3(CO)_{11}$ (48 valence e⁻'s). What happens?

Finally, consider the removal of a second CO group to afford $H_2Os_3(CO)_{10}$. What do we have now?

Compound	Valence e^-	Os–Os Bonds	Geometry	d(Os–Os), pm
$H_2Os_3(CO)_{12}$	50	2		—
$Os_3(CO)_{12}$	48	3		294*
$H_2Os_3(CO)_{11}$	48	3		299 291 286
$H_2Os_3(CO)_{10}$	46	4		282 281 268

Note: ● = Os(CO)₃; * = average value.

Some Osmium Chemistries

Pyrolysis - The heating of $Os_3(CO)_{12}$ to 210°C for 12 hr produces a variety of higher carbonyls: $Os_5(CO)_{16}$ (7%), $Os_6(CO)_{18}$ (80%), $Os_7(CO)_{21}$ (10%), and $Os_8(CO)_{23}$ (2%).

(a) (b) (c)
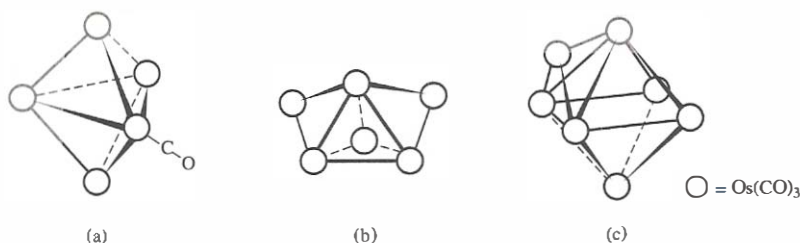
Figure 19.3 The framework structures of three osmium carbonyls: (a) $Os_5(CO)_{16}$, with a trigonal bipyramidal arrangement of osmiums; (b) $Os_6(CO)_{18}$, a copped trigonal bipyramid (or bicapped tetrahedron); (c) $Os_7(CO)_{21}$, a capped octahedron.

Hydrogenation - Triosmium dodecacarbonyl reacts with H_2 under remarkably low pressure (1 atm) to initially form $H_2Os_3(CO)_{10}$. If longer then the tetranuclear cluster $H_4Os_4(CO)_{12}$ is formed.

Reactions with Base - The treatment of $Os_3(CO)_{12}$ with either OH⁻ or BF_4^- gives the $[HOs_3(CO)_{11}]^-$ anion which reacts with protonic hydrogen in two ways: anhydrous Bronsted acids yield the conjugate $H_2Os_3(CO)_{11}$ and rxn with H_3O^+ produces the hydroxo species $HOs_3(CO)_{11}OH$.

$$[HOs_3(CO)_{11}]^- + H_3O^+ \longrightarrow HOs_3(CO)_{11}OH + H_2$$

<u>Substitutions by Other Nucleophiles</u> - Many rxns are known that amount to nucleophilic displacement of CO by other ligands on the $Os_3(CO)_{12}$ substrate.

$$Os_3(CO)_{12} + H_2O \xrightarrow{-CO} [Os_3(CO)_{11}OH_2] \longrightarrow HOs_3(CO)_{11}OH$$

$$Os_3(CO)_{12} + PhCCH \longrightarrow Os_3(CO)_{10}(PhC_2H)$$

$$Os_3(CO)_{12} + H_2S \longrightarrow H_2Os_3(CO)_{19}S$$

$$Os_3(CO)_{12} + Mn(CO)_5^- \xrightarrow{-CO} [Os_3Mn(CO)_{16}]^-$$
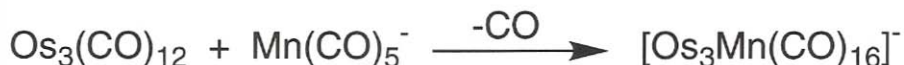
The last two equations represent *cluster expansion* rxns-the # of framework atoms increases from three to four in each case.

<u>Nucleophilic Addition</u> - Because $H_2Os_3(CO)_{10}$ is coordinately unsaturated, it typically reacts with nucleophiles via addition rather than substitution: eg. heating $H_2Os_3(CO)_{10}$ in a CO atmosphere produces $H_2Os_3(CO)_{11}$.

$$H_2Os_3(CO)_{10} + RNC \longrightarrow H_2Os_3(CO)_{10}CNR$$

$$H_2Os_3(CO)_{10} + PPh_3 \longrightarrow H_2Os_3(CO)_{10}PPh_3$$

Tetrahedral Arrays - The Isolobal Analogy

A useful analogy between the bonding properties of organic and inorganic fragments has been pointed out by Hoffman and co-workers as a model for relating the structures of organometallic compounds to organic ones.

If we consider the electronic structure of the 17-e⁻ fragment $Mn(CO)_5^-$, a simple model views the carbonyls as donating e⁻ pairs to five d^2sp^3 hybrids on Mn. Six of the Mn e⁻'s are in t_{2g} orbitals, and the seventh is in the hybrid pointing away from $Mn(CO)_5$. This is analogous to the situation in 7-e⁻ CH_3^- where the sp^3 hybrids on C form C-H bonds and the fourth hybrid points away from the CH_3 group and contains the seventh e⁻.

Table 12.10 Isolobal fragments[a]

Organic Species			
CH_3	CH_2	CH	C
CH_2^-	CH^-	CH_2^-	CH^+
	CH_3^-		

Organometallic Fragment			
$Co(CO)_4$	$Fe(CO)_4$	$Co(CO)_3$	$Fe(CO)_3$
$Mn(CO)_5$	$Cr(CO)_5$	$Mn(CO)_4$	$Cr(CO)_4$
$CpFe(CO)_2$	$CpCo(CO)$	$CpNi$	$CpCo$
$CpCr(CO)_3$	$CpMn(CO)_2$	$CpFe(CO)$	$CpMn(CO)$
	$Ni(CO)_2$	$CpCr(CO)_2$	
	$Ni(CO)_3$		

Read vertically.

In general, we call two fragments isolobal *"if the number, symmetry properties, approximate energy, and shape of the frontier orbitals and the number of e⁻ in them are isolobal."*

CH$_3$ Co(CO)$_4$ Mn(CO)$_5$

(a)

:S̈   CH$_2$ Fe(CO)$_4$

(b)
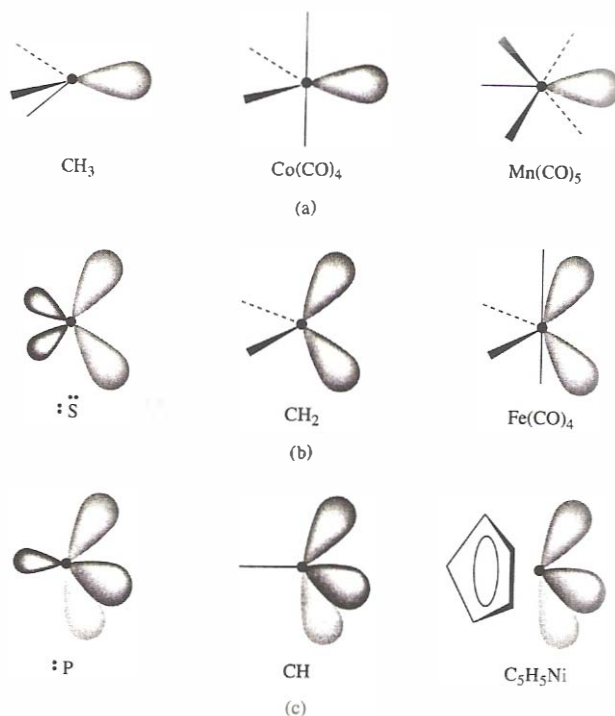
Figure 19.5
Some examples of isolobal molecular fragments: groups having (a) one, (b) two, and (c) three "active" orbitals, respectively.

:P   CH   C$_5$H$_5$Ni

(c)

MO energy and contour diagrams for many organometallic fragments have been calculated. It turns out than an isolobal relation exists between organo-metallic fragments having (18 - *n*) e⁻'s and organic fragments having (8 - *n*) e⁻'s.

eg. 16-*e* Fe(CO)$_4$ is isolobal with 6-*e* CH$_2$.

Table 19.3 Isolobal groups commonly encountered in molecular clusters

0	1	2	3
H$_2$	H		
CH$_4$	CH$_3$	CH$_2$	CH
Cl$_2$	Cl		
		S	
			P
Cr(CO)$_6$			
	Mn(CO)$_5$		
Fe(CO)$_5$		Fe(CO)$_4$	
	C$_5$H$_5$Fe(CO)$_2$		C$_5$H$_5$Fe(CO)
	Co(CO)$_4$		Co(CO)$_3$
C$_5$H$_5$Co(CO)$_2$		C$_5$H$_5$Co(CO)	
Ni(CO)$_4$		Ni(CO)$_3$	
	C$_5$H$_5$Ni(CO)		C$_5$H$_5$Ni

Note: The 0 column lists species that are coordinately saturated; members of the 1 column have one active lobe; etc.

The Bonding in Delocalized Clusters

The Electron Counting (Wade-Mingos) Rules

There is a definite relationship between the framework e⁻ count and the geometry of localized clusters. Unlike e⁻-precise cages, the approach used for clusters is somewhat different: **Wade-Mingos Rules**.

Based on MO theory. It can be shown that a closed polyhedron having n vertices ($n > 4$) has $n + 1$ bonding MO's, which are filled by $2n + 2$ framework e⁻'s. This $2n + 2$ rule is therefore the counterpart of the $6n - 12$ rule for deltahedral cages:

$$T - 2n + 2$$
where T is the total # if delocalized e⁻'s and n is the # of vertices.

Polyhedral e⁻ count versus predicted structure according to Wade-Mingos rules.

Electron Count	# of Vertices	Predicted Structure
12	5	Trigonal bipyramid
14	6	Octahedron
16	7	Pentagonal bipyramid
18	8	Dodecahedron
20	9	Tricapped trigonal prism
22	10	Bicapped square antiprism
24	11	Hexadecahedron
26	12	Icosahedron

The contribution by each vertex unit to the delocalized MO's is determined as follows. For a main group element such as B, three of the four valence orbitals (which are sometimes assued to be sp^3 hybrids) are used to form the cluster MO's. The fourth is involved in exo-cluster bonding (for B, this is usually to a H atom). That leaves two e⁻'s to be donated for the framework bonding.

Figure 19.13
Orientation of the valence orbitals of a BH unit in a polyhedral borane cluster; the boron is assumed to have sp^3 hybridization.

To cluster
3 orbitals
2 electrons
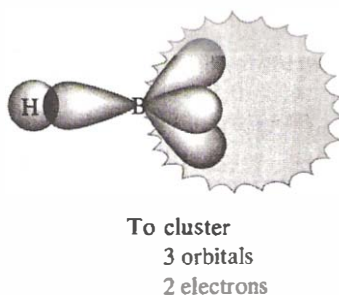
The Boron Hydrides

Polyhedral boron-hydrogen compounds are of historical importance, since they were the first group of compounds to be recognized as clusters. The earliest boron hydrides were prepared by Stock and co-workers, who developed vacuum-line techniques to permit their isolation and study. The Stock series contains the six compounds B_2H_6, B_4H_{10}, B_5H_9, B_5H_{11}, B_6H_{10}, and $B_{10}H_{14}$.

Diborane, B_2H_6, can be considered the parent member of the boron hydrides, since most of the others are prepared-either directly or indirectly-from its thermal decomposition. It can be synthesized by various acid-base and redox reactions.

$$2NaBH_4 + 2H_3PO_4 \longrightarrow B_2H_6 + 2NaH_2PO_4 + 2H_2$$

$$3NaBH_4 + BCl_3 \longrightarrow 2B_2H_6 + 3NaCl$$

$$2NaBH_4 + I_2 \longrightarrow B_2H_6 + 2NaI + H_2$$

Adduct Formation (Nucleophile Cleavage)

The diborane molecule is readily cleaved by nucleophiles. The fragmentation may be either symmetric (to give two BH_3 groups) or asymmetric (forming BH_2^+ and BH_4^-).

$$B_2H_6 + 2CN^- \longrightarrow 2BH_3CN^-$$

$$B_2H_6 + 2NH_3 \longrightarrow [BH_2(NH_3)_2]^+BH_4^-$$

Oxidation-Reduction

A host of reactions are known in which the borons of B_2H_6 are oxidized to B(III).

$$B_2H_6 + 6H_2O \longrightarrow 2B(OH)_3 + 6H_2$$

$$B_2H_6 + 3O_2 \longrightarrow B_2O_3 + 3H_2O$$

The great exothermicity of these rxns (ΔH^o = -2160 kJ.mol) led people to consider B_2H_6 for use as a rocket fuel additive (1950's and 60's).
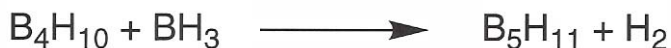
Addition Across Multiple Bonds

$$B_2H_6 + 2H_2C=CHR \longrightarrow 2H_2BCH_2CH_2R$$

H.C. Brown (Purdue)
A. Burg (USC)

Higher Boranes

Higher boranes are formed sequentially via rxns like the following:

$$B_3H_7 + BH_3 \longrightarrow B_4H_{10}$$

$$B_4H_{10} + BH_3 \longrightarrow B_5H_{11} + H_2$$

$$B_5H_{11} \longrightarrow B_5H_9 + H_2$$

$$2B_5H_9 \longrightarrow B_{10}H_{14} + 2H_2$$

The higher boranes generally mimic diborane in their physical and chemical properties, but become less volatile and less chemically reactive with increasing size. For example, B_2H_6 is gaseous well below rt (bp = -93°C), and it explodes on contact with air or water. B_5H_9 is a colorless liquid at rt (bp = 60°C). Like B_2H_6, it explodes on contact with air, but it is easily handled using standard vacuum-line techniques. $B_{10}H_{14}$ is a white solid that decomposes only slowly in air.

Typical reaction of the higher boranes include
1. adduct formation
2. displacement of terminal hydrogen by nucleophiles or electrophiles
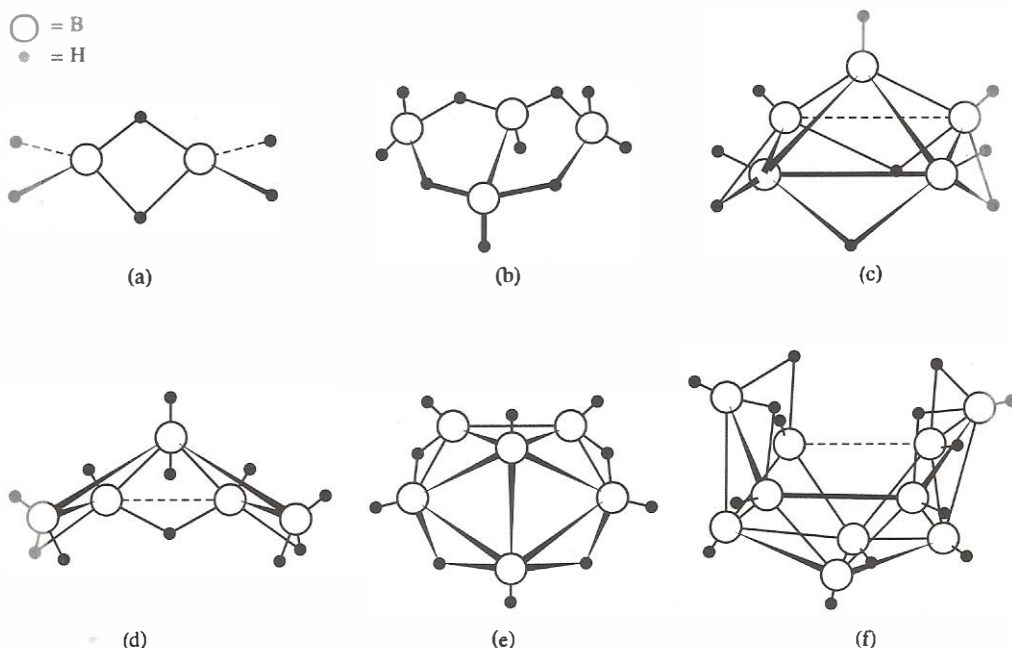3. chemical reduction
4. coupling

Figure 19.16 The structures of Stock's polyhedral boranes: (a) B_2H_6; (b) B_4H_{10}; (c) B_5H_9; (d) B_5H_{11}; (e) B_6H_{10}; (f) $B_{10}H_{14}$.

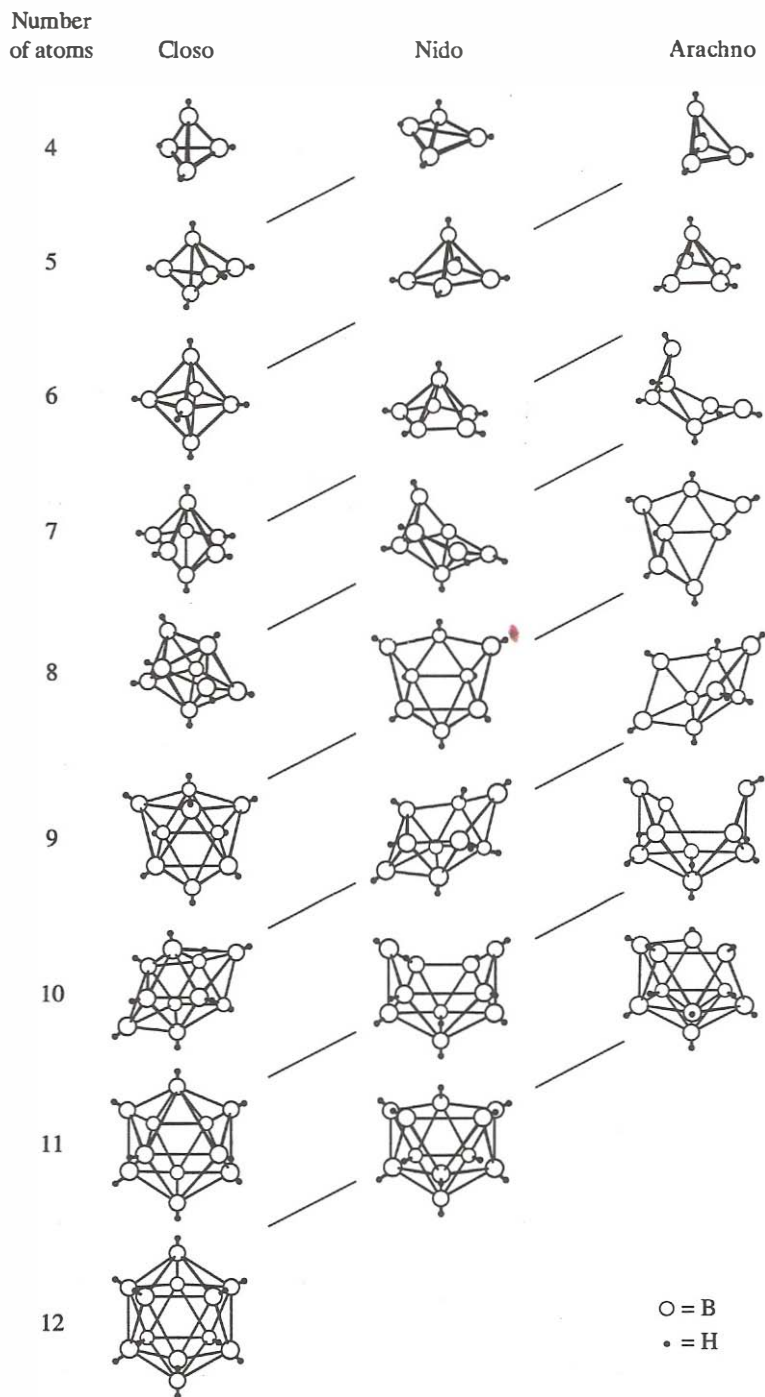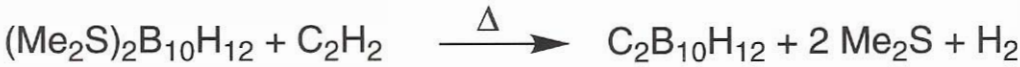| Number of atoms	Closo	Nido	Arachno

Figure 19.15 Structural relationships among closo, nido, and arachno boranes. [Reproduced with permission from Rudolph, R. W. *Acc. Chem. Res.* **1976**, *9*, 446.]

O = B
• = H

Higher Boranes

In a variation of the hydroboration rxn, alkynes can be used to incorporate carbon atoms into polyhedral boranes or their anions or adducts. The rxn products are called carboranes.

$$B_5H_9 + MeCCMe \xrightarrow{\Delta} Me_2C_2B_4H_6 + 0.5\ B_2H_6$$

$$(Me_2S)_2B_{10}H_{12} + C_2H_2 \xrightarrow{\Delta} C_2B_{10}H_{12} + 2\ Me_2S + H_2$$

Many carboranes have been prepared in this matter. For example, all members of the series $C_nB_nH_{n+2}$ (n = 3-10) have long been known.
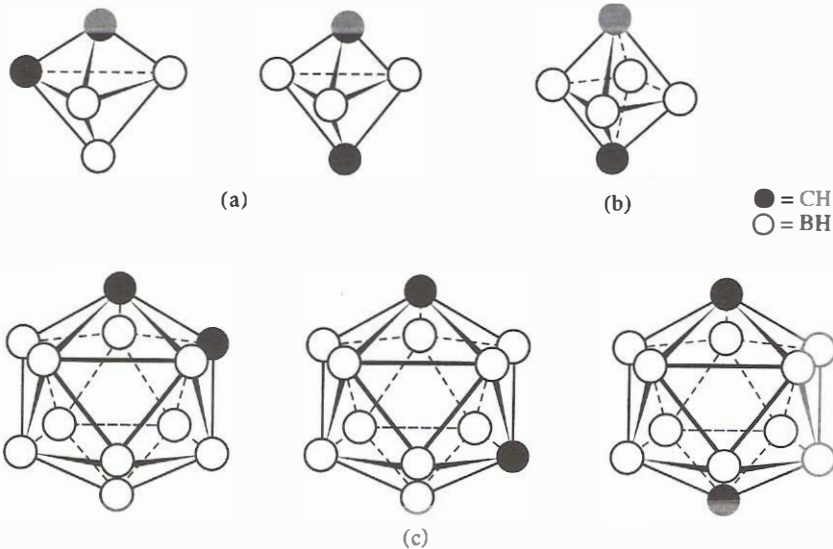

(a)   (b)

● = CH
○ = BH

Figure 19.17
Selected closo carboranes:
(a) the 1,2- and 1,5-Isomers of $C_2B_3H_5$;
(b) 1,6-$C_2B_4H_6$;
(c) the three isomers of $C_2B_{10}H_{12}$.

(c)

Metallaboranes and Metallacarboranes

The incorporation of metals into borane and carborane clusers produces metallaboranes and metallacarboranes, respectively. The synthetic pathways to such species fall primarily into two broad types, depending on whether the initial substrate is a borane/carborane or a metal aggregate.

$$C_2B_3H_5 + C_5H_5Co(CO)_2 \xrightarrow{\Delta} C_5H_5CoC_2B_3H_5 + 2CO$$

$$B_5H_9 + Fe(CO)_5 \xrightarrow{\Delta} (CO)_3C_5H_5FeB_4H_8$$
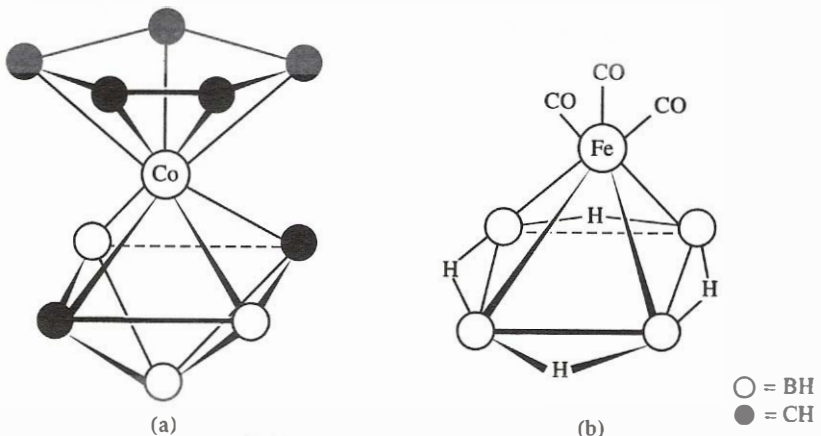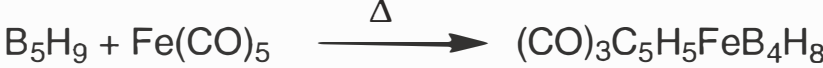
Figure 19.19
The structures of a metallocarborane and a metalloborane:
(a) $C_5H_5CoC_2B_3H_5$;
(b) $(CO)_3FeB_4H_8$.

(a)   (b)

○ = BH
● = CH

The products both have octahedral-based geometries as predicted by the Wade-Mingo rules:

For $C_5H_5CoC_2B_3H_5$: (3×2) (BH) + (2×3) (CH) + (1×2) (C_5H_5Co) = $14e^-$

For $(CO)_3C_5H_5FeB_4H_8$: (4×2) (BH) + (1×2) $[Fe(CO)_3]$ + (4) (H) = $14e^-$

Another approach involves the preparation of a borane or carborane anion by the removal of a bridging hydrogen, followed by reaction with a metal halide. This may lead to metal bridgin, substitution, and/or cluster expansion, depending on the situation.

$$Fe^+ + 2C_2B_9H_{11}^{2-} \longrightarrow [Fe(C_2B_9H_{11})]^{2-}$$

The dicarbollide ion, $C_2B_9H_{11}^{2-}$, and its interactions with various metal ions have been extensively studied by Hawthorne and co-workers.

The $CoCl_2 + C_2B_4H_7^- + C_5H_5^-$ systems is especially interesting. A variety of compounds can be isolated from this reaction, including $C_5H_5CoC_2B_4H_6$ (an addition product), $C_5H_5CoC_2B_3H_7$ (an insertion product), and $(C_5H_5)_2Co_2C_2B_3H_5$ (combination addition and insertion).

$(C_2B_4H_6)Co(C_5H_5)$ $(C_2B_3H_5)Co_2(C_5H_5)_2$ $(C_2B_3H_7)Co(C_5H_5)$

○ = BH
● = CH

○ = BH
● = CH
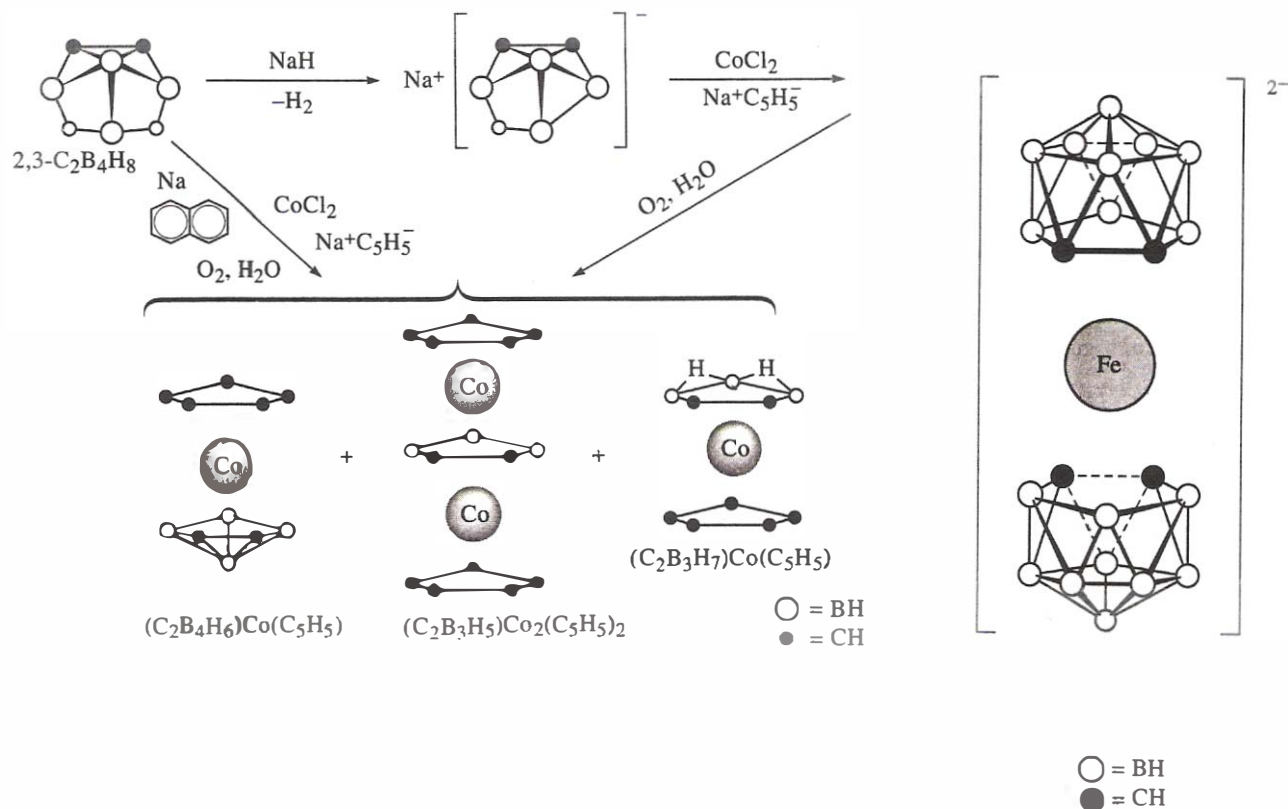
Examples Using the Wade-Mingos Rules

Consider $1,2\text{-}C_2B_4H_6$: octahedral
The framework electron count is
$(2 \times 3)\,(CH) + (4 \times 2)\,(BH) = 14\ e^-$

Based on the $2n + 2$ rule, $14\ e^-$ are the ideal number for an octahedral framework, and the experimental structure coincides with this prediction.

Consider $C_2B_4H_8$: Here, the two "extra" hydrogens are in bridging positions between adjacent borons, and their electrons must be included in the framework count.
$(2 \times 3)\,(CH) + (4 \times 2)\,(BH) + 2 = 16\ e^-$

Solving the $T = 2n + 2$ equation, $n = 7$, so a pentagonal bipyramid framework is predicted.

However, since only six heavy atoms are present, one vertex must remain vacant. The experimental geometry is a pentagonal pyramid, which results from "decapping" one of the apical vertices.

Clusters that are one vertex removed from a closo (all vertices occupied) structure are described as nido ("nestlike). Species lacking two vertices are arachno ("weblike").

Bioinorganic Chemistry

Which of the chemical elements are necessary to sustain life? What are their specific functions? In what chemical forms are they found in vivo? The role of inorganic elements in biological processes has received steadily increasing emphasis since about 1970. This has created *bioinorganic chemistry*.

Essential Elements, Toxins, Abundance, and Availability

The mere presence of an element within an organism does not prove it to be necessary for the organism's survival. Approx. 30 elements are required by all life forms.

H   He

Li Be   B C N O F Ne

Na Mg   Al Si P S Cl Ar

K Ca Sc Ti V Cr Mn Fe Co Ni Cu Zn Ga Ge As Se Br Kr

Rb Sr Y Zr Nb Mo Tc Ru Rh Pd Ag Cd In Sn Sb Te I Xe

Cs Ba La Hf Ta W Re Os Ir Pt Au Hg Tl Pb Bi Po At Rn

Fr Ra

Four of the major categories relate to (1) structure (the proteinaceous elements; Ca for obnes, teeth, and shells, etc.); (2) energy utilization and storage (eg., P in the adenosine phosphates); (3) material transport and storage (eg. of O_2 by certain Fe and Cu complexes); and (4) catalysis (primarily, complexes of mg and the transition metals).

Most of the nonessential elements (and some of the others as well) are toxic above some concentration limit. Toxicity usually arises in one of three ways:

1. **Blockage of an Active Site of Some Biomolecule.** Numberous π acceptor ligands, including CO, CN^-, H_2S, and PH_3, bind strongly do the Fe centers of hemoglobin and myoglobin blocking that coordination site from the weaker ligand O_2, and destroys the ability of those molecules to serve as oxygen carriers.

2. Metal-Metal Displacement. A nonessential metal having chemical properties similar to an essential metal is often toxic: eg., Ba is poisonous to humans, parly because it displace Ca. Also, the toxicity of Cd is due in part to its ability to displace Zn from certain enzymes and thereby deactivate them.

3. Modification of Molecular Structure. The N, O, and S atoms of proteins can serve as ligands for metal ions. However, the H-bonding and other intermolecular interactions that determine the structural conformation of a protein are usually altered upon coordination to a metal. The result is a different molecular shape and, in many cases, deactivation.

A general order of elemental toxicity is Te>Se>Be>V>Cd>Ba>Hg>Tl>As >Pb>Sn>Ni>etc. The order changes somewhat, depending on the organism.

Approximate Concentrations of Selected Elements
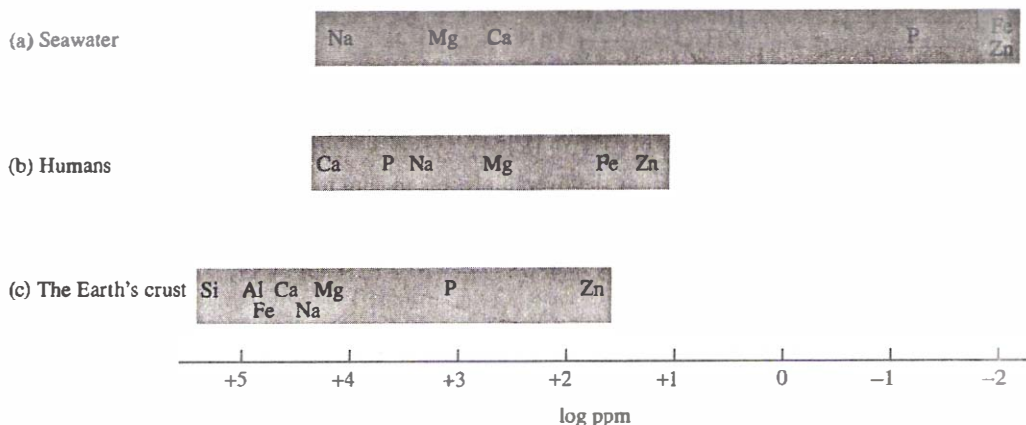
Photosynthesis

Photosynthesis is the use of solar energy by plant cells for the synthesis of cell components. The organic products of photosynthesis are carbohydrates, and the carbon source is CO_2.

$$2H_2Z + CO_2 \longrightarrow 1/x(CH_2O)_x + H_2O + 2Z$$

Here, H_2Z is a H source-reducing agent and Z is its oxidized form. This reagent is H_2S in the so-called *sulfur bacteria*, and an organic alcohol for certain other bacteria. In the most familiar cases (the green plants), water is the source of H and O_2 is the by-product. Hence, photosynthesis is complementary to the process that enables muscle contraction in mammals.

$$2H_2O + CO_2 \longrightarrow 1/x(CH_2O)_x + O_2$$

84

Studies have shown that the molecular oxygen is produced from H_2O rather than CO_2: suggest the oxidation half-rxn is

$$2H_2O \longrightarrow 4H^+ + O_2 + 4e^-$$

The standard potential for this oxidation is -1.23 V. The higher pH of physiological conditions makes it somewhat less disfavored, but still negative (E_{phys} = -0.82 V).

In order for the overall process to sum up to the second eq, the reduction half-rxn must be

$$2CO_2 + 4H^+ + 4e^- \longrightarrow 2/x(CH_2O)_x + O_2$$

When glucose is the product, the physiological potential of the overall rxn is about -1.2 V. The need for an energy source is therefore obvious.

The photosynthesis process can be divided into four sequential steps:
1. Solar energy is absorbed, primarily by biomolecules known as *chlorophylls* and *carotenoids*.
2. Electron transfer occurs from excited-state chlorophyll molecules to and from a series of redox agents, including a *ferrodoxin*. This is accomplished within what is described as *photosystem II*.
3. The oxidation of water to O_2 occurs, being catalyzed by a structurally complex, Mn-containing enzyme. This is *photosystem II*.
4. CO_2 is reduced to carbohydrate.

The Chlorophylls

Chlorophylls are green pigments that are highly efficient at absorbing radiant energy in the visible and near-ultraviolet regions: many are known. One of the best-characterized, chlorophyll *a* is pictured below:

The structure of chlorophyll *a*. Other chlorophylls vary mainly in their substituents at the positions indicated by the arrows.

5.   Strouse, C. E. *Prog. Inorg. Chem.* 1976, *21*, 159.
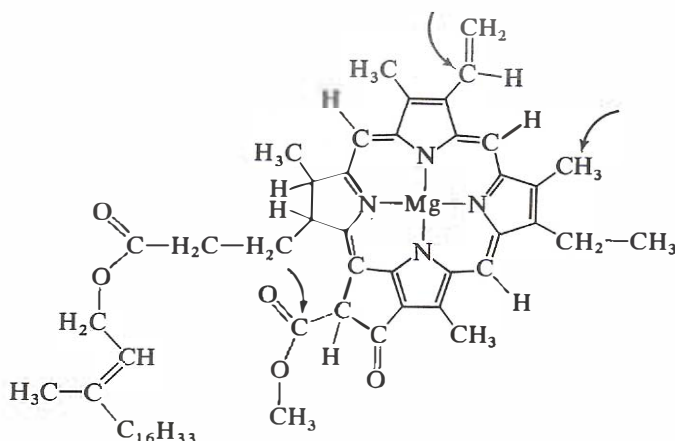
Chlorophyll *a* has three parts:

1. The Mg^{2+} ion is 4-coordinate. (A H_2O molecule acts as a fifth coordination site in aqueous solution.) Four coplanar nitrogens serve as Lewis bases. The metal is raised above the ligand plane by about 40 pm, giving local C_{4v} (square pyramidal) geometry.
2. The porphyrin ring system forms a tetradentate cavity for the metal. There are four C_4N rings, which are interconnected by methine bridges.
3. A long-chain, organic *phytyl* group dangles from one ring; contains 20 C's, linked to the rest of the molecule via an ester functional group.

In an organic solvent: $\pi \longrightarrow \pi^*$, max 420 and 660 nm.
In living cells: max at 685 nm.

Chlorophyll *a* dimerizes in nonpolar solvents by coordination of a carbonyl oxygen to the metal ion of the second molecule: longer oligomers are thought to exist in aqueous solution. The individual molecules are linked by H-bonding between the coordinated H_2O and carbonyl oxygens, pro-ducing a linear chain: crucial to the catalytic activity-the photoelectron "hopped" from one molecule to the next in the chain.

Postulated structure of the dimer of chlorophyll *a*. [Reproduced with permission from Katz, J. J. In *Inorganic Biochemistry*; Elchhorn, G. L., Ed.; Elsevier: New York, 1973; Volume 2, p. 1022.]
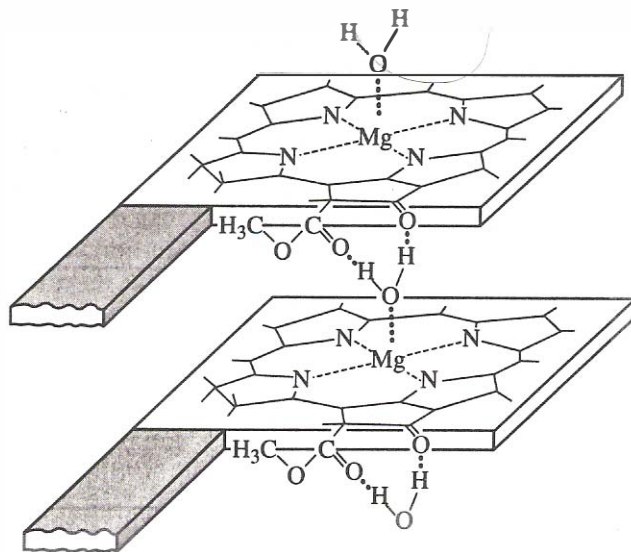
Possible Structure-Function Correlations

How do we rationalize the "choice" of Mg rather than some other metal? We can give at least four reasons:

1. Mg is among the most abundant of all metals.

2. The Mg^{2+} ion is a hard Lewis acid, and therefore has an affinity for the nitrogen bases.

3. The size of Mg(II) is such that it nicely fits the porphyrin cavity. It is small enough to permit strong metal-ligand interactions, but large enough to cause it to lie above, rather than in, the plan of nitrogens. This facilitates interaction with H_2O and, hence, oligomerization.

4. Unlike many divalent metals, Mg(II) has essentially no reduction chemistry. An easily reduced metal center might capture the excited electron via charge transfer. This would prevent the intermolecular electron donation required in photosystem I.

The porphyrin ring stabilizes the complex in several ways. The conjugated double bonds make the organic portion of the molecule stable to photo-decomposition. The chelate effect adds to the stability of the inorganic region. Another benefit of the extended conjugation is that it shifts the $\pi \rightarrow \pi^*$ transitions into the visible region.

Table 22.1 The effect of. conjugation on the $\pi \rightarrow \pi^*$ transitions of some organic species

Compound	Number of Conjugated C=C Bonds	λ_{max}, nm
Ethene	1	165
1,3-Butadiene	2	217
1,3,5-Hexatriene	3	253
β-Carotene	11	465
Chlorophyll a	10 (including C=N linkages)	660

This is important, because the highest-intensity wavelengths of the solar energy reaching Earth are in the visible domain. Furthermore, p-type conjugation gives structural rigidity. This limits the amount of absorbed energy lost to thermal vibration.

The phytyl group provides a hydrophobic region to complement the hydrophilic Mg-porpyrin section, giving the chlorophylls both water and lipid solutibility.

The Role of Mn in Photosystem II

The oxidation of H_2O to O_2 in photosystem II involves catalysis by a Mn-containing enzyme (MW = 25 kD). Exact structure is presently unknown but there has been significant progress toward the understanding of the catalytic mechanism.

ESR. The spin quantum # of ^{55}Mn is 5/2. This results in complex hyperfine splittings and causes the ESR spectra to be difficult to interpret. On the other hand, once the spectra are understood, the amount of structural information gleaned from the hyperfine interactions (along the relaxation effects) is considerable.

The spectrum obtained for the reduced form of the enzyme is consistent with a cluster containing four ligated Mn(II) ions surrounded by a protein. It is now believed that the four metals plus four oxygens form a cubic subunit.

Proposed mechanism of oxidation–reduction for the manganese-containing cluster of photosystem II. The cubic S_0 is the most reduced, and the adamantanelike S_4 the most oxidized, of the five states. [Reproduced with permission from Brudvig, G. W.; Crabtree, R. H. *Proc. Nat. Acad. Sci.* **1986**, *83*, 4586.]
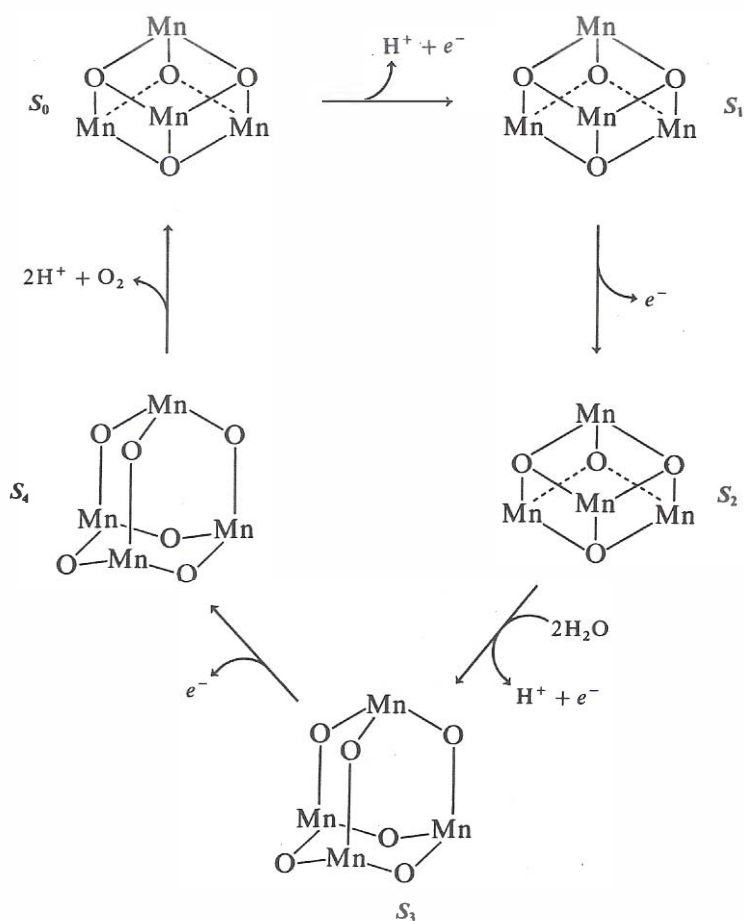
During the course of the postulated catalysis mechanisms, this subunit is oxidized in four sequential steps, ultimately producing a Mn(II) cluster:

$$[Mn_4O_4] + 2H_2O \longrightarrow [Mn_4O_6] + 2H^+ + 4e^-$$
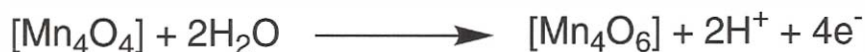
An adamantanelike structure is proposed for this oxidized subunit, with the Mn ions still forming a T_d array.

The overall coordination geometry about each metal is thought to be T_d, with the fourth ligand supplied by the surrounding protein. Subsequent O=O bond formation and the elimination of molecular oxygen returns the system to the reduced state:

$$[Mn_4O_6] \longrightarrow [Mn_4O_4] + O_2$$

Nitrogenases

$$N\equiv N \qquad 942 \text{ kJ/mol}$$

Certain blue-green algae, yeasts, and bacteria are capable of reducing N_2 to NH_4^+, a form amenable to the production of amino acids. Such organisms manufacture an enzyme known as *nitrogenase* for that purpose.

$$N_2 + 8H^+ + 6e^- \longrightarrow 2NH_4^+$$
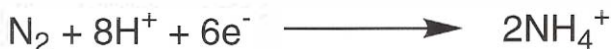
The ability of this enzyme to hydrogenate N_2 under *ambient* conditions is remarkable; consider that the industrial conversion of N_2 to NH_3 involves both very high T (700°C) and P (30 atm).

Like most enzymes, the structure of nitrogenase varies somewhat, depending on the source. Common features include:
1. Nitrogenase actually consists of two separate proteins; neither is catalytically active without the other. The larger of the two has a MW of 230 kD. It contains between 24 and 36 Fe's, and equal number of S's, and 2 Mo's. The smaller protein (60 kD) has an Fe_4S_4 cluster unit (probably a cube).
2. These enzymes appear to operate in an anaerobic atmosphere. This is probably necessary to avoid oxidation to nitrogen oxides and H_2O.
3. The presence of certain small molecules inhibits the process; eg, CO and H_2.

Possible Mechanisms of Action

Very recent developments have confirmed the structure of the nitrogenase (Rees, *et, al*. at Caltech, in some very important *Science* paper of 1993-94.

Dinitrogen Complexes: Model Systems

Many complexes have been synthesized that mimic the behavior of nitrogen. For example, several bis(dinitrogen) complexes produce NH_3 upon treatment with strong acid: eg, *trans*-$Mo(triphos)(N_2)_2(P(C_6H_5)_3)$. The rxn of this species with anhydrous HCl or HBr follows the eq

$$2[Mo^0]\text{-}(N_2)_2 \longrightarrow 2[Mo(III)(] + 3N_2 + 2NH_3$$

Model systems containing Mo and Fe centers connected by one or more bridging ligands also have been reported. In particular, many mixded-- metal Fe-S-Mo clusters are now known.
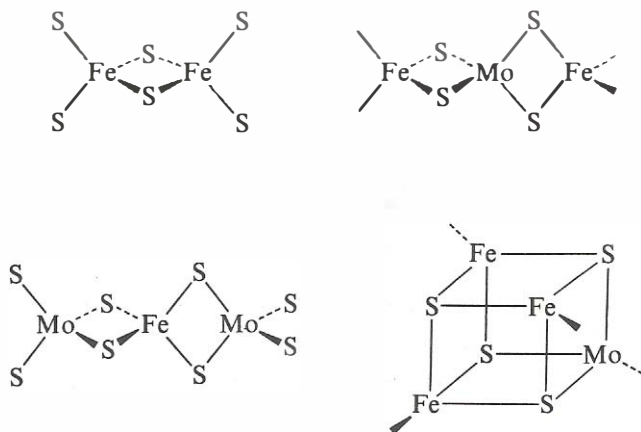
The frameworks of some known iron–sulfur–molybdenum cluster compounds and ions.

11. Holm, R. H. *Chem. Soc. Rev.* **1981**, *10*, 455.

12. Baumann, J. A.; Bossard, G. E.; George, T. A.; Howell, D. B.; Koczon, L. M.; Lester, R. K.; Noddings, C. M. *Inorg. Chem.* **1985**, *24*, 3568.

Zinc-Containing Enzymes

A remarkable number of zinc-containing enzymes-well over 100 in humans alone-have been identified. The broad utilization of Zn by living organisms is remarkable considering its abundance and availability. Based on the functions of many of its enzymes, it can be speculated that the popularity of Zn(II) is due to its ability to act as a Lewis acid w/o engaging in either oxidation or reduction.

We will now examine a few zinc-containing enzymes.

Bioinorganic Chemistry

The catalytic power of proteins comes from their capacity to bind substrate molecules in precise orientations and to stabilize transition states in the making and breaking of chemical bonds.

$$\xrightleftharpoons[K_d]{K_b}$$

This basic principle can be made concrete by a simple example of enzymatic catalysis, the hydration of CO_2 by carbonic anhydrase.

Carbonic Anhydrase

Carbonic anhydrase is important because it brings substrates into close proximity and optimizes their orientation for rxn.

Fig. 39-12. CO_2 exchange in the lungs. CO_2 is carried in solution in the plasma. in combination with hemoglobin in the red cell ($HHbCO_2$), in the form of carbonic acid (H_2CO_3) in the red cell. and as bicarbonate (HCO_3^-) in the red cell and plasma.
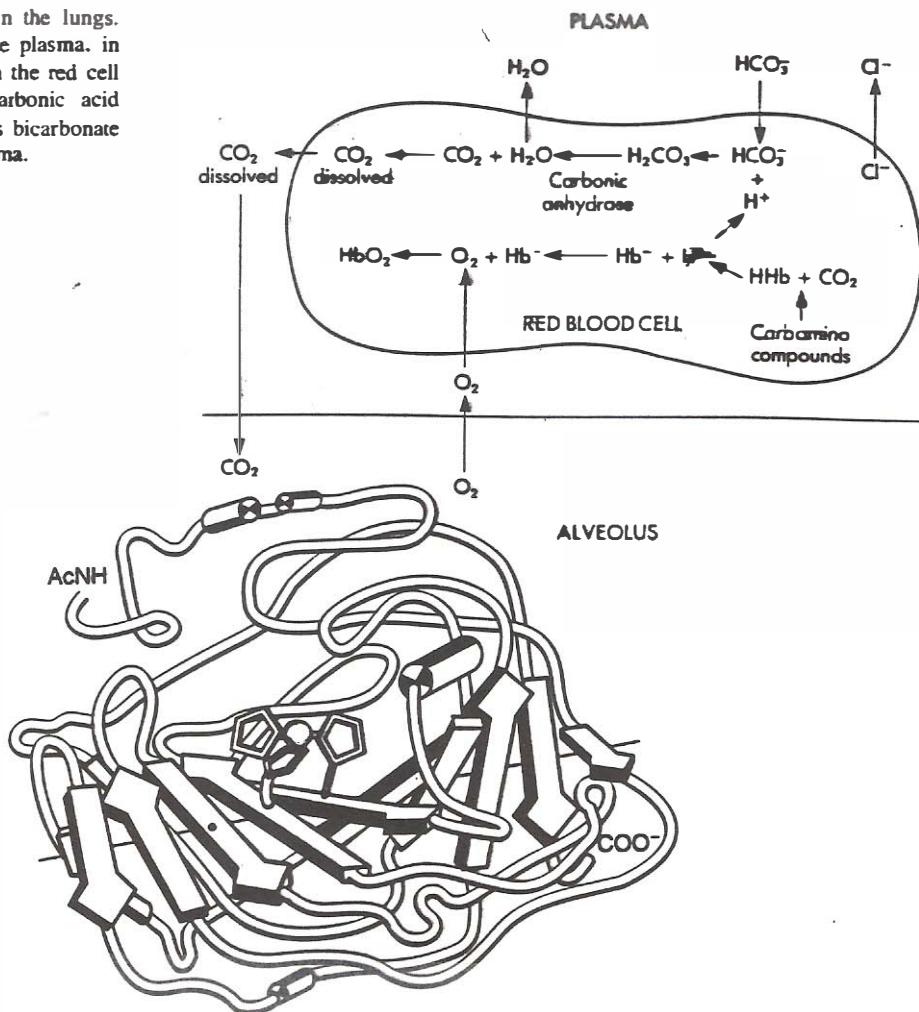
Bovine Pancreatic Carboxypeptidase A

A digestive enzyme that hydrolyzes the carboxyl-terminal bond in poly-peptide chains.
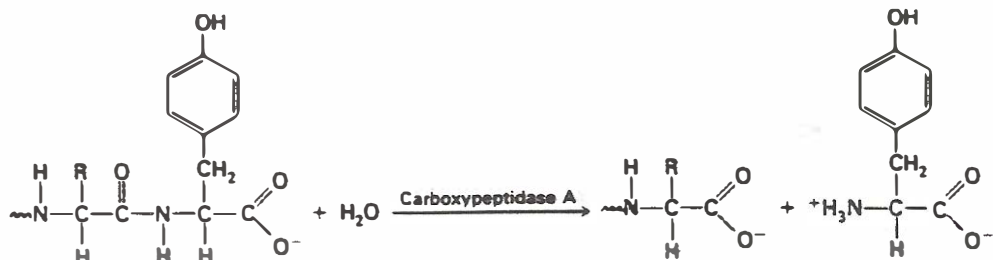
Structure solved by W. N. Lipscomb (Harvard, 1967) and colleagues.

This enzyme is a single polypeptide chain of 307 amino acid residues; dimensions 50 X 42 X 38 Å.

A tightly bound **zinc** ion is essential for enzymatic activity.

Zinc lies in a pocket where it is coordinated in a tetrahedral array to two histidines, one glutamate and one water molecule

A zinc ion is coordinated to two his-tidine side chains and a glutamate side chain at the active site of car-boxypeptidase A. A water molecule coordinated to the zinc is not shown here. [After D. M. Blow and T. A. Steitz. X-ray diffraction studies of enzymes. *Ann. Rev. Biochem.* 39:78. Copyright © 1970 by Annual Reviews, Inc. All rights reserved.]
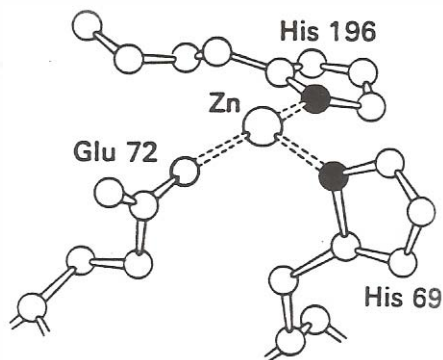
Bovine Pancreatic Carboxypeptidase A

Two facets of the catalytic mechanism of carboxypeptidase A are note-worthy:

1. Induced fit. The binding of substrate is acc. by many changes in the structure of the enzyme.

2. Electronic strain. The enzyme contains a Zn atom and other groups at the active site that induce rearrangements in the distribution of e⁻'s in the substrate, rendering it more susceptible to hydrolysis.
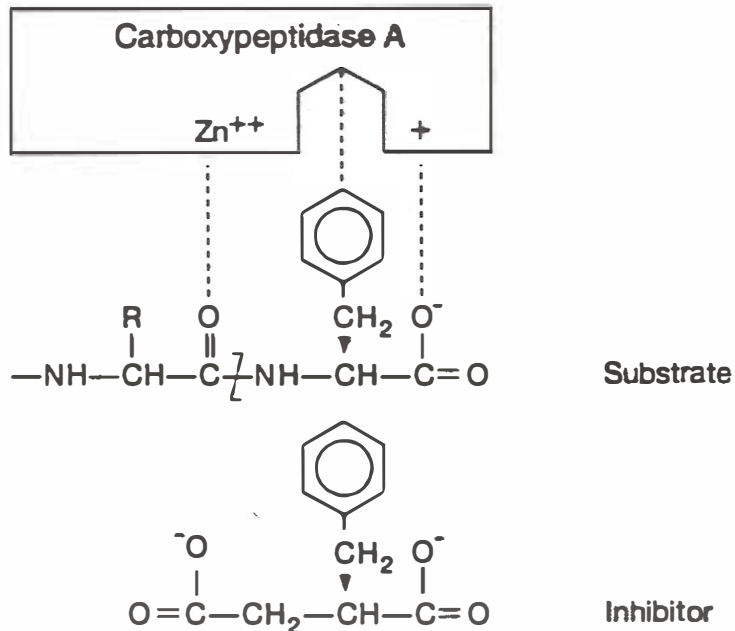
Glycyltyrosine, a slowly cleaved substrate, binds to carboxypeptidase A through multiple interactions.

Let's run through them.
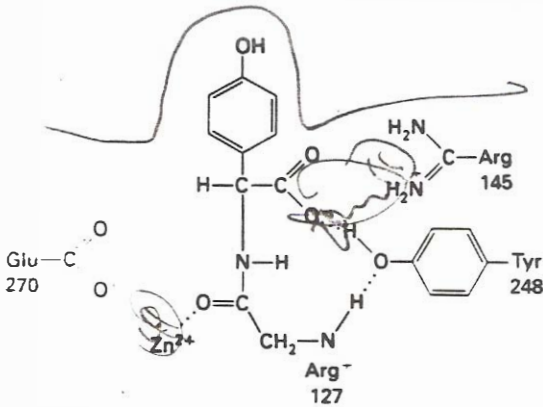
Schematic representation of the binding of glycyltyrosine (black) to the active site of carboxypeptidase A.

Three-dimensional structure of glycyltyrosine at the active site of carboxypeptidase A. Glycyltyrosine, the substrate, is shown in red. [After D. M. Blow and T. A. Steitz. X-ray diffraction studies of enzymes. *Ann. Rev. Biochem.* 39:79. Copyright © 1970 by Annual Reviews, Inc. All rights reserved.]
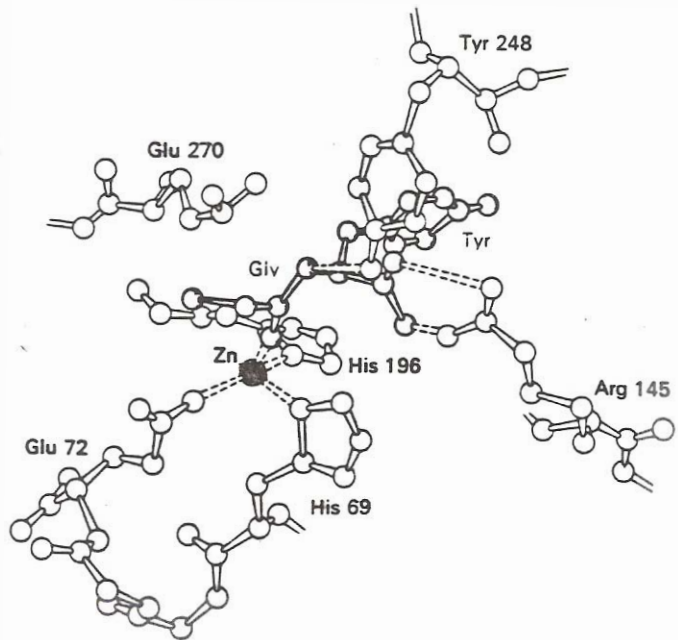
Structural Rearrangement of Carboxypeptidase A on Binding

If we can go back to the induced-fit model of enzyme action: there are some major conformational changes in carboxypeptidase A on binding to substrates, in this case glycyltyrosine.
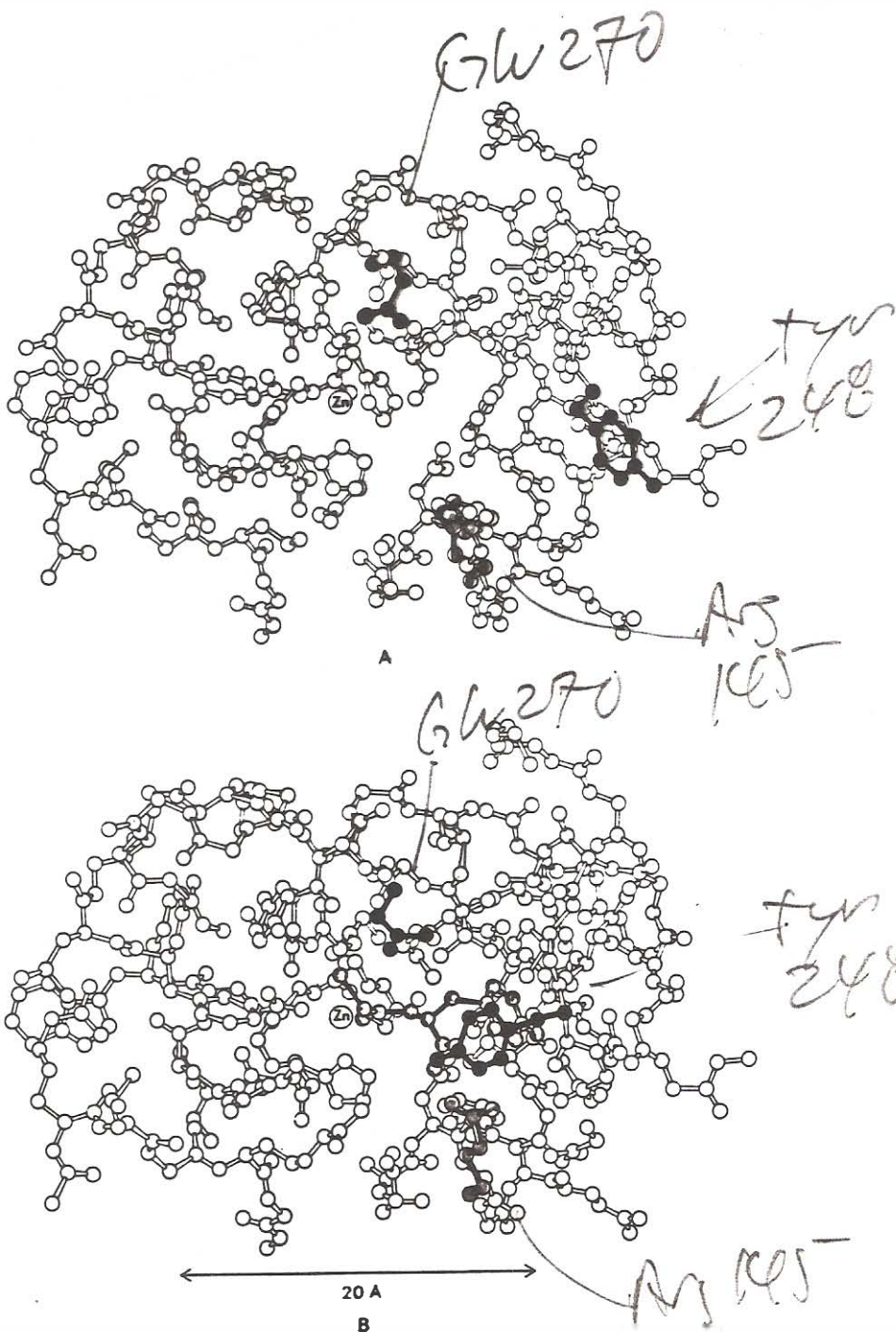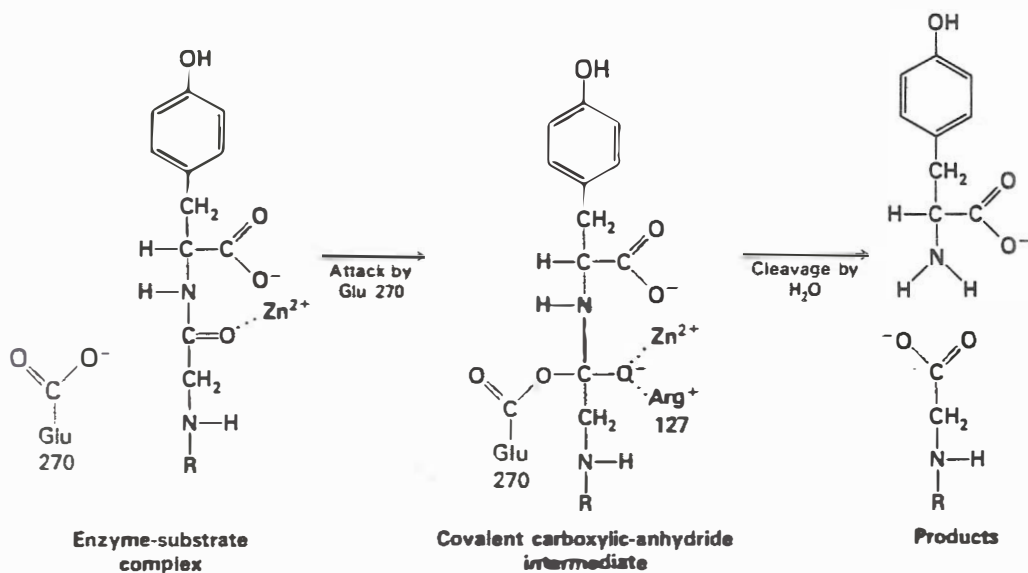
The structure of carboxypeptidase A changes upon binding substrate: (A) enzyme alone (Arg 145 is shown in yellow, Glu 270 in green, and Tyr 248 in blue); (B) enzyme-substrate complex (glycyltyrosine, the substrate, is shown in red). [After W. N. Lipscomb. *Proc. Robert A. Welch Found. Conf. Chem. Res.* 15(1971):140–141.]

Glu 270
tyr 248
Arg 145

A

Glu 270
tyr 248
Arg 145

20 A

B

Catalytic Mechanism of Carboxypeptidase A

A plausible catalytic mechanism for carboxypeptidase A emerges from x-ray and chemical studies.

Three groups are thought to be critical for catalysis: the **zinc** ion, the quanidinium group of arginine 127, and the carboxylate group of glutamate 270.

Enzyme-substrate complex · Attack by Glu 270 → Covalent carboxylic-anhydride intermediate · Cleavage by H_2O → Products

A proposed catalytic mechanism for carboxypeptidase A in which Glu 270 directly attacks the carbonyl carbon atom of the scissile bond to form a covalent mixed-anhydride intermediate.

Angiotensin-Converting Enzyme (ACE)

An exodipeptidase of 140 Kd containing a single polypeptide chain and one **zinc** ion.

Its catalytic properties are similar to those of two other zinc proteases: pancreatic carboxypeptidase A and thermolysin.
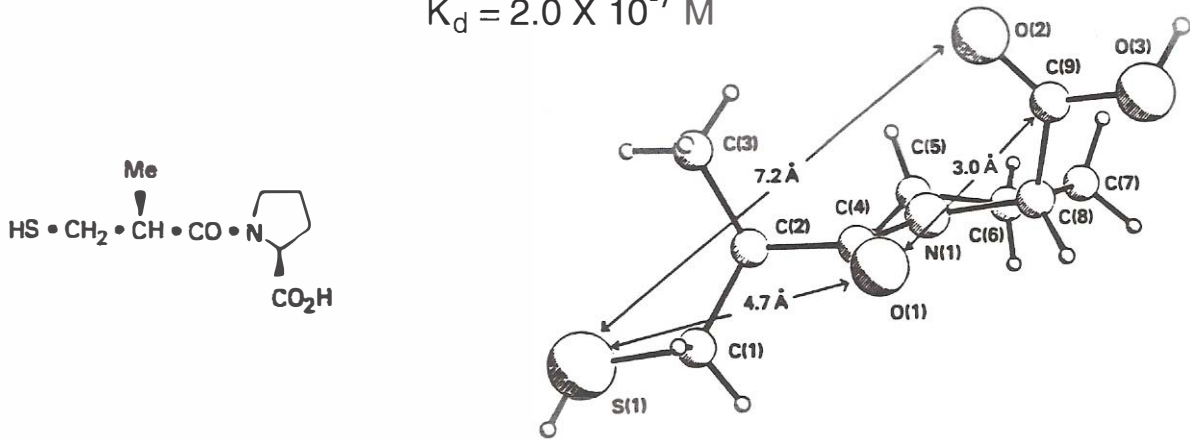
ACE splits off a C-terminal dipeptide in place of the single C-terminal residue cleaved off by carboxypeptidase A.
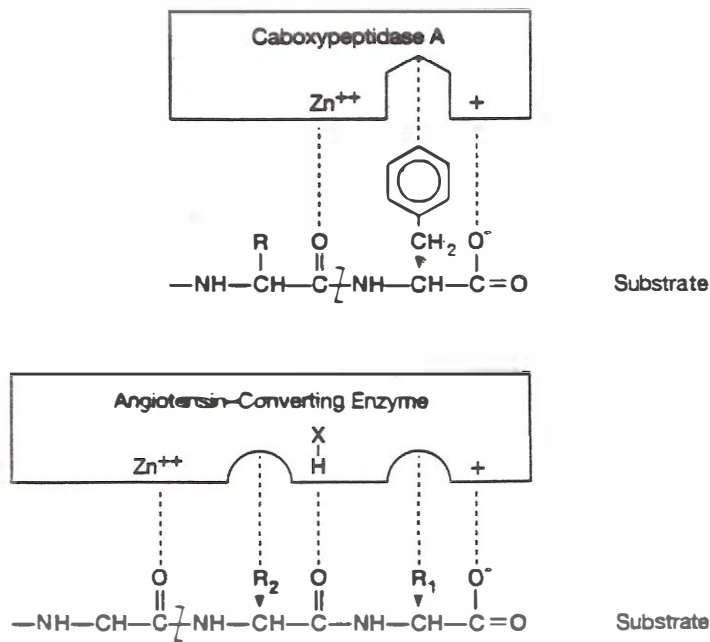
Cushman (1977) assumed that carboxypeptidase A and ACE had similar active sites; first syn. succinylproline ($K_d = 3.3 \times 10^{-4}$ M).

Captopril
$$K_d = 2.0 \times 10^{-7} \text{ M}$$

Angiotensin-Converting Enzyme (ACE)

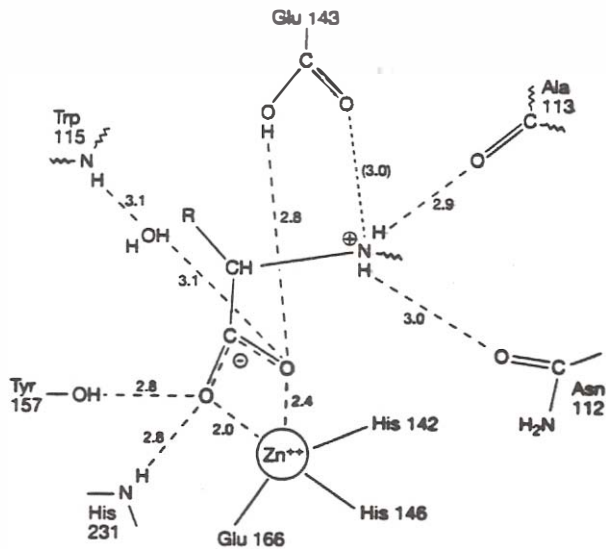Second and third generation inhibitors are even tighter binders

Figure 5.10. Interaction of an inhibitor of the human angiotensin-converting enzyme with the active site of the bacterial zinc endopeptidase thermolysin. The inhibitor is N-(1-carboxy-3-phenylpropyl)-L-leucyl-L-tryptophan. Note the hydrogen bonds between the carboxylate of the inhibitor and the glutamate, tyrosine, and histidine, and its interactions with the zinc ion. (Reproduced, by permission, from Monzingo and Matthews, 1984)
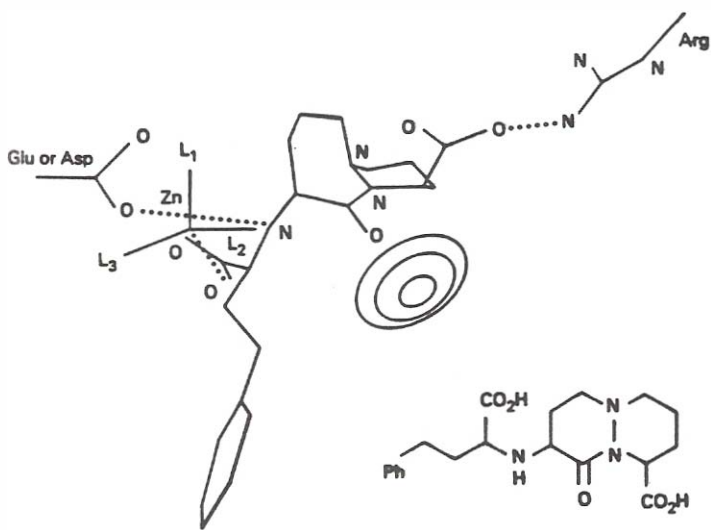

Figure 5.11. Chemical formula and orientation of the antihypertensive drug Cilalapril when bound to the hypothetical active site of the angiotensin-converting enzyme. (Reproduced, by permission, from Attwood et al., 1986)

Remember, this is only a hypothetical active site for the ACE.

Zinc Fingers

In 1985 Miller, McLachlan, and Klug discovered that TFIIIA, a DNA-binding **zinc** protein that controls the transcription of the 5S RNA genes in Xenopus oocytes consists of a tandem repeat of 9 homologous domains of 30 residues, each containing pairs of closely spaced cysteines and histidines.

1 (M G E K A L P V V Y K R)

1	(Y)I (C)S F A D(C)G A A(Y)N K N W K(L)Q · A(H)L C · K(H)	37
2	T G E K · P(F)P(C)K E E G(C)E K G(F)T S L H H(L)T · R(H)S L · T(H)	67
3	T G E K · N(F)T(C)D S D G(C)D L R(F)T T K A N M K · K(H)F N R F(H)	98
4	N I K I C V(Y)V(C)H F E N(C)G K A(F)K K H N Q(L)K · V(H)Q F · S(H)	129
5	T Q Q L · P(Y)E(C)P H E G(C)D K R(F)S L P S R(L)K · R(H)E K · V(H)	159
6	A G - - · -(Y)P(C)K K D D S(C)S(F)V G K T W T(L)Y L K(H)V A E C(H)	188
7	Q D - - · L A V(C)- - D V(C)N R K(F)R H K D Y(L)R · D(H)Q K · T(H)	214
8	E K E R T V(Y)L(C)P R D G(C)D R S(Y)T T A F N(L)R · S(H)I Q S F(H)	246
9	E E Q R · P(F)V(C)E H A G(C)G K C(F)A M K K S(L)E · R(H)S V · V(H)	276

277

(D P E K R K L · K E K C P R P K R S L A S R L T G Y I P P K S K E K[N]A   311

S V S G T E K T D S L V K N K P S G T E T[N]G S L V L D K L T I Q)   344

Figure 3.1. Amino acid sequence of Xenopus zinc finger. Homologous residues are circled. For meaning of single letter amino acid code, see Figure A2.1 on page 278. (Reproduced, by permission, from Miller et al., 1985)

Suggested that each quartet of cysteines and histidines binds one **zinc** ion and that the peptide loop connecting the pair of cysteines to the pair of histidines formed a DNA-binding finger.

Figure 3.2. Miller, McLachlan, and Klug's interpretation of the zinc finger sequence shown in Figure 3.1. Ringed residues are conserved. Black dots mark proposed DNA-binding residues. (Reproduced, by permission, from Miller et al., 1985)
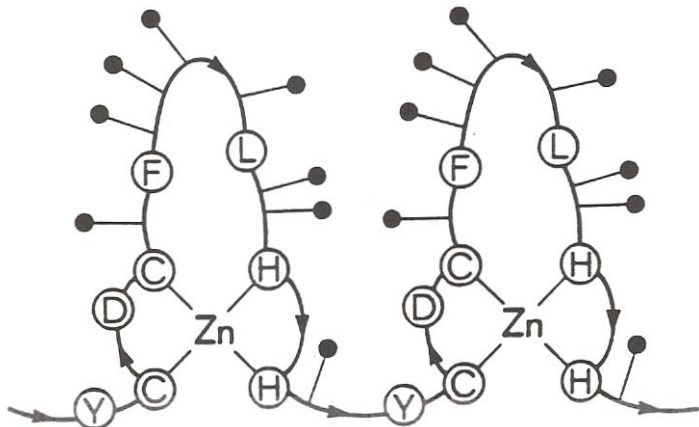
Zinc Fingers

In 1988 Berg proposed a structure for the **zinc** finger from comparisons of its amino acid sequence with those of metalloenzymes of known structure.

It is centered around a **zinc** ion that is tetrahedrally coordinated to the two cysteines and two histidines.
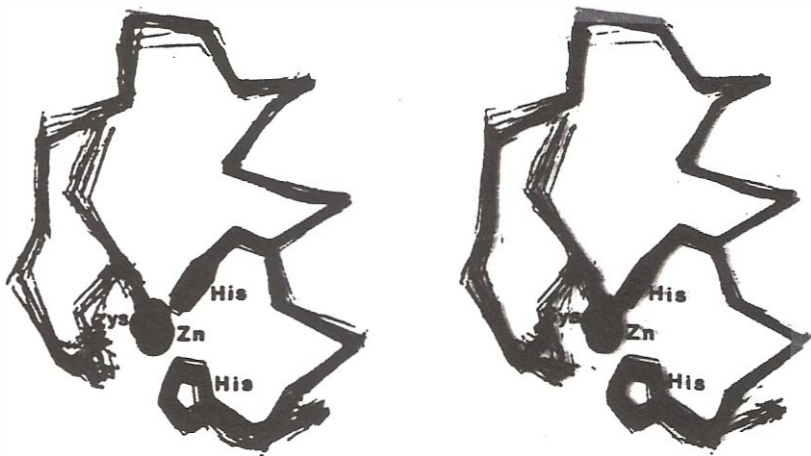

Figure 3.3. Course of the polypeptide chain of the zinc finger and zinc coordination predicted by Berg and then confirmed by NMR. (Reproduced by permission, from Lee et al., 1989)

Berg also predicted that zinc fingers would bind to DNA with their α-helices fitting into its major groove, which would allow successive fingers to wrap around the double helix.

He was correct!

Determined by NMR and X-ray analysis.

The complex was obtained by crystallization of a 90 amino acid residue DNA-binding domain cleaved from a mouse protein and combined with a 10 base-pair double helical DNA.

Zinc Fingers

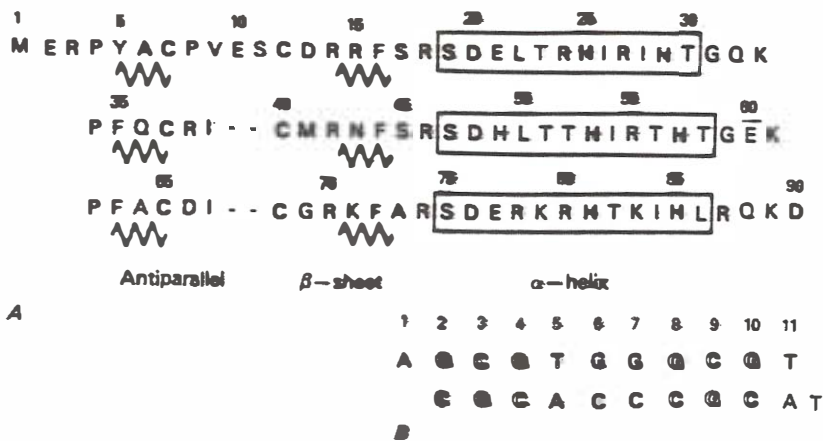Using the DNA-binding domain from the mouse protein:

Figure 3.4. (A) Amino acid sequence of mouse zinc fingers. Bold C's and H's mark the cysteines and histidines coordinated to the zinc ions. (B) Base sequence of double-helical oligonucleotide to which the zinc fingers are bound. (Reproduced, by permission, from Pavletich and Pabo, 1991)

Figure 3.5. Detailed structure of one of the mouse zinc fingers. Note the hydrophobic side chains of phenylalamine 16 and leucine 22 that fill the space between the a-helix on the left and the β-strands on the right. Also note arginines 18, 24, and 27, and lysine 33 that extend from the a-helix toward the DNA. (Reproduced, by permission, from Pavletich and Pabo, 1991)
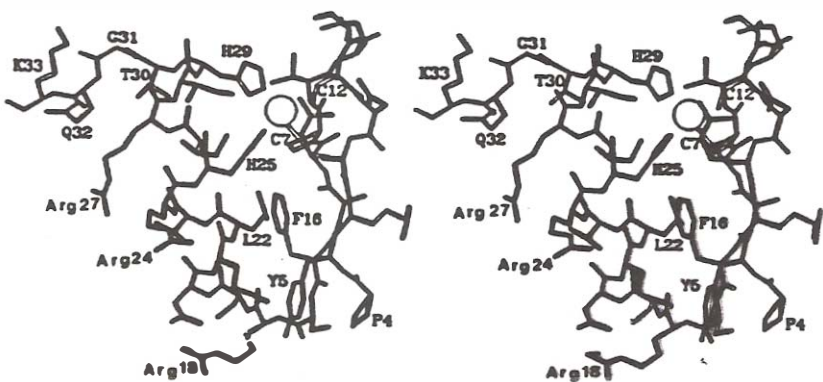
Zinc Fingers

Sidechains in each finger form hydrogen bonds with DNA phosphates and bases.

The arginines immediately preceding the amino-ends of each helix are hydrogen bonded to guanines. Each of these arginines is held in position by a H-bond to an aspartate attached to the α-helix. Two other arginines and a histidine in the α-helices also bind to guanines, while five other arginines and one serine form nonspecific H-bonds with DNA phosphates. In each finger one of the histidines that is coord. to Zn with its N_ε also donates a hydrogen bond to a phosphate O with its N_δ.
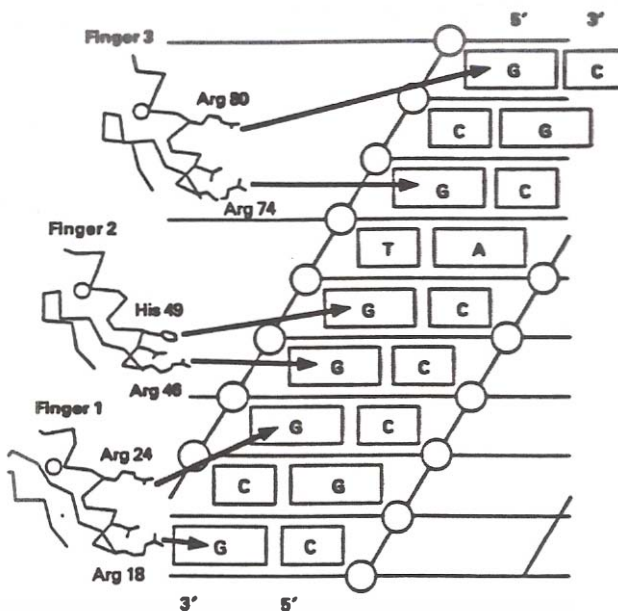

Figure 3.7. Hydrogen bonds from arginines and a histidine in the mouse zinc fingers to guanines in the DNA. (Reproduced, by permission, from Pavletich and Pabo, 1991)

Base pair 10 for finger 1
(Base pair 7 for finger 2;
Base pair 4 for finger 3)

D20 in finger 1
(D48 in finger 2;
D76 in finger 3)
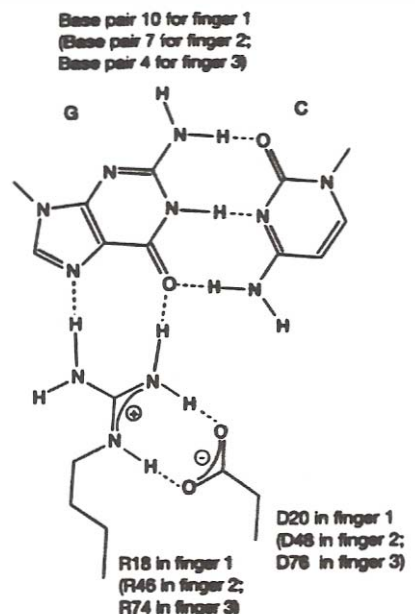
R18 in finger 1
(R46 in finger 2;
R74 in finger 3)

Figure 3.8. Details of hydrogen bonds between the ion pair of arginine and aspartate and the base pair of guanine and cytosine in the mouse zinc fingers. (Reproduced, by permission, from Pavletich and Pabo, 1991).

Zinc Fingers

Zinc fingers are the first known DNA-binding proteins with a variable number of modular repeats that are geometrically adapted to bind to the repeats of the DNA double helix

NMR methods have also been used to solve the structures to two medically important zinc fingers that have not been crystallized.
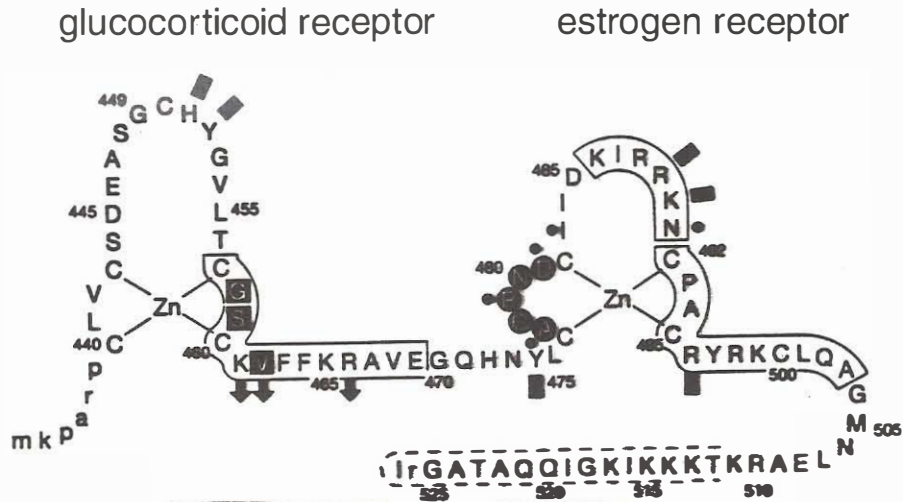
glucocorticoid receptor   estrogen receptor

Figure 3.11. Amino acid sequence of DNA-binding domain of glucocorticoid receptor used for crystallization with the DNA response element. The numbering corresponds to that of the full-length native receptor. The boxed residues are α-helical. Residues that make contact at the dimer interface are indicated by the solid dots (477, 479, 481, 483, and 491). Residues making phosphate contacts (451, 452, 473, 489, 490, and 496) are indicated by solid rectangles. The arrows indicate base contacts. A disordered section at the carboxyl terminus is indicated by the dashed lines. Three amino acid residues that direct the discrimination between glucocorticoid and estrogen response elements are indicated by white lettering in the solid boxes (458, 459, and 462); those that discriminate between estrogen and thyroid response elements are circled (478–481). The lower-case letters indicate artifacts of the expression vector construct.

Figure 3.13. Stereo view of the glucocorticoid receptor protein–DNA complex. The dark circles mark the zinc ions. The domain at the top is the one that is correctly positioned. Protein sidechains that form hydrogen bonds with the DNA are indicated. The α-helix in the major groove is viewed end-on. The residues in the top domain are numbered by the last two digits of the sequence (440-525); those in the bottom domain by subtracting 300 from that sequence. Only the binding of the top domain is likely to be representative of that of the two domains in the natural complex.
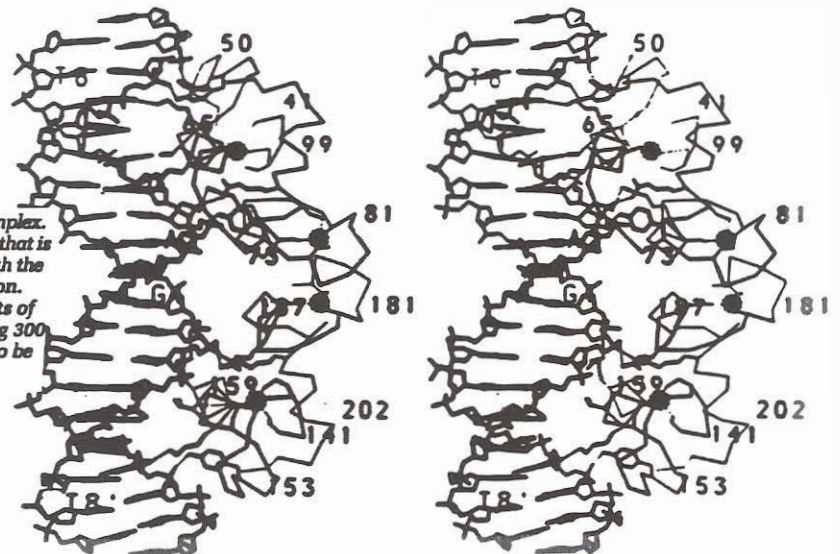
Iron in Biosystems

Fe: most abundant metal in living organisms.
Humans: 60 mg Fe/kg body mass, most of which is involved in oxygen transport.
Much of the biochemistry of Fe relates in some manner or another to the half-reaction

$$Fe^{3+} + 1e^- \longrightarrow Fe^{2+}$$

since both the chemical properties and reactivity of Fe are strongly dependent on its oxidation state. The binding of O_2 to hemoglobin (Fe(II)) is reversible, but that to methemoglobin (structurally similar, but with Fe(III) is not.

Table 22.4 Functions and distributions of some important iron-containing biomolecules

Species	Function	Distribution
Transferrin	Transport of Fe	Animals
Siderochromes	Transport of Fe	Bacteria and fungi
Ferritin	Storage of Fe	Animals
Hemosiderin	Storage of Fe	Animals
Cytochromes	Redox enzymes	Plants and animals
Rubredoxins	Redox enzymes	Bacteria
Ferredoxins	Redox enzymes	Plants and bacteria
Nitrogenase	N_2 fixation	Plants and bacteria
Myoglobin	O_2 transport	Animals
Hemoglobin	O_2 transport	Animals
Hemerythrin	O_2 transport	Marine worms

The solubilities of Fe salts and complexes also vary with the oxidation state. Fe(III) salts have low aqueous solubilities, a fact of biological significance. The recommended daily allowance of Fe in the diet (in which much of the Fe occurs as Fe(III) is about 18 mg; body actually needs only 2 mg/day. The difference reflects the fact that Fe is poorly ingested.

Fe Transport and Storage

The transfer of Fe from the digestive tract to the blood is accomplished in mammals by the protein *transferrin* (80 kD). Transferrin makes up about 2% of the blood serum solids in humans: contains two Fe's in the high spin Fe(III) state. The coordinations appear to be through the surrounding protein, plus one HCO_3^- ligand.

The Fe(III) apotransferrin formation constant is quite large under physiological conditions (10^{30}), and is extremely pH dependent; no complexation is observed below pH 4. This is consistent with the observation that three H ions are released upon complexation. These H's protonate a bicarbonate ion and, probably, two anionic sites of the surrounding protein

In mammals, the long-term storage of excess Fe involves *ferritin* (900 kD). It consists of a protein surrounding a core (420 kD) that contains a variable amount of Fe; up to 4500 Fe's can be accomodated/molecule. Ferritin is nearly spherical, with a diameter of roughly 12,500 pm; the core cavity is thought to be about 7500 pm in diameter. An approx. formulation for the core is $Fe(H_2PO_4) \cdot 8Fe(OH)_3$. The structure is unknown, but is probably similar to that of hydrated ferric oxide.

Heme Redox Agents: The Cytochromes

The term *cytochrome* means "pigment of a cell." There are three major types of cytochromes; *a*, *b*, and *c*, each of which has known variations. They act as electron transfer agents for respiratory metabolism; ie., they manage the transfer of electrons from substrates to O_2. This is accomplished through changes in the metal oxidation state (Fe(II)/Fe(III)).

Cytochrome *c* is the most studied of the three types. Like hemoglobin and myoglobin, it is a *heme* protein-that is, an Fe-porphyrin complex attached to a protein chain. The Fe is also coordinated to the surrounding protein at trans sites through N (histidine) and S (methionine) donors. The protein chain is short compared to other metalloenzymes (104 amino acid residues), giving a relatively low MW (12 kD).

The cytochromes act in sequence: *a* (E°_{red} = +0.24 V), *b* (E°_{red} = +0.04 V), *c* (in the middle). Thus, electrons from the oxidized substrate (glucose) are initially transferred to *b*, which relays them to *c*, which in turn passes them on to *a*. A complex species known as *cytochrome oxidase*, which contains two *a* units and also a Cu atom, provides the ultimate link to O_2.
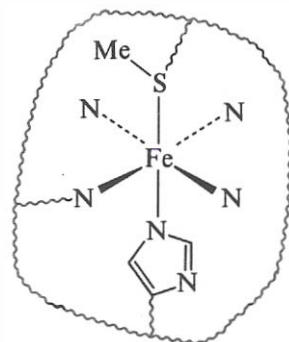
Nonheme Redox Agents: The Doxins

The *rubredoxins* and the *ferredoxins*. Important in the electron transfer aspects of photosynthesis and nitrogen fixation.

Both have Fe coordinated to four S donors, subdivided into two types, *labile* and *nonlabile*. Labile S is ligated S^{2-} (typically in a bridging position betwen two or three Fe's), while nonlabile S is part of an amion acid residue (cysteine or methionine).

The rubredoxins are bacterial enzymes. They contain one Fe, tetrahedrally coordinated to nonlabile S's of a small protein. The ferredoxins (found in plant chloroplasts and certain bacteria) are more complex. At least three categories are known, containing two, four, and eight Fe's, respectively. There is exactly one labile S per Fe in each case. The diiron ferredoxins have 4-coordinate Fe's linked by bridging sulfides.

The tetrairon ferredoxins contain Fe-S cubes resulting in approx. T_d coordination about the metal. Three sites are occupied by labile S's from the adjacent vertices of the cube, with the fourth donor being from a cysteins residue of the protein. The eight-iron ferredoxins contain two Fe_4S_4 cubes, which are connected at two positions by branches of the protein chain.
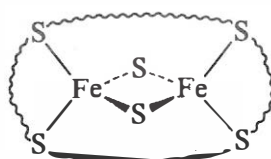
(a)
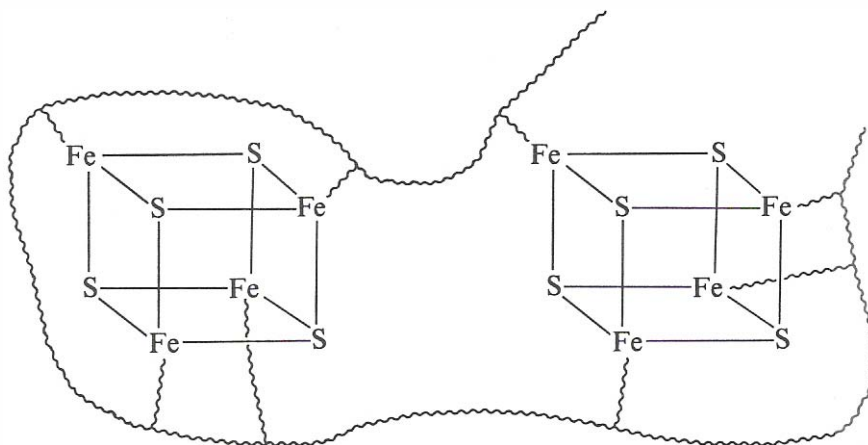
Schematic diagram
of the structure of
(a) a two-iron and
(b) an eight-iron
ferredoxin;
~~= protein.

(b)

Many model systems have been synthesized in efforts to understand the chemistry of these Fe's cubes. One of the best known is the complex anion $[S_4Fe_4(SCH_2(C_6H_5)_4]^{2-}$. The spectroscopic properties of this species is quite similar to those of the four-Fe ferredoxins.

The structure of the model ferredoxin $[S_4Fe_4(SCH_2\phi)_4]^{2-}$; the bond distances are in angstrom units.
[Reproduced with permission from Herskovitz, T.; Averill, B. A.; Holm, R. H.; Ibers, J. A.; Phillips, W. D.; Weiher, J. F. *Proc. Nat. Acad. Sci.* **1972**, 69, 2437.]